BIODETOXIFICATION OF LIGNOCELLULOSIC HYDROLYSATE LIQUOR TO IMPROVE BIOFUEL PRODUCTION

Ph.D. THESIS

by

BHANENDRA SINGH

DEPARTMENT OF BIOTECHNOLOGY
INDIAN INSTITUTE OF TECHNOLOGY ROORKEE
ROORKEE – 247 667 (INDIA)
FEBRUARY, 2019

BIODETOXIFICATION OF LIGNOCELLULOSIC HYDROLYSATE LIQUOR TO IMPROVE BIOFUEL PRODUCTION

A THESIS

Submitted in partial fulfillment of the requirements for the award of the degree

of

DOCTOR OF PHILOSOPHY

in

BIOTECHNOLOGY

by

BHANENDRA SINGH

DEPARTMENT OF BIOTECHNOLOGY
INDIAN INSTITUTE OF TECHNOLOGY ROORKEE
ROORKEE – 247 667 (INDIA)
FEBRUARY, 2019

INDIAN INSTITUTE OF TECHNOLOGY ROORKEE
ROORKEE

CANDIDATE'S DECLARATION

I hereby certify that the work which is being presented in the thesis entitled "**BIODETOXIFICATION OF LIGNOCELLULOSIC HYDROLYSATE LIQUOR TO IMPROVE BIOFUEL PRODUCTION** " in partial fulfillment of the requirements for the award of the Degree of Doctor of Philosophy and submitted in the Department of Biotechnology of the Indian Institute of Technology Roorkee, Roorkee is an authentic record of my own work carried out during a period from July, 2014 to September, 2018 under the supervision of Dr. Saurav Datta, Assistant Professor, Department of Biotechnology, Indian Institute of Technology Roorkee, Roorkee.

The matter presented in this thesis has not been submitted by me for the award of any other degree of this or any other Institution.

(BHANENDRA SINGH)

This is to certify that the above statement made by the candidate is correct to the best of my knowledge.

(Saurav Datta)
Supervisor

The Ph.D Viva-Voce examination of **Bhanendra Singh**, Research Scholar, has been held on 25th February 2019.

Chairman, SRC **Signature of External Examiner**

This is to certify that the student has made all the corrections in the thesis.

Signature of Supervisor **Head of the Department**
Date:

ABSTRACT

Biochemical conversion of lignocellulosic feedstock to biofuels and other valuable chemicals through a sugar-platform process involves pretreatment and hydrolysis steps, which facilitate the conversion of polysaccharides to simple sugars. A major drawback of acid pretreatment and hydrolysis process is formation of lignocellulose-derived by-products, such as furfural and 5-hydroxy-2-methylfurfural (HMF), which inhibit microbial growth during fermentation. Hence, an efficient and environment friendly technique for removal of these inhibitors is essential. We report isolation of a bacterium from soil having excellent capability to degrade furfural and HMF present in lignocellulosic hydrolysate liquor. This isolated bacterium was identified as *Bordetella* sp. BTIITR. Strain BTIITR was observed to be Gram stain-negative, coccobacillus and non-motile. Various biological and biochemical tests were performed to compare the characteristics of the isolated strains with the reported species of *Bordetella.*

The isolated bacterium, *Bordetella* sp. BTIITR, was able to degrade 100 % of furfural and 80 % of HMF from simulated hydrolysate liquor in 16 h of incubation period. For the actual sugarcane bagasse hydrolysate liquor, it was able to remove 100 % of furfural, 94 % of HMF and 82 % of acetic acid in 16 h of incubation period. The isolated bacterium also demonstrated remarkable selectivity for HMF and furfural over the sugars present in hydrolysate liquor. Sugars were not consumed significantly before furfural and HMF were degraded to a low threshold concentration. This substrate priority of *Bordetella* sp. BTIITR for HMF and furfural makes it a potential organism for biodetoxification of inhibitory compounds present in the lignocellulosic hydrolysate liquor. To the best of our knowledge, this is the first study that illustrates the capability of *Bordetella* sp. to degrade the furan derivatives.

The above study was further extended by immobilizing *Bordetella* sp. BTIITR within chitosan beads for detoxification of hydrolysate liquors. We hypothesized that the immobilized cells will enable significant process benefits over the free cells. The immobilized cells were observed to degrade 93 % HMF + 100 % furfural and 86 % HMF + 100 % furfural in 20 h at pH 8 and temperature of 40 ^{0}C from simulated and sugarcane bagasse hydrolysate liquors, respectively. As a significant improvement over the free cells, the immobilized cells were able to detoxify lignocellulosic hydrolysate liquor at broader range of operating pH, temperature

and inhibitor concentration. Besides, the immobilized cells were successfully reused for seven consecutive cycles of operations with nearly constant degradation efficiency.

Furthermore, a packed bed reactor (PBR) was designed and developed with the cell-immobilized chitosan beads. The idea was to employ a bioreactor for continuous detoxification of lignocellulosic hydrolysate for longer period of time, which may potentially lead to an industrially viable detoxification technology. Indeed, the PBR was observed to successfully emulate the performance of the batch operations. The height of the bed and the flow rate were optimized and it was observed that a bed height of 37.5 cm and feed flow rate 4 ml/min were most suitable for detoxification. 86.3 % of total furan was removed from the simulated hydrolysate. To demonstrate the benefit of the bioreactor, experiments were also conducted with continuous flow of sugarcane bagasse hydrolysate liquor for 15 h and a satisfactory degradation of furan inhibitors was observed. A simplified plug flow reactor model was also employed to perform kinetic studies of detoxification reaction within the PBR. It was observed that the degradation reaction followed first order kinetics in the PBR with apparent rate constants of 0.049 min^{-1} and 0.043 min^{-1} for HMF and furfural degradation, respectively.

Finally, advantage of detoxification was established by ethanol formation using *Pichia stipitis* as the fermenting microorganism. Both detoxified simulated and detoxified bagasse hydrolysate liquors demonstrated significantly improved growth of fermenting microorganism and resulted in improved production of ethanol in comparison to the undetoxified hydrolysate liquor. Fermentation results revealed 1.6 times higher ethanol production and 2.6 times higher volumetric productivity from the detoxified sugarcane bagasse hydrolysate liquor in comparison to the undetoxified sugarcane bagasse hydrolysate liquor. Concentration of ethanol was recorded as 8.4 gL^{-1} and 5.2 gL^{-1} for detoxified bagasse and undetoxified bagasse hydrolysate liquors, respectively.

Overall, the substrate priority of the isolated strain and the efficacy of detoxification can potentially lead to a translational technology for efficient degradation of fermentation inhibitors, which subsequently promises to improve the overall economics of ethanol formation from lignocellulosic biomass.

ACKNOWLEDGEMENT

I would like to express my immense gratitude to my supervisor, **Dr. Saurav Datta,** for his continuous encouragement, motivation and guidance towards successful completion of this project. I am grateful to my SRC members, **Dr. Bijan Chaudhury**, **Dr. R.P Singh** and **Dr. Chandrajit Balomajumder**, for their critical suggestions and assessments, which helped me all through to complete my tenure successfully.

I would like to express my gratitude to **Dr. A. K. Sharma**, Head of the Department, for providing all the infrastructural facilities in the department, which helped in completion of this endeavor. I also convey my regards to **Dr. Prabhat Mandal** and **Dr. Sulakshana Mukherjee**, Assistant Professor, Department of Biotechnology, Indian Institute of Technology Roorkee, for helpful discussion in identification of isolated bacterium.

I sincerely and very dearly thank my lab mates, **Ms. Anjlika Yadav, Ms. Ayushi Verma, Ms. Pooja, Mr. Praveen Kumar and Mr. Arpit Maheshwari**, for all of their endless and unconditional help during the lab experiments. I also thank my colleague and lab mate, **Anju Kumari** for helpful discussions.

I would like to mention the unconditional and endless contributions of my family members, especially my parents, **Mr. Malkhan Singh** and **Mrs. Bharti Devi**, who provided each and every support, which I needed in my educational venture. The support and encouragement of my friends, **Mr. Akash Gupta** and **Mr. Raghvendra Singh**, worked as boost towards the completion of my studies.

Finally, I convey my regards to Science and Engineering Research Board (SERB), India and University Grant Commission (UGC), India for financially supporting this research. I am also thankful to Indian Institute of Technology Roorkee, India for providing the much needed infrastructure to conduct this research.

Table of Contents

List of Tables

List of Figures

CHAPTER 1: INTRODUCTION

Energy is an important commodity for human society. The high energy demand for the industrialized and modernized world coupled with the inherent pollution problems of fossil fuels makes it increasingly necessary to explore renewable energy with abundant resources and smaller environmental impact [1, 2]. Currently, all renewable energy sources, such as hydroelectric, solar, wind, tidal and geothermal, target the electricity market, while fuels make up a much larger share of global energy demand. Bioethanol and biodiesel are the alternative liquid fuels for future generations [3]. Biomass is one of the most promising renewable resource used to generate different types of biofuels, such as biodiesel and bioethanol [4]. Biofuels are categorized into primary and secondary biofuels. Primary biofuels, such as fuel wood, is used in an unrefined form primarily for heating, cooking or electricity production. Secondary biofuels, such as bioethanol, is produced by processing of biomass and are used in vehicles and various industrial processes. The secondary biofuels can be divided into three generations, such as first, second and third on the basis of different parameters, such as the type of feedstock, processing technology or their level of development [5].

The first generation biofuels include different fuels obtained from crop plants. Currently, bioethanol from corn starch, sugar cane or sugar beet, and biodiesel from oil crops are the most widely available forms of first generation biofuels. But these crops would compete for arable land with food crops.

The second generation biofuels are produced from non-food crops, such as bioethanol derived from the lignocellulosic materials viz. agricultural residues, straw, grass and wood and biodiesel derived from non-edible oil plant, like Jatropha, Cassava or Miscanthus.

Algal biomass is considered as third generation feedstock. The major drawback associated with it is to produce biomass in large quantity.

Lignocellulosic biomass provides abundant and renewable feedstock for the production of biofuels and biochemicals. As shown in Fig. 1.1 lignocellulosic biomass contains polymeric sugars in the form of cellulose and hemicellulose, which can be converted to simple sugars by hydrolyzing the biomass, and then, can further be converted to ethanol by fermentation using microorganisms, such as *Saccharomyces cerevisiae* [6, 7].

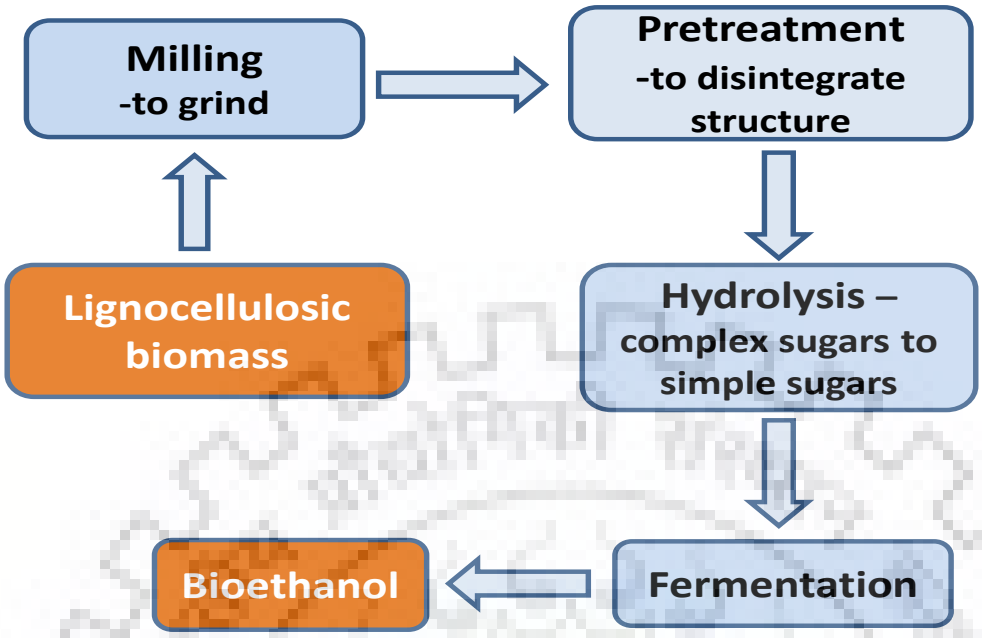

Fig. 1.1 Flow chart showing the steps of ethanol production from lignocellulosic biomass.

Currently, the well-known pretreatment methods used to convert the complex sugar into simple sugars involve dilute acid, steam explosion, alkali, ionic liquids and microwave. The most common method to release sugar in hydrolysate liquor is acid pretreatment followed by enzymatic (cellulase enzyme) or chemical treatment [8]. A major drawback of acidic pretreatment and hydrolysis is the production of several toxic compounds as byproducts that strongly inhibit the activities of fermenting microorganisms essential for downstream processing steps [9, 10].

These toxic compounds can be divided into three major groups based on their chemical nature: (i) organic acids (acetic acid, formic acid, and levulinic acid) that originate from the breakdown of hemicellulose, (ii) phenolic compounds (vanillin, syringaldehyde, 4-hydroxybenzaldehyde, coniferyl aldehyde, ferulic acid, and cinnamic acid) as breakdown products of the phenolic polymer lignin, and finally, (iii) furan derivatives, furfural and HMF (5-hydroxy-2-methylfurfural), that are derived from elimination reactions of pentose and hexose sugars, respectively as shown in Fig. 1.2 [11, 12]. Among all these inhibitors, furfural and HMF are considered as the major inhibitors due to their high concentration and strong inhibition strength to ethanol fermenting strains leading to a noticeable decrease of overall productivity in fermentation processes [10, 13].

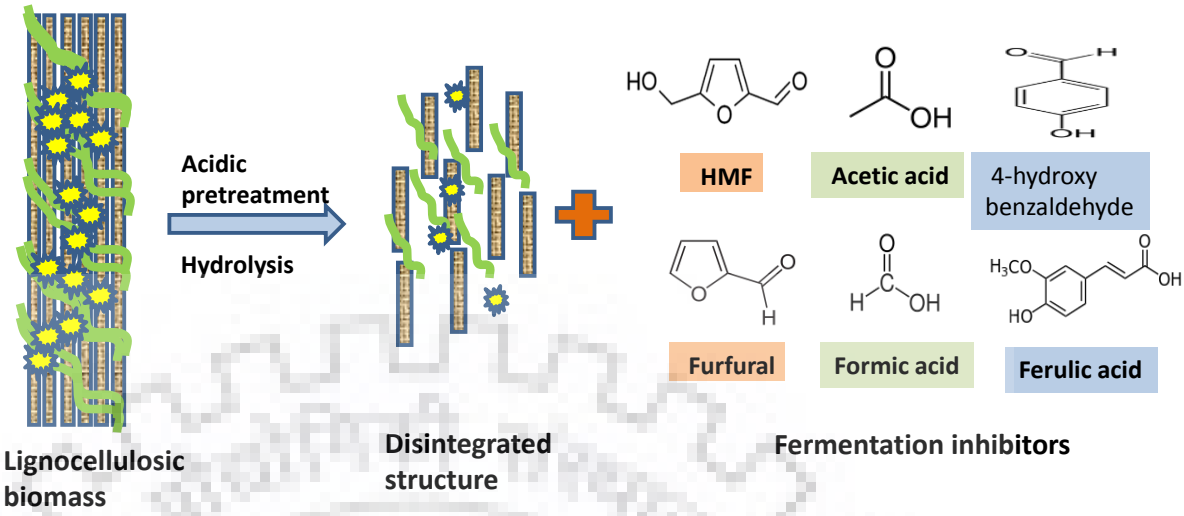

Fig. 1.2 Schematic representation of acidic pre-treatment and possible inhibitors (or toxic compounds) produced as byproducts (adopted from Phitsuwan et al.) [14].

The level of furans (HMF and furfural) produced during pre-treatment varies according to the type of raw material and the pretreatment procedure [15]. Although a mild pretreatment may yield lesser inhibitor compounds, the industries still prefer the intensive pretreatment of lignocellulosic feedstock to get high yield of simple sugars. The inhibitory effect on the growth rate of yeast and fermentation rate is higher for furfural than HMF, but the effect of HMF lasts longer [6]. Furfural and HMF have been shown to inhibit at least three enzymes in the central carbon metabolism in the glycolytic cycle and tricarboxylic acid cycle [16, 17]. Although furfural and HMF can act synergistically, yeast cells are more sensitive to furfural inhibition than the HMF at the same concentration [6, 18]. It has also been reported that furfural and HMF cause oxidative stress and decrease the activities of various dehydrogenase enzymes in yeast cells during the fermentation [17, 19].

To eliminate the problem of toxicity of lignocellulosic hydrolysate liquor, several strategies have been adopted based on physical, chemical or biological detoxification prior to fermentation [20]. Physical and chemical methods involve the removal of inhibitors from lignocellulosic hydrolysate liquor through ether extraction, alkaline precipitation or enzymatic treatment by laccases [20, 21]. Separation of furfural from monosaccharides by nanofiltration was also tried using NF90 and NF270 membranes [22]. Physiochemical methods involve the addition of chemicals/water, which makes the process economically unfavorable and hazardous. Some methods other methods are water washing, over-liming, ammonia

neutralization, ion exchange absorption, solvent extraction and activated charcoal treatment [23, 24]. However, these methods consume huge amount of fresh water and produce a large quantity of waste water, along with notable loss of fermentative sugars [25].

Biological detoxification provides a better alternative to physio-chemical detoxification as it does not involve the addition of chemicals and generates mostly biodegradable waste. Biological detoxification or biodetoxification or bio-abatement depends on microorganisms that specifically remove fermentation inhibitors from the hydrolysate. Biodetoxification has many other advantages, such as significantly decreased use of water, no significant loss of sugars and thus high concentrations of sugars for fermentation. Apart from that, these inhibitors can be converted into valuable chemicals by using specific microorganisms. Production of such valuable chemicals from fermentation inhibitors may further improve the economics of biofuel production. Bio-transformed *Pseudomaonas putida* S12 was developed by Koopman et al. to produce 2,5-furandicarboxylic acid (FDCA) from HMF. FDCA has the potential to replace terephthalic acid as a 'green' substitute for the production of polyesters [26]. Biological detoxification needs specific microorganism, which can utilize the fermentation inhibitory compounds for its metabolism.

Use of free cells requires an additional downstream step of separation of cells from the process stream, which makes the process costlier and lengthier. As an alternative, immobilization of microorganisms on inert supports or entrapment inside the bead has been drawing significant attention, because this technique provides several advantages over free cells, such as easy cell recovery, prevention of cell washout, cell recycling in repeated batch operations, and the flexibility of bioreactor designing and the improved operational stability [27]. Bead structure may also provide increased protection to the entrapped microorganisms against the adverse conditions, such as high/low temperature, pH variation and concentrations of toxic chemicals [28].

In the present study, soil samples were collected from different locations of Dehradun (30.34° N and 77.99° E) in India to isolate microorganisms capable of degrading the model fermentation inhibitors, HMF and furfural. Screening, isolation and characterization were done to select the best microorganism for the study. Then, the selected bacterium was used for removal of fermentation inhibitors from simulated and sugarcane bagasse hydrolysate liquors. Furthermore, immobilization of the isolated bacterium was explored within chitosan beads for

degradation of HMF and furfural. Characterization of the immobilized cells was conducted to verify that the desired properties were achieved. Effects of biomass loading, pH, temperature and inhibitor concentration on the detoxification efficiency of the immobilized cells were investigated and compared with that of the free cells. The reusability of the immobilized cells was demonstrated by conducting seven consecutive cycles of detoxification. After that an attempt was made to develop a packed bed reactor system containing the immobilized cells within chitosan beads for long term biodetoxification of hydrolysate liquors under convective mode of flow. Finally, comparative study on bioethanol production was investigated from the biodetoxified and the undetoxified hydrolysate liquors.

CHAPTER 2: LITERATURE REVIEW

Today's society is largely dependent on fossil resources for the production of chemicals and transportation fuels. The constant exploration of oil and gas has increased the exploitation of these fossil resources. The over exploitation of these resources has a profound negative impact on society, economy and environment. The major concern is that consumption of fossil fuels is increasing drastically with the increase in population, transportation and lifestyle advancement [29, 30]. But, the fossil resources are limited, and hence they will exhaust in future. Furthermore, fossil fuels lead to CO_2 and other greenhouse gas emission, which adversely affects climate and air quality. Therefore, there is immediate necessity to develop sustainable and renewable alternatives for fossil resources. Lignocellulosic biomass presents a potential alternative feedstock for the production of fuels. They are carbon neutral, meaning the amount of CO_2 produced during combustion of biofuels is recycled back and stored in biomass again via the process of photosynthesis in a relatively short time period. In contrary, storage of CO_2 in fossil fuels takes millions of years as schematically represented in Fig. 2.1.

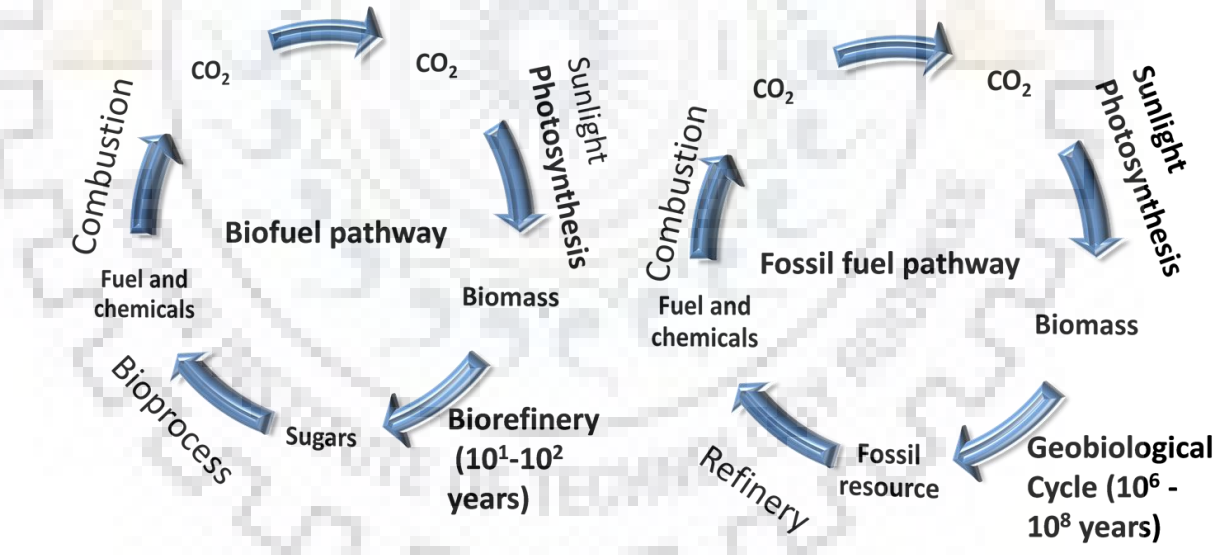

Fig. 2.1 The carbon cycle for fossil fuel formation and biofuel formation showing the difference in time period (adopted from Van Maris et al.) [31].

2.1. Bioethanol feedstocks

The world is exploring new carbohydrate resources for bioethanol production. Mainly following factors are considered for selecting a feedstock for bioethanol. (1) Chemical composition of biomass, (2) availability of biomass, (3) emission of greenhouse gasses, (4) absorption of water and minerals from the soil, (5) its role in the biodiversity and landscape value, (6) cost of the biomass, and (7) productivity [32]

Bioethanol feedstocks can be divided into three categories – (1) First generation feedstocks, (2) Second generation feed stocks, and (3) Third generation feed stocks.

2.1.1. First generation feedstocks

First generation bioethanol feed stocks come from agricultural cereal and sugar crops that are also sources of animal food. In tropical areas, such as India, Brazil and Colombia, mainly sugarcane is used as feedstock to produce bioethanol, while corn dominates in other part of world, like USA, European Union and China. The increasing demand for ethanol and shortage of first generation feedstock are responsible for the rise in the price of ethanol. Further use of many of these feedstocks for bioethanol production opens the debate on food versus fuel. Hence, for sustainable bioethanol production, non-food feedstock should be used. Therefore, there is an immediate need for development of technology, which can produce the ethanol from second generation feedstocks [33].

2.1.2. Second generation feedstocks

The second generation biofuels are produced from non-food crops, such as bioethanol derived from the lignocellulosic materials viz. agricultural residues (corn stover, wheat and barley straws), grasses and wood and biodiesel derived from non-edible oil plant like jatropha, cassava or miscanthus [34]. Agri-processing by products, such as corn fibers, sugarcane bagasse and seed cake, are also considered to be a good feedstock for ethanol production [35, 36] Lignocellulosic biomass is a complex structure consisting primarily of cellulose, hemicellulose and lignin bonded to each other in the plant cell wall. Second generation feedstocks do not compete with the food, hence they are considered as promising renewable feedstocks for ethanol production.

2.1.3. Third generation feedstocks

Algal biofuel is considered as third generation biofuels. Microalgae are capable to produce many fold high oil for biodiesel production than traditional crops on the area basis. Apart from that, microalgae have a very short harvesting cycle compared to conventional crop plants, thus allows multiple or continuous harvests with significantly increased yields [37, 38]. High class agricultural land is not required to grow the algal biomass [39].

2.2. Ethanol from lignocellulosic biomass

The quantity and quality of ethanol produced from lignocellulosic biomass depends on the conversion route. Bioethanol production involves several steps, like pretreatment, hydrolysis, detoxification, fermentation and distillation [40].

2.2.1. Pretreatment

Pretreatment is a crucial step, which exposes cellulose and hemicellulose for the hydrolysis by disrupting the rigid lignin structure to release the sugar compounds [41, 42]. Pretreatment can be done by physical, chemical, physiochemical or biological methods as shown in the Fig. 2.2 [43, 44]. Dilute acid treatment and steam explosion are considered most cost effective methods [45-47]. Pretreatment can be done in a number of ways, like using dilute acid (sulphuric acid or hydrochloric acid), alkali (calcium oxide), liquid ammonia or steam explosion [48-50]. Dilute acid pretreatment is generally considered as most efficient [33]. Cellulose and hemicellulose are sufficiently exposed to breakdown into simple sugars for fermentation. A major drawback of dilute acid treatment is formation of several toxic inhibitors as byproducts. These toxic compounds can be divided into three major groups based on their chemical nature: (i) organic acids (acetic acid, formic acid, and levulinic acid) that originate from the breakdown of hemicellulose, (ii) phenolic compounds (vanillin, syringaldehyde, 4-hydroxybenzaldehyde, coniferyl aldehyde, ferulic acid, and cinnamic acid) as breakdown products of the phenolic polymer lignin, and finally, (iii) furan derivatives, furfural and HMF (5-hydroxy-2-methylfurfural), that are derived from elimination reactions of pentose and hexose sugars, respectively. These inhibitors need to be removed as they inhibit the growth of fermenting microorganism resulting into lesser yield of ethanol.

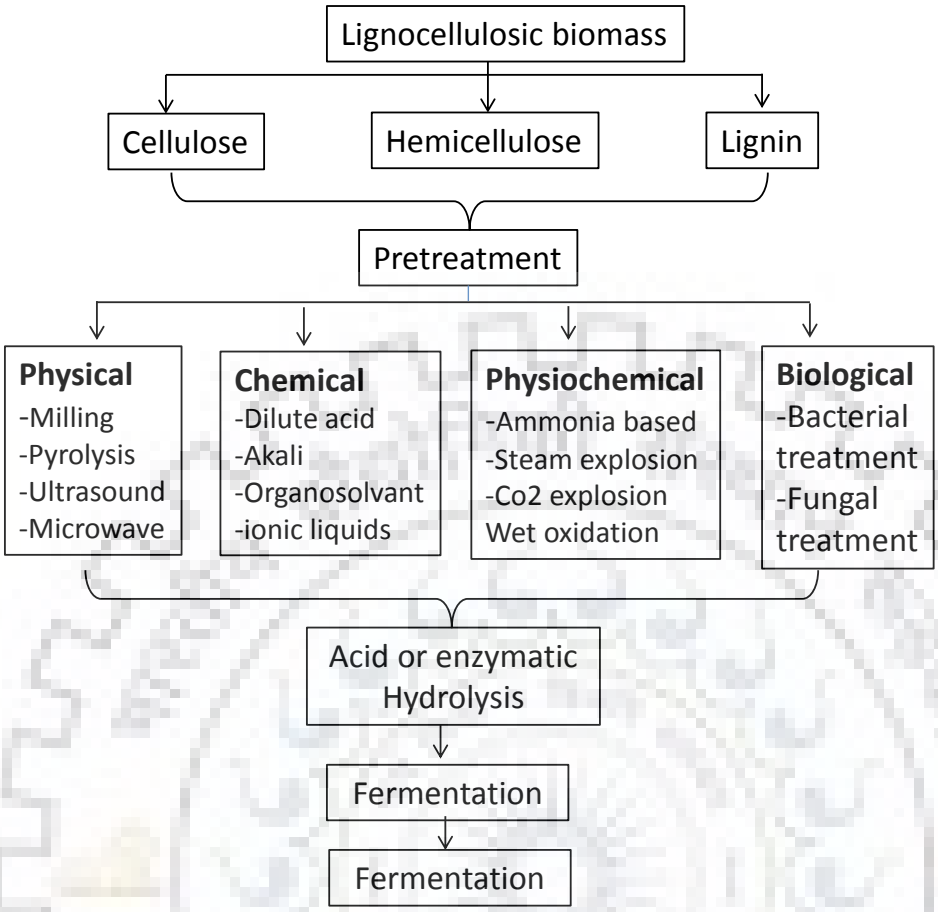

Fig. 2.2 Schematic diagram showing different methods of pretreatment (adopted from Kumar and Sharma) [51].

2.2.1.1. Merits and Demerits of different pretreatment methods

Each method from the available methods gives different outcome, advantage and disadvantage. Table 2.1 provides a comparative detail of advantages and disadvantages of some commonly used pretreatments methods.

Table 2.1comparative detail of advantages and disadvantages of some commonly used pretreatments methods [52]

Pretreatment Method	Effect	advantage	disadvantage
Dilute acid	Hydrolyses of hemicelluloses Renders cellulose more amenable for further enzymatic treatment	Less corrosion problems Low formation of inhibitors Cost effective	Generation of toxic inhibitory products due to high temperature Low sugar concentration
Concentrated acid	Hydrolyses both hemicelluloses and cellulose	High glucose yield moderate operation temperature No enzymes are required	Acid recovery is mandatory Equipment corrosion Generation of inhibitory compounds
Alkali	Removes lignin and hemicelluloses Increases accessible surface area	High digestibility High lignin removal	Long residence times Irrecoverable salts formation
Ionic liquids	Reduces cellulose crystallinity Removes lignin	High digestibility Green solvents	Large-scale application still under investigation
Mechanical method	Reduces cellulose crystallinity	No formation of inhibitors	High power and energy consumption
Organic solv	Hydrolysis of lignin and hemicellulose	Pure lignin recovery High digestibility	High cost Solvents need to be drained and recycled
Ammonia fiber explosion (AFEX)	Increases accessible surface area Removes lignin and hemicelluloses to an extent	Low formation of inhibitors	Not efficient for biomass with high lignin content High cost of large amount of ammonia
Biological pretreatment	Degrades lignin and hemicellulose	Low energy consumption	Low rate of hydrolysis

2.2.2. Inhibitors in lignocellulosic hydrolysate

As described earlier, acid pretreatment of lignocellulosic biomass leads to formation of three different groups of inhibitory compounds – weak organic acids, phenolic compounds and furanic compounds [53]. Each of them is associated with specific toxicity problems for microorganisms. Among all the inhibitors, furfural and HMF are considered as the major ones due to their high concentration and strong inhibition strength to ethanol fermenting strains leading to a marked decrease in overall productivity in fermentation [10, 13]. Furfural and HMF are formed by degradation of pentose and hexose sugars, respectively at high temperatures and low pH as shown in the Fig. 2.3.

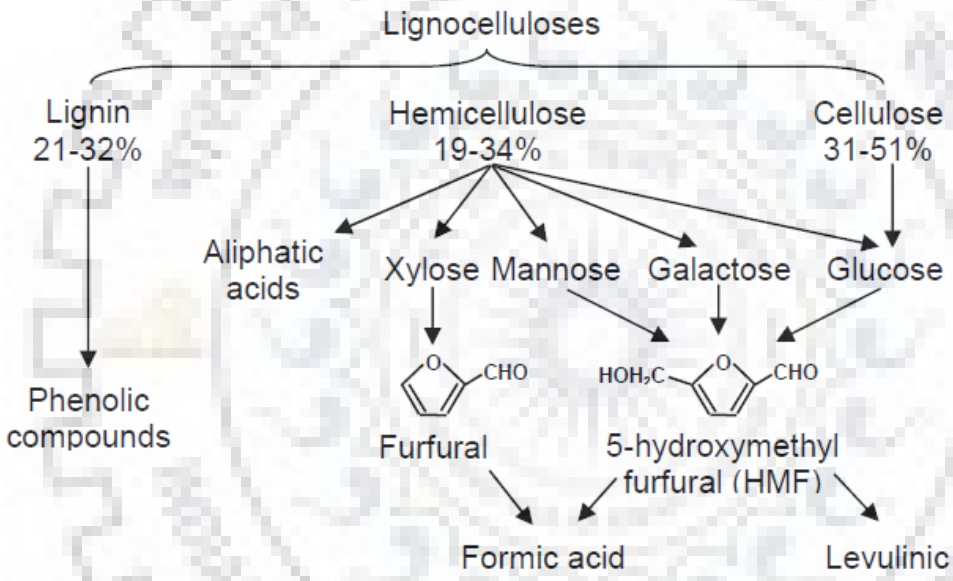

Fig. 2.3 Reactions occur during the acid hydrolysis of lignocellulosic hydrolysate.

2.3. Inhibitory effects of HMF and furfural on fermenting microorganism

The effect of inhibitors on the growth rate of yeast and the fermentation rate is higher for furfural than for HMF, however the effect of HMF lasts longer [6]. Furfural has been shown to inhibit at least three enzymes in the central carbon metabolism in the glycolytic cycle and the tricarboxylic acid cycle [16, 17]. Although furfural and HMF can act synergistically, yeast cells are more sensitive to furfural inhibition than the HMF at the same concentration [6, 18]. It has also been reported that furfural and HMF cause oxidative stress and reduce the activities of various dehydrogenase enzymes in yeast cells [17, 19]. The toxic effect of furfural and HMF on

yeast cells can be attributed to the attenuation of bulk translation activity and the accumulation of cytoplasmic mRNP granules within the cell. A combination of furfural and HMF induced the notable repression of translation initiation and stress granules formation [54]. Possible routes to inhibit the cell growth by HMF and furfural are demonstrated in the Fig. 2.4.

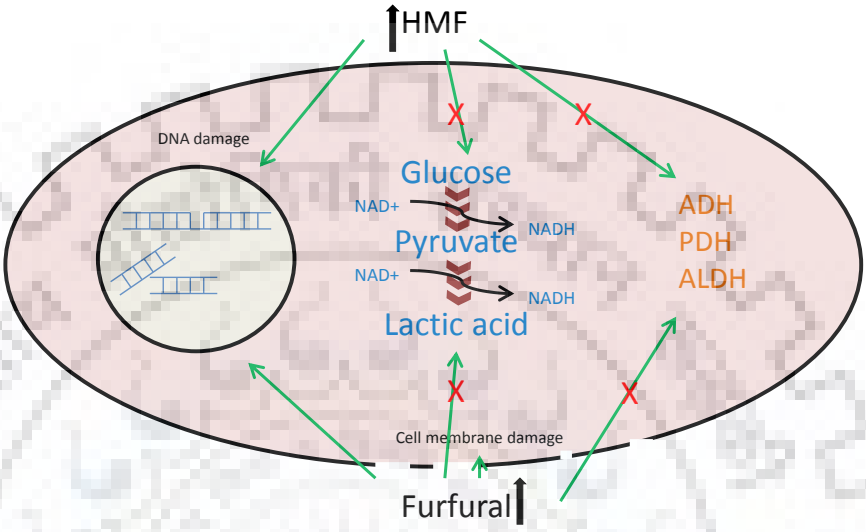

Fig. 2.4 Effect of HMF and furfural on the different metabolic pathways of the cell (adopted from de Oliveira et al.) [55].

2.4. Detoxification of lignocellulosic hydrolysate

Different measures are taken to avoid the toxic effect of inhibitors. The quantity and type of inhibitors formed in the hydrolysate greatly depend upon the feedstock and methods adapted during the pretreatment and hydrolysis [56]. Hence, one way to avoid the problem of inhibitory effect is decreasing the production of inhibitory chemicals by selecting suitable feedstock and by adopting mild conditions for pretreatment and hydrolysis. But these strategies provide poor yield of sugars, which cannot be accepted for bulk production of biofuels.

Another strategy is to design a fermentation process, which can omit the problems associated with the inhibition. Solid state fermentation is one of the examples to avoid inhibition of cellulolytic enzymes by sugars [57, 58]. Another approach is to develop an inhibitor-tolerating fermentation strain [59]. An example is the adapted strain of *Pichia stipits*, which was able to produce more ethanol as compare to the wild strain from the undetoxified hydrolysate [60]. Landaeta et al. [61]achieved 10 % enhanced ethanol volumetric productivity

and 70 % higher growth rate for adapted *Saccharomyces cerevisiae* strain as compare to the parent strain. Furthermore, genetic manipulation can be done to obtain recombinant hyper resistant yeast for increased resistance to fermentation inhibitors by overexpression of enzymes responsible to improved resistance to phenolics [62, 63], furan aldehydes [64], and aliphatic acids [65].

An alternative strategy is to remove the inhibitory chemicals from hydrolysate prior to fermentation, so that the fermenting microorganism is not subjected to inhibition. This strategy is considered to be the most efficient. There are several methods to eliminate the inhibitory chemicals from lignocellulosic hydrolysate liquor, based on physical, chemical or biological methods [20, 66]. Physical and chemical methods involve the removal of inhibitors from lignocellulosic hydrolysate liquor through ether extraction, alkaline precipitation or enzymatic treatment by laccases [20, 21]. Separation of furfural from monosaccharides by nanofiltration was also tried using NF90 and NF270 membranes [22]. Chandel et al. [67] reported 47.1 % removal of furfural from *Saccharum Spontaneum* hydrolysate by over-liming and Zhuang et al. [68] reported 59.76 % removal of furfural from wheat straw hydrolysate by ethyl acetate and over liming. Physiochemical methods involve the addition of chemicals/water, which makes the process economically unfavorable and hazardous. Some methods include water washing, over-liming, ammonia neutralization, ion exchange absorption, solvent extraction and activated charcoal treatment [23, 24]. However, these methods consume huge amount of fresh water and produce a large quantity of waste water, along with notable loss of fermentative sugars [25, 69]. Biological detoxification or bio-abatement depends on microorganisms that specifically remove fermentation inhibitors from the hydrolysate. Microorganisms, *Coniochaeta ligniaria*, *Trichoderma reesei*, *Cupriavidus basilensis*, *Amorphotheca resinae ZN1* and *Ureibacillus thermosphaericus* were reported to degrade the inhibitors from lignocellulosic hydrolysate liquor [70-73]. Comparative study of different methods for detoxification suggests that they differ significantly with respect to effects on hydrolysate chemistry and fermentability [23]. Some detoxification techniques are summarized in the table 2.2.

Table 2.2 Techniques for detoxification of lignocellulose hydrolysate

Technique	Procedure	References
Chemical additives	Alkali [such as $Ca(OH)_2$, NaOH, NH_4OH]	[74]
	Reducing agents [such as dithionite, dithiothreitol, sulfite]	[75]
	Sodium Borohydrite	[76]
	Ferrous sulfate and hydrogen peroxide	[77]
	Polyelectrolyte flocculants	[78]
Enzymatic treatment	Laccase	[79]
	Peroxidase	[79]
	RW-EDI	[80]
Liquid–solid extraction	Activated carbon	[81]
	Ion exchange	[82]
Filtration	NF90 and NF270 membranes	[22]
Microbial treatment	*Coniochaeta ligniaria*	[83]
	Trichoderma reesei	[84]
	Ureibacillus thermosphaericus	[73]
	Amorphotheca resinae ZN1	[72]
	Cupriavidus basilensis	[71]

Each method represents its specificity to eliminate particular inhibitor from the hydrolysate as shown in the table 2.3. It is difficult to compare different methods of detoxification on the basis of their efficiency. Inhibitor concentration and type of inhibitors greatly depends upon feedstock and pretreatment methods.

Table 2.3 Summary of different hydrolysate detoxification methods employed to the variety of lignocellulosic hydrolysate liquors.

Lignocellulosic Hydrolysate	**Detoxification methods**	**Changes in hydrolysate composition**	**References**
Sugarcane bagasse	Neutralization	NA	[85]
Saccharum spontaneum	Over-liming	Removal of furfurals (41.75%), total phenolics (33.21%), no effect on acetic acid content. Reduction of reducing sugars (7.61%)	[86]
Oak wood	Activated charcoal	Removal of phenolics (95.40%)	[87]
Wheat straw	Ion exchange-D 311 + over-liming	Removal of furfurals (90.36%), phenolics (77.44%) and acetic acid (96.29%)	[68]
Wheat straw	Ethyl acetate + Overliming	Removal of furfurals (59.76%), phenolics (48.23%) and acetic acid (92.19%)	[68]
Aspen	Roto-evaporation	Removal of acetic acid (54%), furfural (100%) and vanillin (29%)	[88]
Corn stover	Membrane based organic phases alamine 336	60% acetic acid removal	[89]
Corn stover	*Coniochaeta ligniaria*	80% Removal of furfural and 5-HMF	[83]
Sugarcane bagasse	*Issatchenkia occidentalis* CCTCC M 206097	Reduction of syringaldehyde (66.67%), ferulic acid (73.33%), furfural (62%), and 5-HMF (85%)	[90]

2.5. Immobilization

Immobilization is a process by which a molecule is immobilized to restrict its movement either completely or to a small limited space by attaching it to a solid structure. Immobilization of enzymes, cellular organelles, animal, plant cells and whole cell microorganisms can be conducted [91]. Recently, immobilization of whole cells was conducted to implement them as biocatalysts in environmental pollutions. Immobilization can be done with three physiological states of cells – dead, living and growing states. It is necessary to select the appropriate state depending on the application [92].

2.5.1. Types of Immobilization

There are several methods for immobilization of cells, which include adsorption, covalent binding, entrapment and encapsulation [93] as demonstrated in Fig. 2.5.

Adsorption is a reversible method based on the physical interaction between cells and surface. Immobilization by adsorption is easy, quick and cost effective. Drawback of cell immobilization by adsorption is high cell leakage from matrix due to poor interactions [94].

Covalent binding is based on covalent bond formation between support material and cell with the help of binding agent. This method is mainly deployed for the enzyme immobilization [95].

Entrapment is technique based on fixing of particles or cells within a support matrix by non-covalent interactions. Entrapment is fast, required mild conditions and has limited cell leakage. Drawbacks associated with the entrapment are cost of immobilization, diffusion limitations and low loading capacity [96]. A range of support materials like, chitosan, alginate, collagen, gelatin, polyester and polyacrylic polymers are used for the entrapment of cells [97]. Encapsulation is a technique similar to entrapment, where cells are confined within spherical solid support matrix [98].

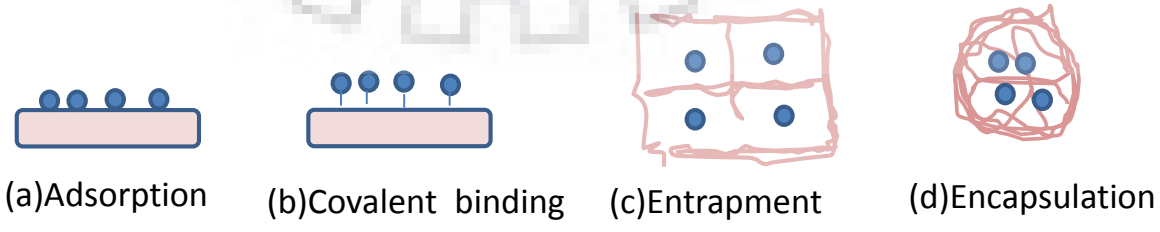

Fig. 2.5 Different methods of cell immobilization (adopted from Bayat et al.) [99].

2.5.2. Immobilization of cells

Use of free cells requires an additional downstream step of separation of cells from the process stream, which makes the process costlier and lengthier. As an alternative, immobilization of microorganisms on inert supports or entrapment inside the beads has been drawing significant attention. These techniques provide several advantages over free cells, such as easy cell recovery, prevention of cell washout, cell recycling in repeated batch operations, and the flexibility of bioreactor designing and the improved operational stability [27]. Bead structure may also provide increased protection to the entrapped microorganisms against the adverse conditions, such as high/low temperature, pH variation and concentrations of toxic chemicals [28]. The major limitation of immobilized cells is substrate/ product diffusional resistance across the bead structure. Microorganism growth and fluid exchange further may disturb or reduce the mechanical strength of the bead [28, 100]. Therefore, the material used for microorganism entrapment must meet the requirements of mechanical and chemical stability, porosity and high microorganism viability as well as low cost.

2.5.3. Advantages of immobilized cells

1. Provide high quantity of cell biomass.
2. Provide cell reuse and reduce the cost of cell recovery and cell recycle.
3. Eliminate cell washout problems at high dilution rates.
5. Provide favorable micro-environmental conditions for the cells.
6. Improve genetic stability of the microorganism.
7. Provide protection against shear damage.
8. Provide resistance to toxic chemicals, variation in pH and temperature, organic solvents and other adverse conditions.

2.5.4. Degradation of different compounds by immobilized system

Immobilized cells are being used in biodegradation of various compounds. Most of the studies of immobilized cells were done for degradation of toxic chemicals for water treatment. Few of the studies are summarized in Table 2.4.

Table 2.4 Showing the degradation of different chemicals by immobilized cells

Compound degraded	Materials	Microorganism	Reference
Cadmium and Zinc	Alginate	*Pseudomonas fluorescens* G7	[101]
2-chloroethanol	Sand	*Pseudomonas putida* US2	[102]
Phenol	Polyvinyl alcohol (PVA)	*Acinetobacter* sp.strain PD12	[103]
Phenol	Agar	*methanogenic consortium*	[104]
Oil wastewater	Calcium alginate	*Yarrowia lipolytica* W29	[105]
2,4,6-trinitrotoluene (TNT)	Alginate	*Arthrobacter* sp.	[106]
Phenol and trichloroethene (TCE)	Chitosan	*Pseudomonas putida*	[107]
Petroleum hydrocarbon	Chitosan	*Bacillus subtilis* LAMI008	[108]
Sulfur dyes	Chitosan	laccase	[109]
Phenol	Sodium tripolyphosphate-crosslinked chitosan	*Pseudomonas putida*	[110]
Acrylamide	Calcium Alginate	*Pseudomonas* sp. and *Xanthomonas maltophilia*	[111]

2.5.5. Chitosan as a base material to immobilize whole cell

Researchers have explored various materials to immobilize whole cells. The selection of material is based on mechanical and chemical stability, porosity and high microorganism viability as well as low cost. Chitosan is a natural nontoxic copolymer of β-1,4-linked D-glucosamine and n-acetyl-D-glucosamine residues derived by the deacetylation of chitin (Fig.

2.6 (a)) [112]. Chitin is the second most plentiful polysaccharide in nature, which is the main component of the shells of crustaceans, the exoskeletons of insects and the cell walls of fungi. The amino groups of the polymer in weak acidic conditions can interact with polyanionic counter ions to form gels, which can be used for efficient entrapment of cells.

Chitosan's unit structure, glucosamine contained hydroxyl and amine groups, which can be used to develop various derivatives by chemical modifications. Chitosan dissolves in the weak acid solutions and repolymerizes in the basic solutions. Mechanical and chemical stability of the chitosan can be improved by crosslinking. Crosslinking may be covalent or ionic. Glutaraldehyde and glyoxal are commonly used for covalent crosslinking. These cross linkers are toxic in nature. To overcome this toxicity problem, natural chemical genipine and low molecular weight anions like citrate, tripolyphosphate (TPP) and sulfate have been used [113]. At low pH, the amine groups of chitosan are protonated and on addition of pentasodium tripolyphosphate solution, they electrostatically interact with the anionic tripolyphosphate to form crosslinked networks, i.e. chitosan – TPP gels as demonstrated in the Fig. 2.6. (b) [113]. TPP-crosslinked chitosan beads can be obtained by dipping chitosan drops into TPP solution [110].

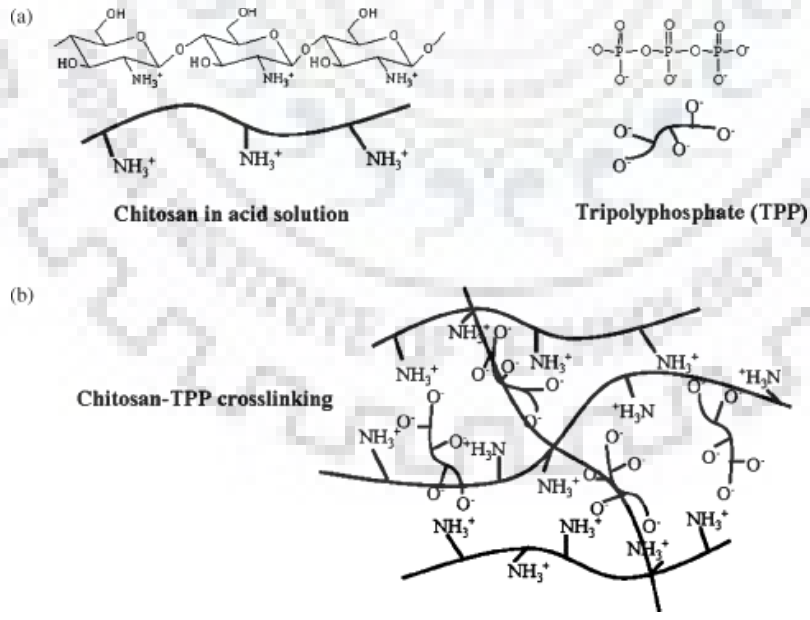

Fig. 2.6 (a) Structure of chitosan molecule at low pH and structure of TPP (b) structure of chitosan-TPP cross-linked matrix (represented from Hsieh et al.) [110].

2.6. Improved ethanol from detoxified lignocellulosic hydrolysate

Previous studies have established that detoxification step eliminates inhibitors and leads to higher fermentation efficiency for improved ethanol production [114]. Zhu et al. [115]reported that detoxification of corn stover hydrolysate by trialkylamine extract improved the ethanol production. They observed maximum 3.79 g/L of ethanol from the undetoxified hydrolysate, while 21.8 g/L of ethanol from the detoxified hydrolysate with the sugar utilization ratio of 93.2 %.

Yu et al. [116] reported high residual glucose in the undetoxified fermentation liquor, which suggested that fermenting microorganism, *S. cerevisiae*, was strongly inhibited by the inhibitors. They observed 3.25 times higher ethanol production in the detoxified hydrolysate as compare to the undetoxified steam exploded corn stover. Chandel et al. [85] observed enhanced ethanol production with different methods of detoxification. E.g. ion exchange detoxified hydrolysate gave maximum ethanol of 8.67 g/L, followed by activated charcoal (7.43 g/L), laccase treatment (6.50 g/L), overliming (5.19 g/L), and neutralized hydrolysate (3.46 g/L).

2.7. Continuous reactor for degradation

Continuous reactor containing immobilized cell biomass for inhibitor degradation offers several benefits over the batch reactor. These include continuous processing of large volume of hydrolysate liquor, which leads to decreased working cost and boosted degradation. The packed bed reactor (PBR) is the most suitable one among the wide range of reactor designs available for continuous operation with immobilized cells. A PBR has various advantages including high-yield process, ease of scaling-up, promising automation of separation process, opportunity to handling large volume of lignocellulosic hydrolysate and reuse of biomass. Successful biodegradation of various toxic materials, such as phenol, by immobilized cells in PBR has been widely reported [117]. There is no report on continuous degradation of HMF and furfural.

Banerjee and Ghoshal [117] reported the biodegradation of phenol by calcium-alginate immobilized *Bacillus cereus* in an upflow PBR. Pazarlioglu and Telefoncu [118] tested the performance of the bioreactor for five runs and it was observed that the degradation rates were not changed for the first four runs. They found that the reactor can tolerate high concentration of phenol (1.25 g/L). Biodegradation of an actual petroleum wastewater was conducted in a

PBR by *Bacillus cereus* immobilized in calcium alginate beads. It was observed that the initial COD of 9200 mg/L, TOC of 4548 mg/L, phenolics of 3561 mg/L, PO_4^{3-} of 121.1 mg/L and NH_4^+ of 121.09 mg/L were reduced to 70 mg/L, 184.97 mg/L, 8 mg/L, 67.3 mg/L and 61.3 mg/L, respectively by biodegradation within the PBR by immobilized cells [119]. Kumar et al. [120] reported that the cells of *Ochrobactrum* sp. DGVK1 entrapped in PVA–alginate matrix tolerated higher concentration of DMF (2.5%, v/v) and effectively removed DMF (N,N-dimethylformamide) from industrial effluents. Cr (VI) was removed using calcium alginate immobilized *Bacillus* sp. in PBR. In this study, theoretically calculated rate constants for different flow rates were analyzed and external mass transfer effect was correlated with a model of the type $J_D = K R_e^{-(1-n)}$ [121]. Biodegradation of chlorpyrifos by *Pseudomonas* sp. in a continuous PBR was studied. This continuous PBR was operated at various flow rates (10-40 ml/h) under the optimum conditions. In the steady state more than 91 % chlorpyrifos removal efficiency was observed up to the inlet load of 300 mg/L/d [122].

CHAPTER 3: OBJECTIVES

Objectives

1. To isolate, characterize and identify the HMF and furfural degrading microorganism from soil.

2. To study the HMF and furfural degradation capability of the isolated microorganism in simulated and actual lignocellulosic hydrolysate liquors.

3. To immobilize the isolated microorganism within chitosan beads and study HMF and furfural degradation from simulated lignocellulosic hydrolysate liquor.

4. To develop a packed bed reactor using immobilized microorganism for detoxification of lignocellulosic hydrolysate liquor.

5. To study the effect of biodetoxification on bioethanol production.

Graphical representation of the objectives

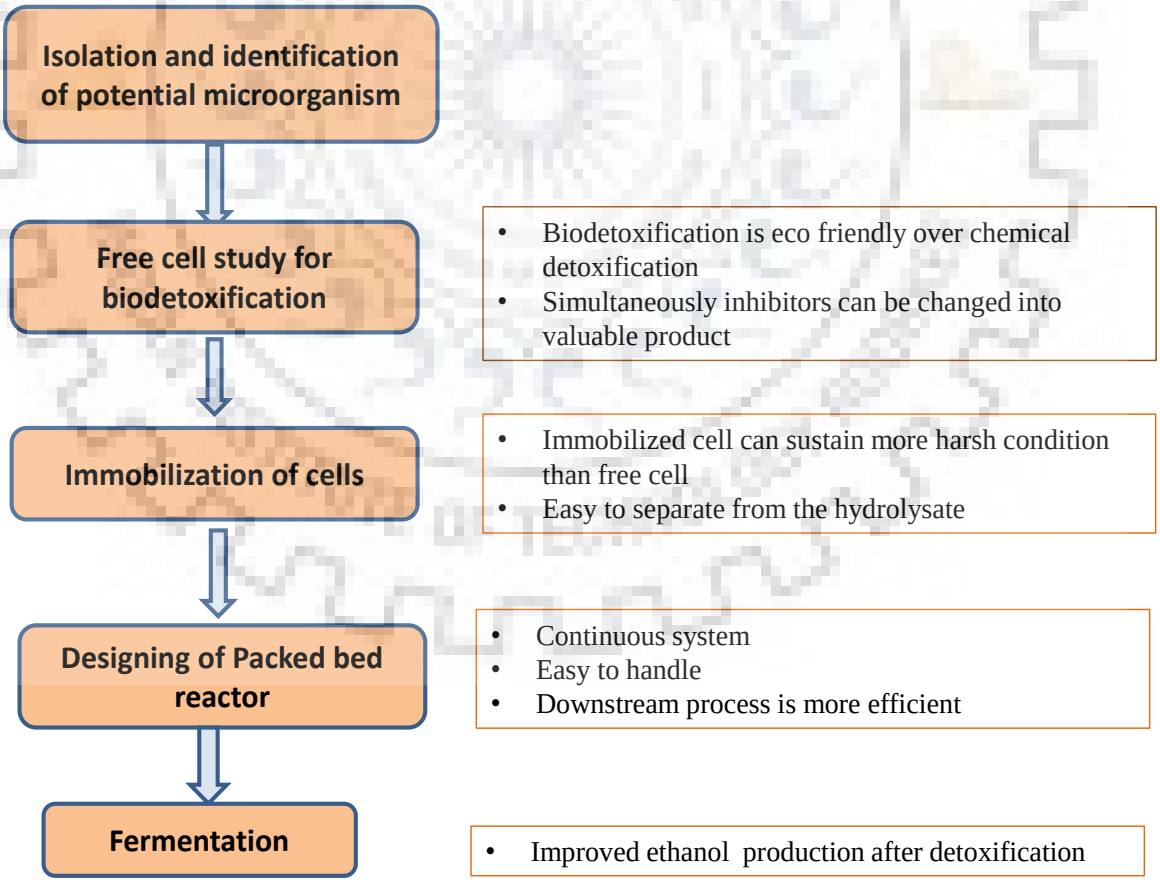

CHAPTER 4: MATERIALS AND METHODS

This chapter contains detailed description of the equipments, materials, experimental methods and analytical procedures used for isolation, identification and characterization of the bacterium isolated from soil. This chapter also includes the experimental methods used to describe the potential of soil isolated bacterium to detoxify the lignocellulosic hydrolysate. Further, this chapter provides the experimental details on cell immobilization and their characterization and application to detoxify the lignocellulosic hydrolysate. Detailed methods to design a packed bed reactor using immobilized cells are also included in this chapter. Finally, this chapter describes the method used to ferment the detoxified and undetoxified hydrolysate liquors for production of bioethanol.

4.1. Materials

4.1.1. Chemicals

Different salts used in media preparation were purchased from Himedia, India. 5-Hydroxy-2-methyl furfural (HMF) was purchased from Matrix Scientific, India. Furfural, 2- Furoic acid and 5-hydroxymethyl-2-furancarboxylic acid (HMF acid) were purchased from Avra chemicals, India. Acetic acid, xylose and glucose were also purchased from Himedia. Kits (KB002 HiAssorted^{Tm} Biochemical test kit, KB009 Hicarbo^{Tm} kit for 36 carbohydrate test and K001 gram staining kit) used for characterization of bacterium were purchased from Himedia, India. Agar powder was purchased from s d fine-chem Limited, India. Chitosan was procured from Sigma-Aldrich, India. Sodium tripolyphosphate (STPP) and furfural were purchased from Sisco Research Laboratories, India.

All other chemicals and solvents used in the project were purchased from HiMedia and Sisco Research Laboratories, India, unless stated otherwise.

4.1.2. Equipments

A temperature controlled incubator-shaker (Daihan-labtech) was used for bacterial cell culture. Centrifuge (Eppendorf, USA) was used to separate the cells from the culture. . Laminar air flow (Clean air, India) was used to maintain the aseptic conditions during inoculation. Optical density of culture was measured using UV-VIS spectrophotometer (Cary 60 UV-VIS, Agilent). Analysis of samples was done using HPLC (Shimadzu,Corp., Kyoto, Japan) equipped with a RI

detector. The column used was Hi-Plex H, 7.7 × 300 mm, 8 μm, (Agilent, Santa Clara, California, United States).

4.2. Analytical procedures

4.2.1. Quantification of the growth of microorganisms

Growth of bacteria and yeast was monitored by measuring the optical density at 600 nm wavelength using UV-VIS spectrophotometer (Agilent, Cary 60 UV-VIS) at required time intervals using the media as a blank. To calculate dry cell weight (dcw gL^{-1}) of the bacterial cells, a standard curve was obtained for dry cell weight vs. optical density of culture at 600 nm wave length. Cultures of different optical density were taken and centrifuged at 10000 rpm to get the pellet. Now these biomass pellets were dried in the vacuum oven at 60 °C till a constant weight was obtained. Then a graph was plotted between biomass (dcw gL^{-1}) and optical density at 600 nm [123].

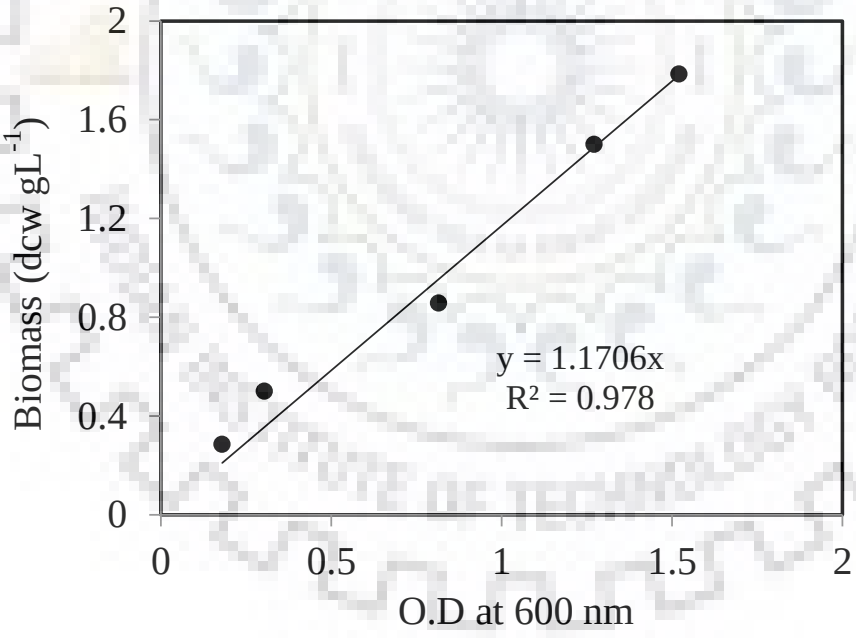

Fig. 4.1 Standard curve for biomass (dcw gL^{-1}) calculation using optical density of cell culture.

4.2.2. Quantification of HMF, furfural, glucose and xylose

HMF, furfural, organic acids, carbohydrates and ethanol were quantified with HPLC (Shimadzu Corp., Kyoto, Japan) equipped with a RI detector. The column used was Hi-Plex H, 7.7 × 300 mm, 8 μm, (Agilent, Santa Clara, California, United States), where 0.005 M H_2SO_4 was used as the mobile phase in isocratic mode with a flow rate of 0.7 ml/min. The mobile phase was prepared using degassed ultrapure type-I water. Degassing of water was done using vacuum pump for 50 min. The oven temperature and pressure were set up at 60 °C and 4.6 MPa, respectively. The sample injection volume in HPLC was 20 μl. All the samples, prior to injection, were filtered with 0.2 μm pore size syringe filter (PALL Life sciences, ValuPrep 25 mm Syringe Filter with PVDF Membrane). Retention times for glucose, xylose, acetic acid, HMF and furfural were observed to be 8.53 min, 9.02 min, 13.5 min, 27.8 min and 42.03 min, respectively at the above mentioned operating conditions.

To quantify the chemicals standard curves were made for each component as represented below.

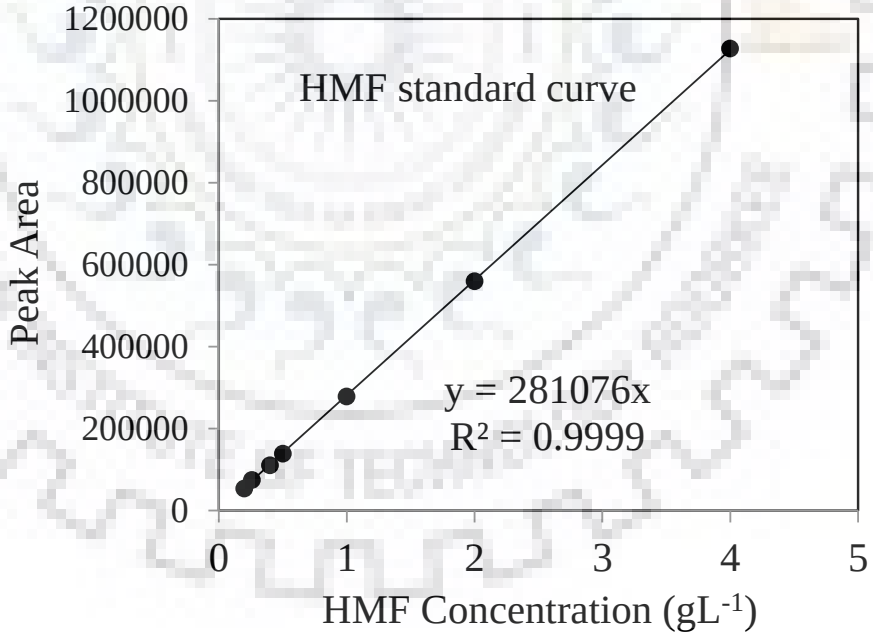

Fig. 4.2 Standard curve for HMF quantification.

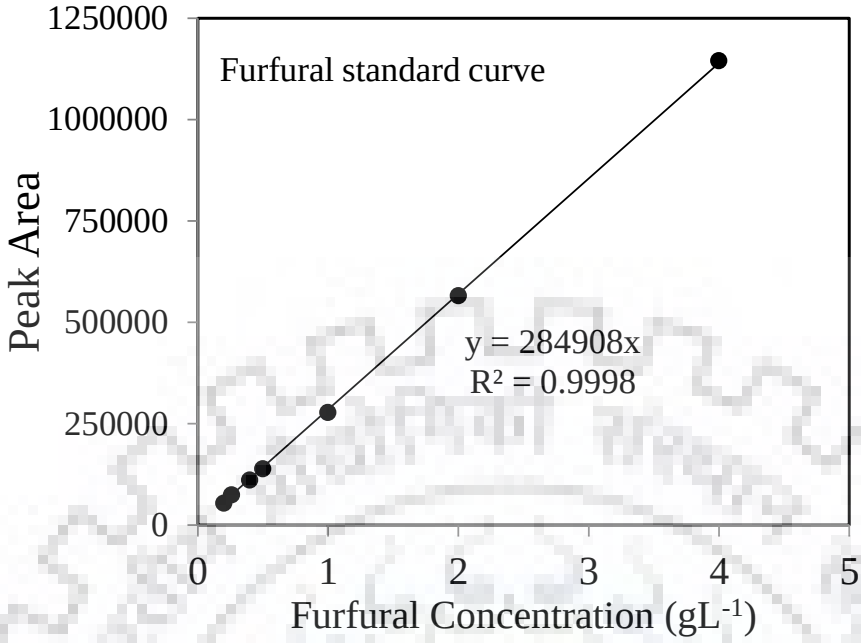

Fig. 4.3 Standard curve for furfural quantification.

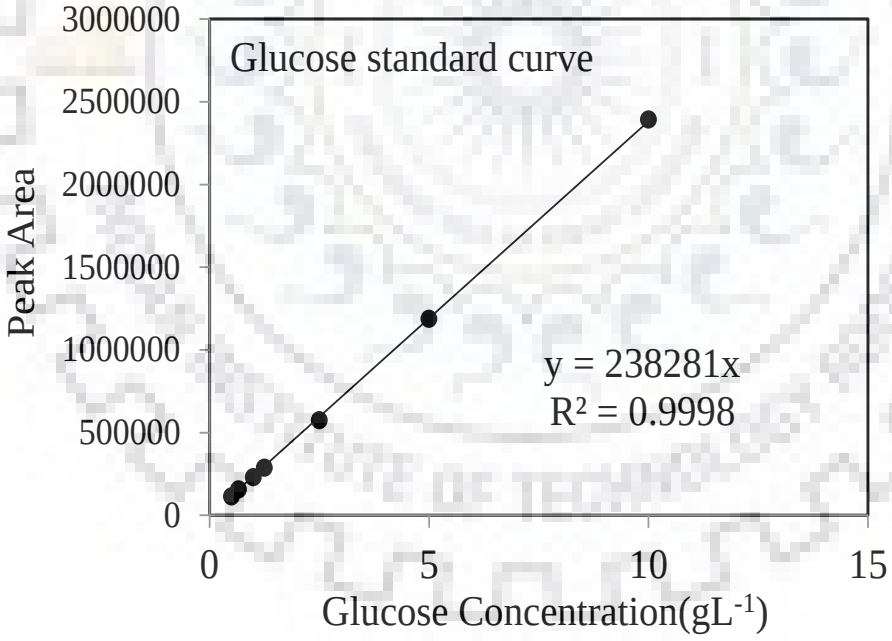

Fig. 4.4 Standard curve for glucose quantification.

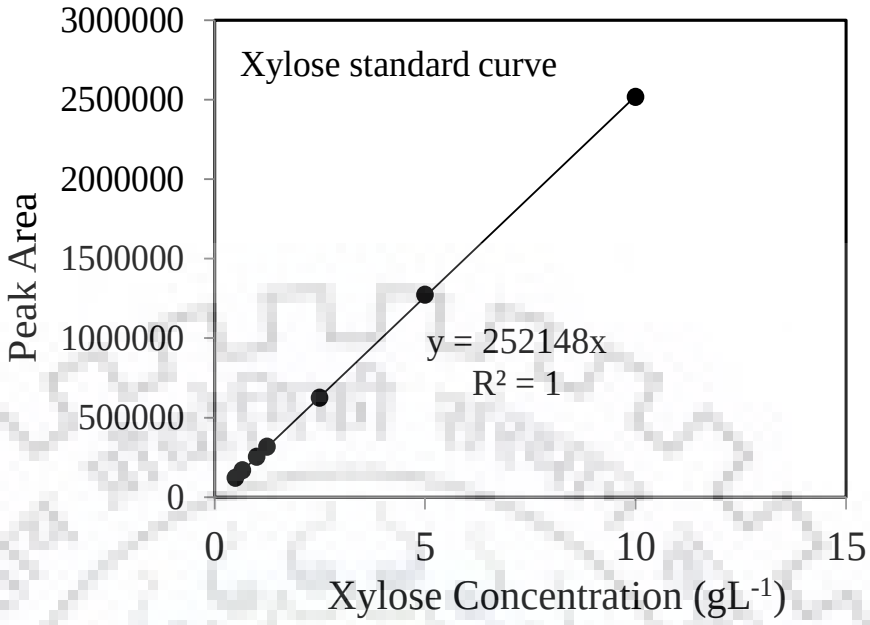

Fig. 4.5 Standard curve for xylose quantification.

4.3. Experimental methods

4.3.1. Strain isolation and culture conditions

Soil samples were collected from three locations in Dehradun, India – Forest Research Institute (FRI) Dehradun, Robber's cave (ROC) Dehradun and Botanical Survey of India (BSI). Dehradun is located at 30.3°N and 78.04°E having Pinus trees in abundant. The rationale of collecting soil samples from these places was the fact that the undisturbed terrain at the foothills of Himalayas is rich in lignocellulosic biomass and could be a potential incubation zone for the inhibitor-resistant microorganism.

A minimal medium (MM) or salt medium was prepared, which consists of salts, such as 1.55 g of K_2HPO_4, 0.85 g of $NaH_2PO_4.2H_20$, 2.0 g of $(NH_4)_2SO_4$, 0.1 g of $MgCl_2.6H_20$, 10 mg of EDTA, 2 mg of $ZnSO_4$ .7H20, 1 mg of $CaCl_2.2H_20$, 5 mg of $FeSO_4.7H_20$, 0.2 mg of $Na_2MoO_4.2H_2O$, 0.2 mg of $CuSO_4.5H_2O$, 0.4 mg of $CoCl_2.6H_2O$, and 1 mg of $MnCI_2.2H_2O$ per liter of demineralized water [124]. Enrich culture was performed in the medium having carbon source in the form of either 10 mM HMF (MMH10) or 10 mM furfural (MMF10) or 10 mM HMF and 10 mM furfural (MMHF10). 1 g of each soil sample was inoculated to the 50 ml MMH10 medium in 250 ml Erlenmeyer flask and was incubated at 30 °C at 200 rpm for 2 days

in a rotary shaking incubator. 1 ml of these culture samples were transferred thrice to fresh medium and incubated until bacterial growth was apparent (OD_{600} > 1). The final enrichment cultures were streaked onto MMH10 medium solidified with 1.5 % (w/v) agar plates. The plates were incubated at 30 °C until colonies appeared. Now the single colonies were streaked on the separate agar plates containing MMH10 medium. A comparative growth study of different isolates was done in MMH10 liquid medium to screen the most suitable bacterial species for removal of the inhibitory compounds from hydrolysate.

4.3.2. Genomic DNA isolation and PCR amplification of 16s ribosomal DNA

Identification of isolated bacterium from MMH10 culture was performed by the partial sequence analysis of the 16s ribosomal DNA gene. Total DNA was extracted manually and the procedure in brief is as follows. Around 1.5 ml culture grown for 48 h in MMH10 culture media was centrifuged at 10000 rpm for 30 sec at room temperature (RT). The cell pellet was dissolved in 400 µl $T_{10}E_1$ buffer (10 mM Tris-Cl pH 8.0, 1 mM EDTA). Cells were then lysed by adding SDS and proteinse K followed by incubation at 37 °C for one h. The final concentration of SDS and proteinase K was 1% (w/v) and 2 mg/ml, respectively. The lysate was then passed through 26 gauge needle for 5-6 times to reduce the viscosity of the solution. Equal volume of phenol and chloroform (1:1) was then added and mixed properly by vortexing. The sample was centrifuged for 10 mins at 10000 rpm at room temperature and the upper aqueous phase was transferred to a new tube. The procedure was repeated one more time with equal volume of phenol : chloroform and another time with equal volume of chloroform. Finally the upper aqueous phase was separated in a new 1.5 ml tube and the DNA was precipitated by adding salt and ethanol followed by washing with 70 % ethanol. The pellet was dried and dissolved in TE buffer. The quality of genomic DNA was checked by resolving in 0.8 % Agarose gel. The quantity of DNA was measured by using Nanodrop Spectrophotometer. To amplify the conserved 16s ribosomal DNA the following primers set were used

27F- AGAGTTTGATCMTGGCTCAG, (M is A or C nucleotide)

1492R- CGGTTACCTTGTTACGACTT (Y is T or C nucleotides)

Around 50 ng genomic DNA was amplified using the above set of primers in 25 µl reaction volume. DNA isolated from *E.coli* (DH5α strain) was used as positive control. The following program was used for PCR amplification: one cycle at 95 °C for 5 min followed by 30 cycles at

94 °C for 30 sec, 55 °C for 30 sec and 72 °C for 60 sec and finally one cycle at 72 °C for 5 min. The PCR product was resolved in 0.8 % Agarose gel, distinct 1.6 kb band was gel purified and send for sequencing (Fig. 4.6).

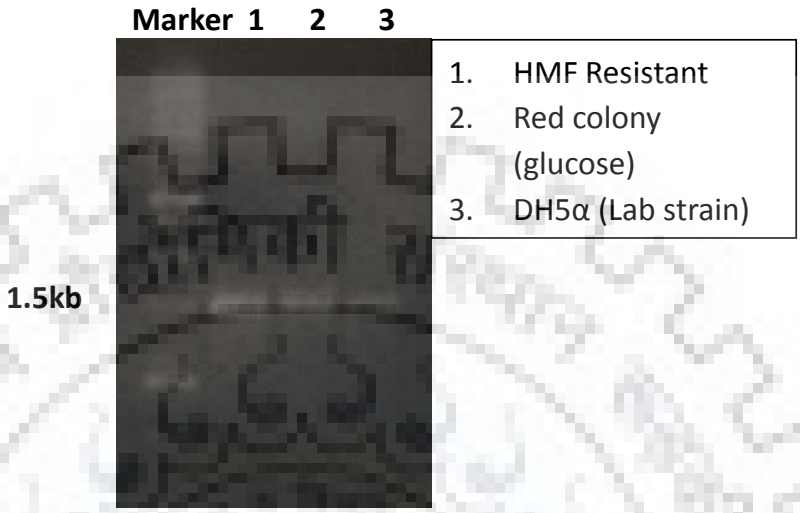

Fig. 4.6 Gel image of 16 S rDNA of isolated strain with control.

4.3.3. Construction of phylogenetic tree

The partial 16s rDNA sequence of the isolated bacteria was deposited to the NCBI with the Accession Number of KY411825.1. The sequence obtained for the 16S rDNA (1432 bp) gene was used for identity searches using the EzTaxon-e server [125] and NCBI BLAST sequence similarity [126] to identify the nearest taxa. CLUSTAL W program of MEGA version 7 [127] was utilized to align all the previously downloaded 16S rDNA sequences of the nearest type strains. The evolutionary distances were computed using the Tajima-Nei method [128]. A phylogenetic tree was constructed using the neighbour-joining tree-making algorithm in MEGA version 7.0. The stability of phylogenetic tree was assessed based on 1000 replicates. The reliability of the clustering results was assessed by bootstrap analysis [129].

4.3.4. Phenotypic and biochemical characteristics

Morphological features of the strain were observed under a Field Emission-Scanning Electron Microscope (FE-SEM) (FE-SEM QUANTA 200 FEG from FEI Neitherlands). Gram-staining was performed by using a Gram Stain Kit (K001; HiMedia) according to the manufacturer's instructions. HiCarbohydrate^{TM} Kit (KB009; HiMedia) was employed to determine the ability

of the strain to utilize various sugars as carbon source. Citrate utilization, lysine utilization, orinithine utilization, urease test, phenylalanine deamination, nitrate reduction and H_2S production were analyzed with the HiAssorted^{TM} Biochemical Test Kit (KB002; Himedia). Motility was determined by stabbing 2 cm into the center of the medium (SIM, Motility medium modified; Himedia) in a test tube. Indole test was performed by adding 2-3 drops of Kovac Reagent after bacterial growth in SIM medium. Oxidase activity was tested by using oxidase disc (Himedia, India). Growth at pH 5.0–10.0 was evaluated in MMH10 broth at 35°C. The pH of the medium was maintained using three buffers (final concentration of 50 mM): acetate buffer (for pH 4.0–5.5); phosphate buffer (for pH 6.0–8.0); and Tris buffer (for pH 8.5–10.0). Growth at 10, 25, 30, 37, and 42°C was assessed on MMH10 agar.

4.3.5. Cellular Fatty acids analysis

The fatty acids of strain were analyzed using the cells grown in MMH10 agar for 2 days at 35 °C. The cellular fatty acids were saponified, methylated and extracted according to Sherlock Microbial Identification System (MIDI) protocol. Fatty acid methyl esters were then analyzed by Gas Chromatography and Microbial Identification Software (Sherlock TSBA, version 6.0) [130].

4.3.6. G+C content of genomic DNA

The G+C content was determined by thermal denaturation method [131]. Briefly, the temperature of the genomic DNA (25 µg/ml) in buffer (0.15 M NaCl with 0.015 M sodium citrate) was increased slowly (0.5 °C/min) from 25 °C and the absorbance of the solution was monitored continuously at 260 nm against a blank sample containing buffer only. The T_m of the DNA is defined as the temperature at which 50 % DNA is double stranded and 50% DNA is single stranded. The G+C content of the genomic DNA was calculated by the following equation: percent (G+C) = $2.44T_m$ -169 [132].

4.3.7. Effect of HMF concentration and temperature on the growth isolated strain

To investigate the HMF tolerance level of the selected bacterial species, bacterium was inoculated in the HMF enriched media containing HMF concentrations of 3 mM, 6 mM, 9 mM, 12 mM, 15 mM, 18 mM, 21 mM and 24 mM. 50 ml of each medium was taken in the Erlenmeyer flask of 250 ml and inoculated with 1 ml of seed culture in the aseptic conditions in

the laminar autoflow. After inoculation, culture was incubated at 30 °C and 150 rpm in the shaking incubator for 48 h of incubation period. Bacterial growth was measured at every 4 h time interval by measuring optical density at 600 nm wavelength and a growth curve was plotted to compare the growth at different concentration of HMF. To analyze the suitable temperature for the growth of isolate, culture was grown at 20 °C, 25 °C, 35 °C and 40 °C in medium MMH10 at 150 rpm within the shaking incubator. Growth was measured at every 4 h time interval.

4.3.8. Degradation of HMF and furfural from MMH10 and MMF10 media

HMF and furfural degradation time courses were established by culturing the selected bacterial species in MMH10 and MMF10 media separately. Synergic effect of inhibitors was observed by culturing the species in the MMH10F10 medium.

4.3.9. Degradation of HMF and furfural from GXH10, GXF10 and GXHF10 simulated hydrolysate

To check the substrate priority of the isolated bacteria, simulated hydrolysates of different compositions were prepared. Salt medium (as described in Section 4.3.1) enriched with 10 mM each of xylose, glucose and HMF (GXH10), salt medium enriched with 10 mM each of glucose, xylose and furfural (GXF10) and salt medium enriched with 10 mM of each glucose, xylose, furfural and HMF (GXHF10) were used to check the substrate priority of the bacterium. To conduct the experiment, 50 ml of each medium was taken in conical flask, inoculated with 1 ml of seed culture (O.D~0.6) in aseptic conditions and incubated at 30 °C and 200 rpm in shaker incubator. 1 ml of sample was collected at each 4 h of time interval for 48 h. All the samples were collected under aseptic conditions inside a laminar air flow hood. The collected samples were centrifuged at 10000 rpm for 10 min followed by membrane filtration with 0.2 µm syringe filter prior to the analysis with HPLC.

4.3.10. Degradation of inhibitory compounds present in sugarcane bagasse hydrolysate liquor

Locally collected sugarcane bagasse was dried overnight in a vacuum oven at 60 °C. Bagasse was milled to achieve particle size range between 5 to 10 mm. 100 gL^{-1} of bagasse was loaded with 1.25 % H_2SO_4 w/w and pretreated in an autoclave at 121 °C with residence time of 2 h

[133]. The liquid fraction was separated by centrifugation at 10000 rpm for 10 min followed by membrane filtration. pH of hydrolysate liquor was maintained at 7 using 5 N NaOH. This neutralized hydrolysate liquor was supplemented with necessary salts as described earlier in the minimal media preparation and sterilized with 0.2 µm pore size membrane. Glucose, xylose, acetic acid, HMF and furfural were analyzed using HPLC. 50 ml of hydrolysate was taken in 250 ml Erlenmeyer flasks. This hydrolysate was inoculated with 1 ml seed culture, which was prepared in MMH10 medium by culturing the selected bacterium for 20 h and incubated in a shaking incubator at 30 °C and 150 rpm shaking speed. Samples were analyzed at every 4 h intervals.

4.3.11. Preparation of bacterial cell-immobilized chitosan beads

1 g of chitosan was dissolved in 50 ml of 0.6 % acetic acid solution to make 2 wt% chitosan solution. To prepare a homogenous solution, it was mixed on the magnetic stirrer for 2 h and kept overnight. Then, the biomass pellet (equivalent to 10 mg dry cell weight (dcw)) was suspended in 1 ml of autoclaved water and mixed with 50 ml 2 wt% chitosan solution on a magnetic stirrer. This mixture, under ice bath, was added into 2 wt% sodium tripolyphosphate (STPP) solution in drop wise manner using a 10 ml syringe to obtain gel beads of approximately 2 mm diameter. A constant distance between the solution surface and the syringe tip was maintained to obtain uniform size of the beads. The beads were allowed to cure in the same STPP solution for 30 min. Then, the beads were washed with 100 ml of 0.15 M K_2HPO_4 solution thrice. The collected washing solutions were analyzed by viable cell count method. The cell count was very low or nearly undetectable in the washing solution. The entire procedure was carried out under aseptic conditions in a laminar air flow hood. The cell-entrapped beads were stored in sterile water at 4 °C temperature.

4.3.12. Characterization of chitosan beads

4.3.12.1. SEM images of immobilized cells

Extra water of the beads was absorbed with tissue paper. Then, cross sections of the beads were obtained using a sharp knife. The sections were left for air drying for 6-8 h. The bead samples were then coated with gold and attached onto the microscope supports with sliver tape. SEM images were taken at10 kV using a Field Emission Scanning Electron Microscope.

4.3.12.2. Water uptake ratio

The swelling ability of the cell-immobilized chitosan beads was determined by measuring the water uptake ratio on the basis of the weight of the beads right after immobilizing the cells. A known weight of the cell-immobilized chitosan beads was taken right after formation, surface water was removed by tissue paper, and then, it was placed in phosphate buffer at 30 °C with shaking. The swollen beads were separated by filtration, surface water was removed by tissue paper, and then, the beads were weighed immediately using an electronic balance. Water uptake was determined as a function of pH using phosphate buffers of pH 6, 7, 8 and 9. The water uptake ratio of the immobilized beads was then calculated as given below.

$W_u = [(W_w - W_{w0})/W_{w0}]$

Where, W_u is the water uptake ratio of the cell-immobilized chitosan beads, W_w is the final weight of the cell-immobilized chitosan beads and W_{w0} is the initial weight of the cell-immobilized chitosan beads right after formation. Hence, $W_w - W_{w0}$ is the water uptake of the cell-immobilized beads.

4.3.12.3. FTIR analysis

Fourier transform infrared (FTIR) spectroscopy was conducted for empty beads, fresh immobilized beads and used immobilized beads after detoxification by an infrared spectroscope (Thermo Nicolet Nexus FT-IR). Samples for FTIR analysis were prepared by mixing 1 % (w/w) of dry bead with 100 mg of KBr powder and pressing into a sheer slice [134].

4.3.13. Optimization of cell biomass loading within the chitosan beads

Various amounts of bacterial cells were entrapped within chitosan beads and used for biological detoxification of simulated lignocellulosic hydrolysate. The major sugar components of actual lignocellulosic hydrolysate are xylose and glucose and major inhibitors are HMF and furfural. Considering this, simulated hydrolysate liquor was prepared with 16 gL^{-1} xylose, 8 gL^{-1} glucose, 1.25 gL^{-1} HMF and 0.5 gL^{-1} furfural. This simulated hydrolysate was supplemented with the salts of minimal medium as described in Section 2.2. Dry cell weight (dcw) of bacterial cells was estimated by following the procedure described by Rai et al. [135]. Bacterial culture was centrifuged at 10,000 rpm for 10 min and the harvested biomass was dried under vacuum at 60 °C till a constant weight was attained. Dry cell weight was estimated

gravimetrically. To measure biomass directly, a standard calibration curve between OD_{600} and biomass concentration (dcw/ml) was prepared.

A range of 2.5 mg dcw to 20 mg dcw biomass was loaded per 50 ml of 2 wt% chitosan solution and the beads were prepared as described in section 2.3. The beads prepared from 50 ml chitosan solution were equally distributed and inoculated in two beakers with each containing 100 ml of sterile simulated hydrolysate. Then, they were incubated at 35 °C and 150 rpm in a shaker incubator for 28 h. 1 ml of sample was collected at each 8 h of time interval in the laminar air flow hood to avoid contamination. The samples were filtered with 0.22 µm pore size membrane and stored at 4 °C for analysis.

4.3.14. Study of effect of pH and temperature on HMF and furfural degradation

The effect of pH on HMF and furfural degradation was investigated by conducting cell culture at various initial pH of 6, 7, 8 and 9. pH of simulated hydrolysate was adjusted with 5 M NaOH and HCL. A comparative study for free cells and immobilized cells was done. For temperature optimization, immobilized cells were inoculated in the simulated hydrolysate and incubated at the temperatures of 25 °C, 30 °C, 35 °C, 40 °C and 45 °C in a shaker incubator at 150 rpm. Beads used in this experiment were prepared with 10 mg biomass/50 ml of 2 % chitosan solution. Experiments were conducted for 48 h of incubation period and 1 ml of sample was collected at every 4 h time interval in sterile conditions.

4.3.15. Effect of HMF concentration on the immobilized biomass

The effect of inhibitor concentration on the degradation capability was examined by growing the immobilized cells in variable concentration of HMF (5 mM, 10 mM, 15 mM, 20 mM and 25 mM) present in simulated hydrolysate.

4.3.16. Reusability of the cell-immobilized chitosan beads

Reusability of the cell-immobilized beads was examined for seven successive cycles of detoxification. Beads were incubated in simulated hydrolysate for 20 h for each cycle. After each cycle, beads were filtered, washed with water and transferred to fresh simulated hydrolysate. This procedure was repeated for 7 times.

4.3.17. Design of a packed bed reactor

Degradation of fermentation inhibitors was studied in a packed bed reactor with flow of biomass hydrolysate liquor. A schematic diagram of the experimental set-up is demonstrated in Fig. 4.7. A cylindrical acrylamide column (inner diameter 4.4 cm, outer diameter 4.5 cm and height 70 cm) was taken and packed with cell-immobilized chitosan beads. A porous fiber plate was inserted at the bottom of the column to provide support to the beads. An adjustable porous fiber plate was installed at the top of the column and was moved up and down to obtain the required bed height. This column was having two openings both at the bottom and the top. The openings at the bottom were used as inlets for feed and air and the openings at the top were used as outlets for detoxified hydrolysate liquor and air. To control the temperature inside the column, it was surrounded by a cylindrical jacket (outer diameter - 6 cm). Water was circulated through the jacket with the help of a pump to maintain the desired temperature. For different set of experiments, the reactor was packed with immobilized cells to a height of 25 cm, 37.5 cm and 50 cm. Aeration was maintained at a constant rate throughout the column, so that the culture medium was well mixed.

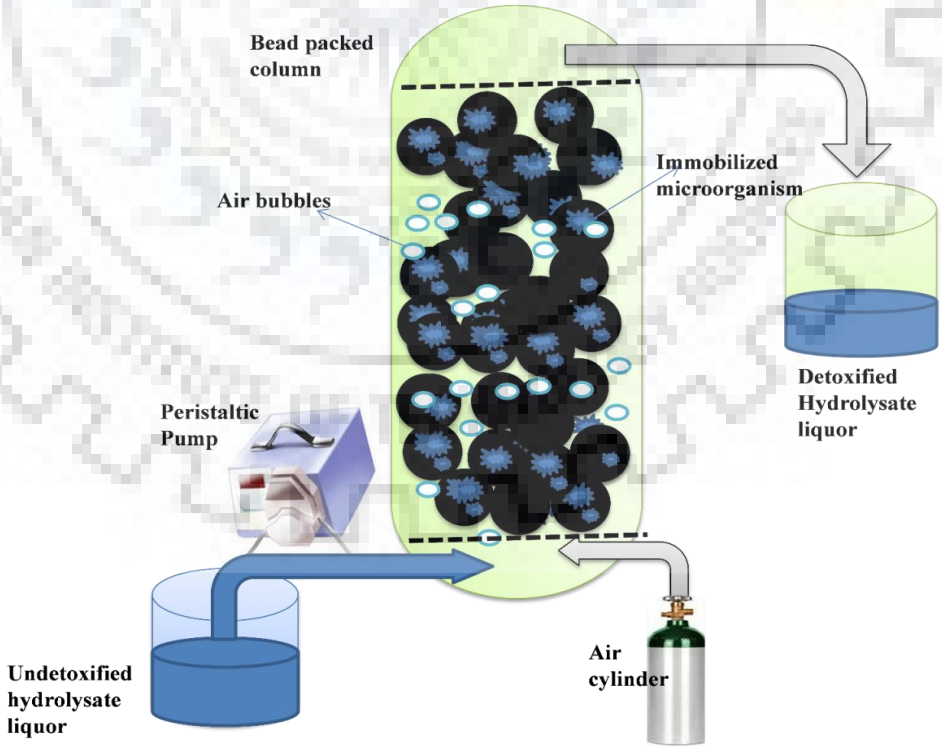

Fig. 4.7 A schematic diagram of the experimental set-up.

The influent lignocellulosic hydrolysate, containing the fermentation inhibitors, were fed into the reactor from bottom side using a peristaltic pump at a flow rate of 4 ml/min. Samples were collected from the outlet at the top at every 30 min h interval to analyze the inhibitor removal efficiency. Inlet and outlet ports were closed by silicon tubing with pinch cork to avoid contamination.

To observe the effect of flow rate on the detoxification capability of PBR flow rate was varied from 2 to 5 ml/min at fixed bed height of 37.5 cm.

Continuous removal of fermentation inhibitors from lignocellulosic hydrolysate in the packed bed reactor was studied as a function of packed bed height and flow rate. The performance of a packed bed column is usually described by the characteristic breakthrough curve. The shape of breakthrough curve and the time required for breakthrough appearance are important factors in designing and operation of the packed bed column [136]. Generally, breakthrough curve is described in terms of degraded inhibitor concentration ($C_d = C_0 - C$) or the ratio of the inhibitor concentration in the effluent (exit stream) to that in the feed (C/C_0) as a function of time or volume of effluent (V_{eff}) [137]. Where, C_d is the degraded inhibitor concentration from the effluent, C_0 is the inhibitor concentration in the feed and C is the inhibitor concentration in the effluent at any time (t). Total volume of the effluent can be calculated from Eq. (1).

$$V_{eff} = Qt_{total} \quad (1)$$

where, Q is the volumetric flow rate of the feed solution and t_{total} is the total flow time. The total degraded quantity of inhibitor (q_{total}) at a given inhibitor concentration and flow rate can be calculated from Eq. (2).

$$q_{total} = QA = Q\int_{t=0}^{t=t_{total}} C_d dt \quad (2)$$

Where, A is the area under the curve on X-axis of the C_d vs. time plot.

Total amount of inhibitor passed through the column (m_{total}) can be calculated from Eq. (3).

$$m_{total} = (C_0 Qt_{total}) \quad (3)$$

Total inhibitor removal percentage (% removal) can be calculated from Eq. (4).

$$\% \text{ removal} = (q_{total}/m_{total}) \times 100 \quad (4)$$

Void fraction of the column (E) was calculated by filling the water in the column up to the bed height then water was withdrawn gently from the bottom. Ratio of volume of water eluted out from the column (W) and total volume of effective column (W_h) gave the void fraction.

$$E = W/W_h \quad (5)$$

where, W_h can be calculated from Eq. (6)

$$W_h = \pi r^2 h \quad (6)$$

r is the internal radius of the column and h is the effective bed height

4.3.18. Fermentation of detoxified and undetoxified hydrolysates

Pichia stipitis NCIM 3498, obtained from the National Collection of Industrial Microorganisms, NCL, Pune, India, was used to ferment the detoxified and undetoxified hydrolysate liquors. The yeast was grown in sterilized MGYP broth containing 30 gL^{-1} yeast extract, 50 gL^{-1} peptone, 10 gL^{-1} glucose, and 30 gL^{-1} malt extract. When the culture reached to log phase, the cells were inoculated (1 %) into the hydrolysate liquor. Fermentation was carried out in a 250 ml flask containing 100 ml of hydrolysate liquor supplemented with 30 gL^{-1} of yeast extract. Then, it was allowed to incubate in shaker incubator at 150 rpm and 30 °C for 48 h. Sterilization of hydrolysate was done by autoclaving at 15 psi pressure and 120 °C for 15 min or by membrane filtration. Fermentation broth was analyzed at every 8 h by collecting 1 ml sample in aseptic conditions.

CHAPTER 5: RESULTS AND DISCUSSION

This chapter includes the results and discussion pertaining to all the experiments conducted during the dissertation research. The Chapter is divided into five sections based on the objectives of the proposed research plan. Section 5.1 deals with screening, isolation, identification and characterization of the inhibitor degrading bacterium, *Bordetella* sp. BTIITR. Section 5.2 consists of the analysis of degradation capability of *Bordetella* sp. BTIITR in both simulated and actual lignocellulosic hydrolysate liquors. Section 5.3 includes immobilization of the bacterium within chitosan beads and their ability to detoxify lignocellulosic hydrolysate liquor. Section 5.4 describes the design of a packed bed reactor and its application for the detoxification of lignocellulosic hydrolysate liquor. Section 5.5 represents a comparative study of bioethanol production from the detoxified and the undetoxified lignocellulosic hydrolysate liquors.

5.1. Isolation, identification and characterization of the microorganism capable of detoxifying lignocellulosic biomass hydrolysate liquor

This Section describes screening and isolation of a bacterium from soil, which demonstrated the capability to survive with HMF as the sole carbon source. Further, identification and characterization of the bacterium using various biochemical tests are thoroughly discussed.

5.1.1. Strain isolation and screening

In search of microorganism, which can utilize fermentation inhibitory compounds, such as HMF as the sole carbon source, we collected 6 soil samples from different locations of Dehradun, India The samples were designated as FRI I, FRI II, FRI III, BSI, ROC I, and ROCII. Since HMF is one of the major inhibitory compounds in lignocellulosic biomass hydrolysate liquor [11], HMF-enriched minimal medium (MMH10) was used for screening and isolation of bacteria capable of degrading the inhibitory compounds. After incubation of 48 h in MMH10 medium, no turbidity was observed in the cultures of ROC II and BSI I, indicating the inability of the microorganisms present in these soil samples to survive in HMF-enriched medium. Hence, they were not considered for further study. From the remaining four cultures, 1 ml from each was transferred to fresh MMH10 liquid medium. This process was repeated thrice. Then, the final enriched cultures were streaked onto MMH10 medium solidified with 1.5

% (w/v) agar plates to isolate individual bacterium having the potential to degrade HMF. After three or four trials of streaking on agar plates, we were able to obtain prominent single colonies from all of the four (FRI I, FRI II, FRI III and ROC I) plate cultures. Only single large colony was taken from each sample for further evaluation. For screening the most suitable bacterium for HMF biodetoxification, a comparative growth study was conducted. All the four samples were inoculated in medium MMH10 in the previously described culture conditions. The results of the observed growth is demonstrated in Fig. 5.1, which depicts significantly better growth for FRI I sample compare to the other three samples. This suggested that the microorganism isolated from FRI I sample was a better candidate for removal of HMF than the other three soil samples. Hence, microorganism isolated from FRI I sample was selected for further study.

E. coli BL21 was also plated in the MMH10 and MMH10G10 medium containing 1.5 % agar as solidifying agent. In both the cases no colony was observed in the petri plate as shown in the Fig. 5.2 (c). This experiment revealed that *E. coli* BL21 cannot metabolize HMF as a carbon source. *E. coli* was also unable to metabolize glucose in presence of HMF. This suggested that HMF worked as a glycolysis inhibitor and *E. coli* did not possess the enzymes, which can covert the toxic HMF into nontoxic compounds. However, the isolated microorganism from FRI I sample was able to grow in both the media, suggesting the presence of the enzymes in the microorganism, which can convert toxic HMF into nontoxic compounds, thereby aiding the metabolism of HMF.

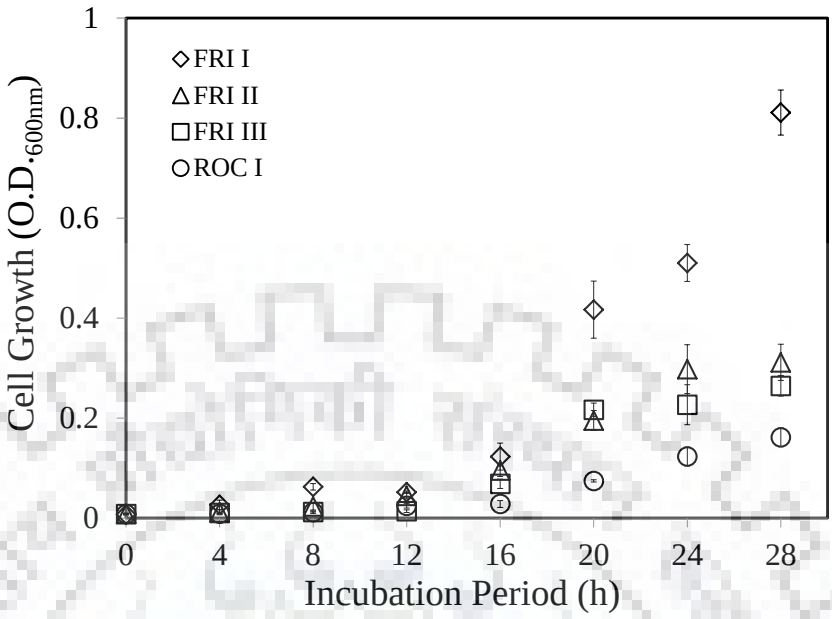

Fig. 5.1 Comparative cell growth of FRI I, FRI II, FRI III and ROC I samples in minimal medium enriched with 10 mM HMF. O.D. represents optical density. The error bar represents the standard deviation, where n=3.

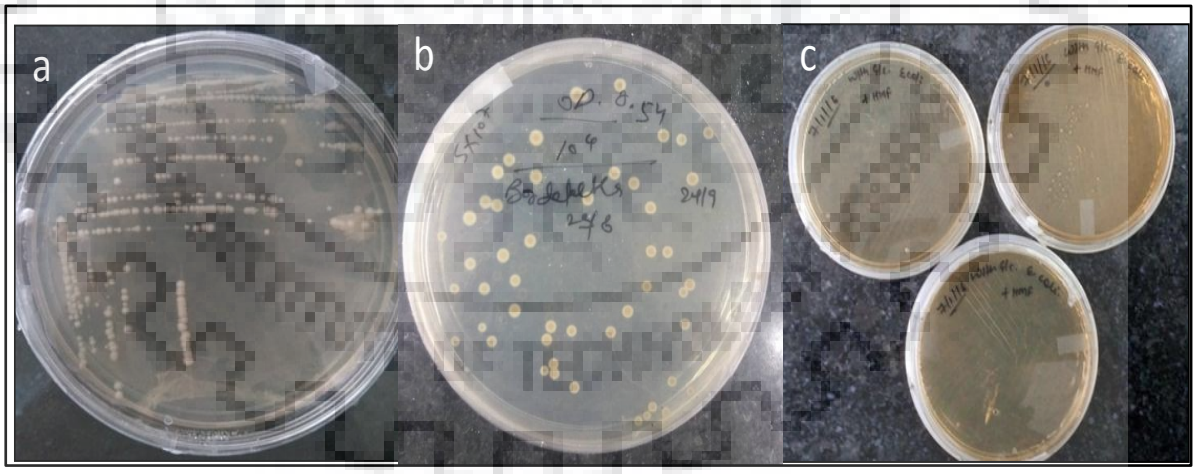

Fig. 5.2 (a and b) Colonies of the soil isolated HMF degrading bacteria in presence of 10 mM HMF as a sole carbon source (c) No colony was observed for *E. coli* (control) in presence of 10 mM HMF

5.1.2. Identification of the isolated strain

In order to identify the isolated bacterial species from FRI I soil sample, we have amplified the conserved 16s rDNA region using universal primers set (details are in Materials and Methods Section). *E. coli* laboratory strain was used as a control. Partial sequencing followed by alignment of the sequences with the bacterial database available in NCBI (National Center for Biotechnology Information) showed that the positive control and the isolated bacterium matched with *Bordetella* species (strain PDD9 with accession # JQ394931.1) and *E. coli* (strain 44A with accession # KP789331.1), respectively (Fig. 5.3 and Fig. 5.4). The 16s rDNA sequence of the isolated bacterium did not completely match with any reported species of genus *Bordetella* available in the NCBI database. So, to identify the isolated bacterium up to the level of species, several other characterization studies of the cells were conducted.The partial rDNA sequence of the isolated bacterium was deposited to the NCBI GenBank with a nomenclature of *Bordetella* sp. BTIITR and an accession number of KY411825.1.

Description	Max score	Total score	Query cover	E value	Ident	Accession
Bordetella sp. PDD-9 16S ribosomal RNA gene, partial sequence	1168	1168	99%	0.0	100%	JQ394931.1
Bordetella sp. T6713-1-3b gene for 16S ribosomal RNA, partial sequence	1162	1162	99%	0.0	99%	LC053656.1
Bordetella sp. T6220-3-2b gene for 16S ribosomal RNA, partial sequence	1162	1162	99%	0.0	99%	LC053647.1
Bordetella petrii strain BjF2 16S ribosomal RNA gene, partial sequence	1162	1162	99%	0.0	99%	KP259605.1
Bordetella sp. PDD-10 16S ribosomal RNA gene, partial sequence	1162	1162	99%	0.0	99%	JQ394933.1
Bordetella sp. R-8 16S ribosomal RNA gene, partial sequence	1151	1151	98%	0.0	99%	JX130378.1
Bordetella sp. B4 16S ribosomal RNA gene, partial sequence	1151	1151	99%	0.0	99%	EU140499.1
Uncultured bacterium partial 16S rRNA gene, clone SICC952_N11D2_16S_B	1146	1146	99%	0.0	99%	LN562261.1
Uncultured bacterium partial 16S rRNA gene, clone SINW1324_N11D0_16S_B	1146	1146	99%	0.0	99%	LN560757.1
Bordetella sp. p23(2011) 16S ribosomal RNA gene, partial sequence	1146	1146	99%	0.0	99%	HQ652588.1
Bordetella sp. e3(2011) 16S ribosomal RNA gene, partial sequence	1146	1146	99%	0.0	99%	HQ652587.1
Bordetella sp. JC15 partial 16S rRNA gene, strain JC15	1146	1146	99%	0.0	99%	AM402948.1

Fig. 5.3 Comparison of the blast results of the 16s rDNA sequence of the isolated bacterium with the NCBI database showing the isolated bacterium belongs to *Bordetella* genus.

Description	Max score	Total score	Query cover	E value	Ident	Accession
Escherichia coli strain 44A 16S ribosomal RNA gene, partial sequence	1085	1085	99%	0.0	100%	KP789331.1
Cronobacter sakazakii strain M.D.E.NA1-8 16S ribosomal RNA gene, partial sequence	1083	1083	99%	0.0	100%	JF690871.1
Escherichia fergusonii strain Sw2 16S ribosomal RNA gene, partial sequence	1081	1081	99%	0.0	100%	KF938590.1
Uncultured bacterium clone 14L-63 16S ribosomal RNA gene, partial sequence	1081	1081	99%	0.0	99%	HM021535.1
Escherichia coli strain 13A 16S ribosomal RNA gene, partial sequence	1079	1079	99%	0.0	99%	KP789326.1
Escherichia coli strain E84-1 16S ribosomal RNA gene, partial sequence	1079	1079	99%	0.0	99%	KJ477001.1
Escherichia fergusonii strain Z4 16S ribosomal RNA gene, partial sequence	1079	1079	99%	0.0	99%	HQ259937.1
Escherichia sp. 3-26(2010) 16S ribosomal RNA gene, partial sequence	1079	1079	99%	0.0	99%	HM489943.1
Escherichia coli strain CZ-BHG010 16S ribosomal RNA gene, partial sequence	1077	1077	98%	0.0	100%	KT765844.1
Escherichia coli strain RCB932 16S ribosomal RNA gene, partial sequence	1077	1077	99%	0.0	99%	KT261144.1
Escherichia coli strain 42L 16S ribosomal RNA gene, partial sequence	1077	1077	99%	0.0	99%	KP789329.1
Escherichia coli strain 35A 16S ribosomal RNA gene, partial sequence	1077	1077	99%	0.0	99%	KP789327.1

Fig. 5.4 Comparison of the blast results of the 16s rDNA sequence of the *E. coli* (used as a positive control) with the NCBI database.

5.1.3. Morphological and biochemical characteristics of the isolated strain

Cells of the strain BTIITR were observed to be Gram stain-negative, coccobacillus and non-motile as shown in Fig. 5.7 (a) and (b). The optimum temperature and pH for growth were found to be 30-35 °C and 6-7, respectively. White colored colonies were observed on the MMH10 agar plates. Strain BTIITR can grow on MacConkey agar, Blood agar, Simmons' citrate agar and LB agar. The growth of strain BTIITR on Simmons's citrate agar differentiated it with its phylogenetically closer neighbour, *B. tumulicola*. *B. tumblicola* can grow on MacConkey agar, but did not show growth on Simmons' citrate agar (Table 5.1). On the HiCarbohydrate™ Kit, strain BTIITR was positive for xylose, maltose, fructose, dextrose, galactose, raffinose, trehalose, melibiose, sucrose, L-arabinose, mannose, inulin, glycerol, salicin, dulcitol, inositol, sorbitol, mannitol, adonitol, arabitol, rhamnose, cellobiose, melezitose, xylitol, ONPG, esculin hydrolysis, D-arabinose, citrate utilization, and malonate utilization and negative for lactose, sodium gluconate, erythritol, α-methyl-D-mannoside, α-methyl-D-glucoside and sorbose. Strain BTIITR assimilated D-xylose, which distinguished it from closely related species, *B. tumulicola and B. tumbae* (Table 5.1). Assimilation of D-

glucose also distinguished strain BTIITR from other members of genus *Bordetella*. Urease test was positive for strain BTIITR, which distinguished it from *B. muralis* (Table 5.1). Indole test was positive for BTIITR, while it was negative for other species of *Bordetella* those were subjected to this test. Strain BTIITR was also positive for lysine and ornithine, and negative for phenyl alanine deamination, H_2S production and Voges–Proskauer test.

Table 5.1 Comparison of the phenotypic characteristics of strain BTIITR with its closest phylogenetic relatives in the genus *Bordetella*

Strains/species: 1, Strain BTIITR; 2, *B. muralis* sp. nov. T6220-3-2b^T [138]; 3, *B. tumulicola* sp. nov. T6517-1-4b^T [138]; 4, *B. tumbae* sp. nov. T6713-1-3b^T [138]; 5, *B. petrii* [139]; 6, *B. hinzii* [140]; 7, *B. avium* [141-143]; 8, *B. trematum* [142]; 9, *B. holmesii* [142, 144]; 10, *B. bronchiseptica* [145]; 11, *B. parapertussis* [142, 143]; 12, *B. pertussis* [142, 143]; 13, *B. ansorpii* [146]; 14, *B. bronchialis* [147]; 15, *B. flabilis* [147]; 16, *B. sputigena* [147]. +, Positive; –, negative; W, weakly positive; V, strain-dependent; ND, no data available; Cb, coccobacillus; C, coccus; R, rod shaped

Characteristic	1	2	3	4	5	6	7	8	9	10	11	12	13	14	15	16
Shape	Cb	Cb	Co	Cb	R/C	R	R	R	R	R	R	R	R	R	R	R
Motility	-	-	-	-	-	+	+	+	-	+	-	-	+	+	+	+
Oxidase	+	+	+	+	+	+	+	-	-	+	-	+	-	+	+	+
pH range	5-10	5-10	5-10	5-10	ND	ND	ND	ND	ND	ND	ND	ND	ND	ND	ND	ND
Optimum pH	6-7	7-8	7-8	7-8	ND	ND	ND	ND	ND	ND	ND	ND	ND	ND	ND	ND
Growth on																
MacConkey agar	+	+	+	+	+	+	+	+	+	+	+	-	+	ND	ND	ND
Blood agar	+	ND	ND	ND	+	+	+	+	+	+	+	-	+	+	+	+
Simmons'citrate agar	+	+	-	+	+	+	+	-	-	+	v	-	ND	ND	ND	ND
10º C	-	W	W	W	-	ND	ND	ND	ND	ND	ND	ND	ND	ND	ND	ND
25º C	+	+	+	+	+	+	+	+	V	+	V	-	+	+	+	+
42º C	W	-	-	-	+	+	+	+	-	V	V	-	ND	+	+	+
Optimum temp(º C)	30-35	25-30	25-30	25-30	ND	37	37	ND	35-37	35-37	ND	ND	37	30-37	30-37	30-37
Acid production from D-glucose	-	-	-	-	-	-	-	-	-	-	-	-	ND	-	-	-
Citrate utilization	+	+	-	+	+	+	+	ND	ND	ND	ND	ND	+	+	+	+
Indole	+	ND	ND	ND	-	-	ND	-	ND	ND	ND	ND	-	-	-	-
Urease	+	-	+	+	_	-	-	-	-	+	+	-	-	-	-	-
Lactose	-	-	-	-	-	ND	ND	-	ND	ND	ND	ND	ND	-	-	-
Nitrate reduction	+	+	+	+	-	-	-	V	-	+	-	-	-	-	-	-
D-Glucose	+	-	-	-	-	-	-	-	-	-	-	-	-	-	-	-
Sorbitol	+	ND	ND	ND	-	ND	ND	-	ND	ND	ND	ND	ND	ND	ND	ND
Arabinose	+	+	-	+	-	-	-	-	ND	ND	ND	ND	-	-	-	-
D-Xylose	+	+	-	-	-	-	-	-	-	-	-	-	ND	-	-	-
Adonitol	+	ND	ND	ND	-	ND	ND	-	ND	ND	ND	ND	ND	-	-	-
G+C content (mol%)	60.5	59.8	59.6	60.0	65.8	65-67	61.6-62.6	64-65	61.5-62.3	68.2-69.5	66-70	66-70	63.8	67.5	65.9	65.9
Isolation source	Forest soil	Mural painting	Mural painting	Mural painting	River sediment	Chicken	Respiratory tracts of Turkey	Chronic otitis	Human blood	Mammalian respiratory tract	Human respiratory tract	Human respiratory tract	Epidermal cyst	Respiratory System	Respiratory System	Respiratory System

Fig. 5.5 HiAssorted™ Biochemical Test kit (KB002) showing the results of different biochemical test

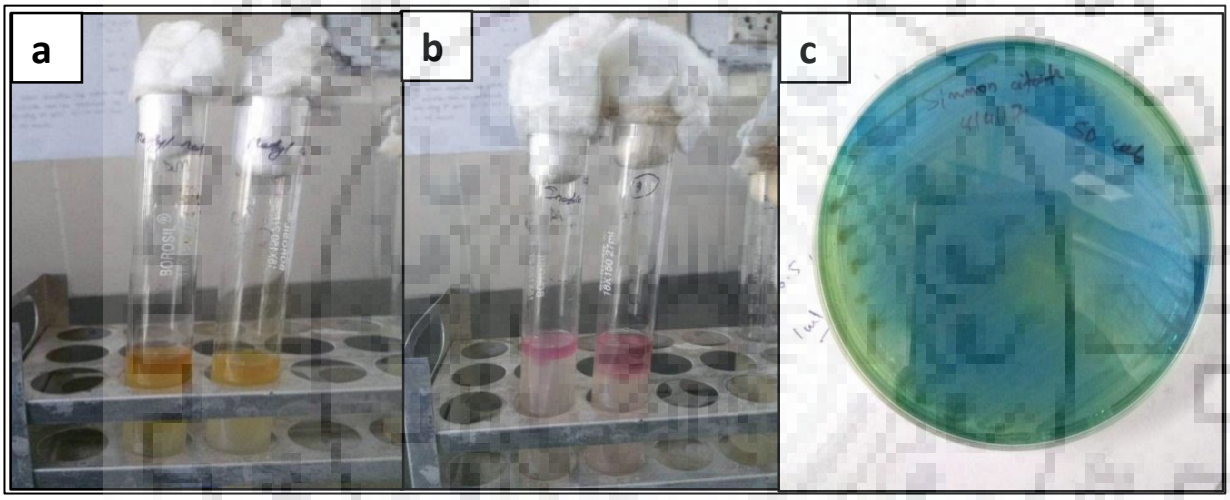

Fig. 5.6 Images of (a) methyl red test (b) indole test (c) Simmon's citrate test

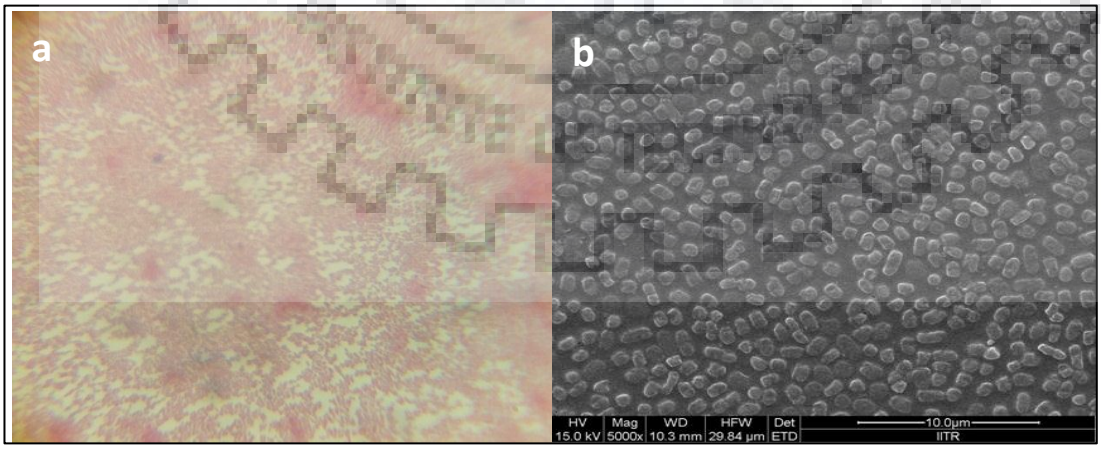

Fig. 5.7 (a) Gram staining image of the isolated strain BTIITR showing its gram stain-negative nature (b) SEM image of the strain showing its coccobacillus shape.

5.1.4. Phylogenetic analysis

16S rDNA sequence analysis using the EzTaxon-e server showed the highest degree of similarity with *Bordetella tumabe* T6713-1-3b (99.5 %) followed by *Bordetella muralis* T6220-3-2b (99.4 %), *Bordetella tumulicola* T6517-1-4b (98.5 %), *Bordetella petrii* DSM 12804 (98.1 %), *Bordetella trematum* NCTC 12995 (97.6 %), *Bordetella avium* 197N (97.6 %), *Bordetella sputigena* R-39474 (97.6 %), *Bordetella hinzii* LMG 13501 (97.6 %), *Bordetella flabilis* AU10664 (97.4 %), *Bordetella bronchiseptica* ATCC 19395 (97.4 %), *Bordetella ansorpii* NCTC 13364 (97.2 %), *Bordetella parapertussis* NCTC 5952 (97.2 %), *Bordetella bronchialis* (97.2 %) and *Bordetella pertussis* Tohama I (97.2 %). Phylogenetic analysis as determined by various tree-making algorithms, including the neighbour-joining and maximum-likelihood, revealed that strain BTIITR belongs to the genus *Bordetella* of the family *Alcaligenacae* in the phylum, order *Burkholderiales*, class *Betaproteobacteria* and phylum *Proteobacteria* grouped with *Bordetella tumbae* with bootstrap value of 72 % as demonstrated in Fig. 5.8.

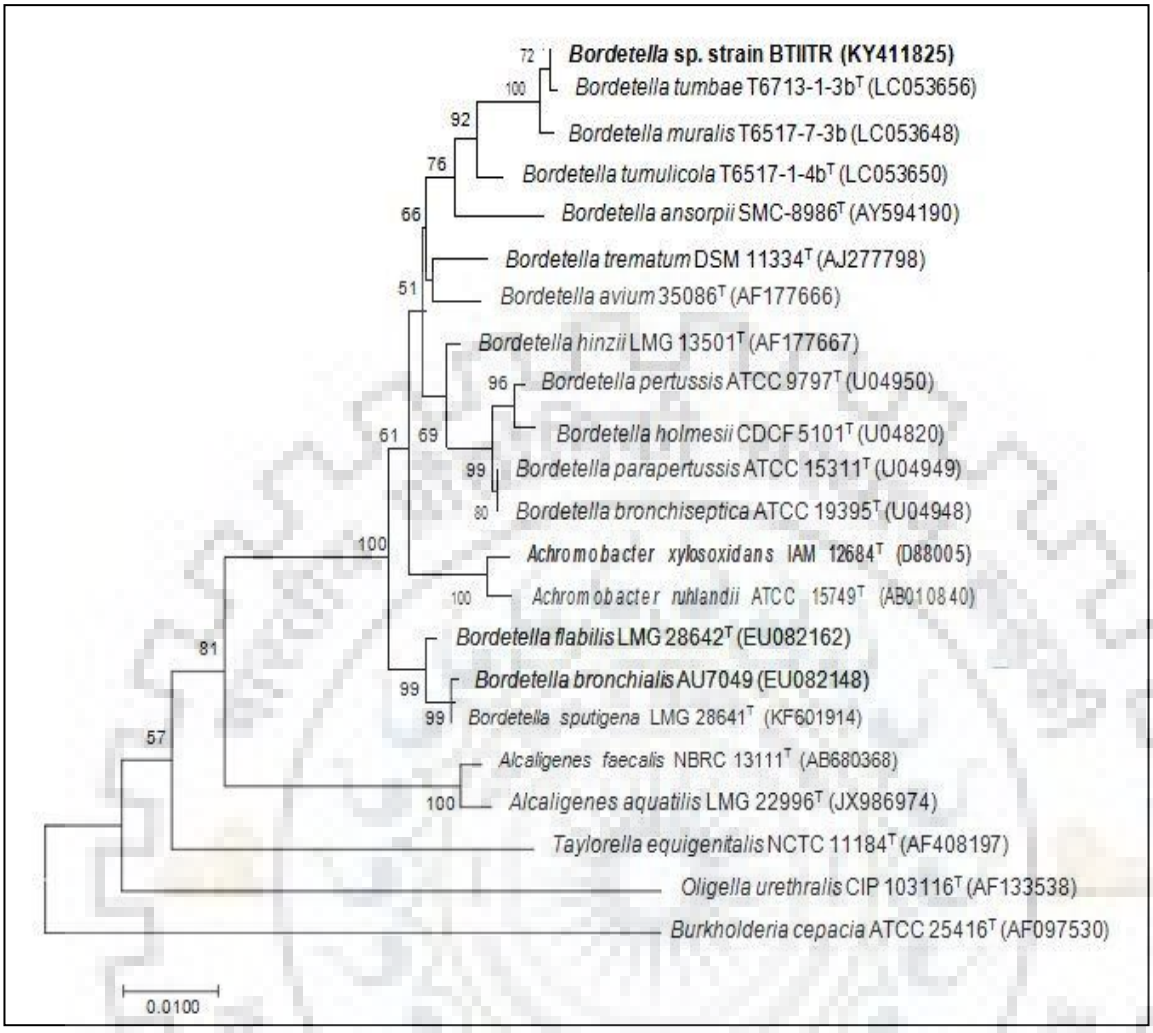

Fig. 5.8 Neighbour-joining tree based on 16S rRNA gene sequences (1432 bases) showing the phylogenetic relationships between the strain BTIITR and other species of the genus *Bordetella*. Bootstrap values (percentages of 1000 replications) of >50% are shown at branches. *Burkholderia cepacia* ATCC 25416^T was used as an out group. Bar, 0.01 substitutions per nucleotide position.

5.1.5. Genomic characteristics

The G+C content of the DNA of strain BTIITR was calculated as 60.5 mol %, which falls near the G+C content of phylogenetically closest species, *B. tumbae*, *B. muralis* and *B. tumlicola* as they have G+C content of 59.6 to 60 % [138].

5.1.6. Cellular fatty acid analysis

The profile of the cellular fatty acids (CFA) of the strain was obtained (Fig. 5.9) and compared with that of the closely related strains of species in the genus *Bordetella*. CFA analysis results are represented in Table 5.2. The CFA profiles of the isolated strain was consistent with the description of the family Alcaligenaceae provided by Busse & Auling [148] and Austin [149]. The analysis revealed that the CFA composition of strain BTIITR was dominated by C_{16} fatty acid and summed 3 ($C_{16:1}$ ω7c and/or $C_{16:1}$ ω6c). The prominent fatty acid in strain BTIITR was $C_{16:0}$ (31.24 %) and summed feature 3 (35.65 %), which are also present in other species of the genus *Bordetella*. However, strain BTIITR could be differentiated from its close relatives in the high fraction of the structurally unresolved summed 3 ($C_{16:1}$ ω7c and/or $C_{16:1}$ ω6c) and summed 8 ($C_{18:1}$ ω7c and/or $C_{18:1}$ ω6c), which were measured as 35.65 % and 5.8 %, respectively (Table 5.2). Strain BTIITR also contained least amount (2.65 %) of fatty acid $C_{17:0}$ cyclo as compared to the other species of *Bordetella* genus. The library data (CLIN6 6.10) of MIDI showed the maximum similarity index (.769) for *Bordetella bronchiseptica*, which also confirmed that strain BTIITR belongs to genus *Bordetella* as shown in the Fig. 5.10.

Table 5.2 Total cellular fatty acid composition (%) of strain BTIITR and other related species of the genus *Bordetella*

Strains/species: 1, Strain BTIITR; 2, *B. muralis* sp. nov. T6220-3-2bT; 3, *B. tumulicola* sp. nov. T6517-1-4b^T; 4, *B. tumbae sp.* nov. T6713-1-3b^T; 5, *B. petrii* DSM 12804^T; 6, *B. hinzii* JCM 15550^T; 7, *B. avium* DSM 11332^T; 8, *B. trematum* DSM 11334^T; 9, *B. holmesii* DSM 13416T; 10, *B. bronchiseptica* NBRC 13691^T; 11, *B. parapertussis* DSM 13415^T; 12, *B. pertussis* DSM 5571^T; 13, *B. ansorpii* SMC-8986^T; 14, *B. bronchialis* AU7049; 15; *B. sputigena* LMG 28641^T; 16, *B. flabilis* LMG 28642^T;

Fatty acid	1	2	3	4	5	6	7	8	9	10	11	12	13	14	15	16
$C_{12:0}$	1.07	-	4.3	-	-	1.2	-	-	-	-	-	-	-	-	-	-
$C_{12:0}$ 2-OH	1.66	3.0	1.9	3.1	4.2	4.3	5.8	2.6	4.8	4.4	1.0	-	1.1	5.27	4.66	5.44
$C_{12:0}$ 3-OH	0.10	-	-	-	-	-	-	-	-	-	-	1.8	-	-	-	1.1
$C_{14:0}$	5.29	6.6	1.8	5.4	7.0	-	1.1	-	-	6.0	6.3	3.6	2.4	4.11	3.78	2.80
$C_{14:1}$ ω5c	0.14	-	-	-	-	-	-	-	-	-	-	-	-	-	-	-
$C_{14:0}$ 2-OH	0.70	2.5	3.4	-	1.3	4.4	5.3	3.0	4.8	-	-	-	4.9	4.55	5.02	3.65
$C_{15:1}$ ω6c	0.15	-	-	-	-	-	-	-	-	-	-	2.6	-	-	-	-
anteiso-$C_{15:0}$	0.09	-	-	-	-	-	-	6.9	-	-	-	-	-	-	-	-
$C_{15:0}$ 2-OH	-	-	-	-	-	-	-	1.3	-	-	-	-	-	-	-	-
$C_{16:0}$	31.24	30.0	41.8	-	-	-	-	1.1	-	-	-	-	32.4	33.55	33.72	28.47
iso- $C_{16:0}$	-	-	-	-	-	-	-	-	-	-	-	-	6.7	-	-	-
$C_{16:0}$ 3-OH	0.38	-	-	-	-	-	-	-	-	-	-	-	1.1	-	-	-
$C_{16:1}$ ω7c	-	-	-	-	-	-	-	-	-	-	-	-	17.6	-	-	-
$C_{17:0}$	0.56	-	-	-	-	-	-	-	-	-	7.7	3.9	-	-	-	-
$C_{17:0}$ cyclo	2.56	10.8	23.8	16.5	12.7	14.2	32.2	12.0	19.5	15.5	24.7	-	9.6	29.28	26.77	35.90
anteiso $C_{17:0}$	0.18	-	-	-	-	-	-	1.2	-	-	-	-	-	-	-	-
$C_{17:1}$ ω5c	-	-	-	-	-	-	-	4.7	-	-	-	-	-	-	-	-
$C_{17:1}$ ω7c	-	-	-	-	-	-	-	-	1.1	-	-	-	-	-	-	-
anteiso-$C_{17:1}$ ω9c	-	-	-	-	-	-	-	4.8	-	-	-	-	-	-	-	
$C_{18:0}$	5.04	1.9	1.3	3.4	2.6	3.9	3.4	2.5	6.4	2.3	3.4	3.6	1.9	1.28	T	1.5
$C_{18:1}$ ω7c	-	-	-	-	-	-	-	-	-	-	-	-	12.9	1.36	2.09	4.82
$C_{18:3}$ ω6c(6,9,12)	0.07	-	-	-	-	-	-	-	-	-	-	-	-	-	-	-
iso- $C_{19:0}$	-	-	-	-	2.8	-	-	1.1	4.6	-	4.0	-	-	-	-	-
$C_{19:0\ cyclo}$ ω8c	-	-	-	-	-	-	-	-	-	-	-	-	4.6	-	-	-
iso- $C_{20:0}$	-	-	-	-	-	-	-	3.3	-	-	-	-	-	-	-	-
Summed features*																
2	9.02	12.0	9.1	9.0	11.1	10.4	11.3	10.6	11.5	8.9	15.0	9.6	-	14.19	12.56	11.28
3	35.65	27.0	10.1	26.3	19.2	25.5	1.3	14.4	-	22.6	2.3	42.2	-	5.37	8.89	4.38
5	0.20	-	-	-	-	-	-	-	-	-	-	2.3	-	-	-	-
8	5.80	2.3	1.3	4.7	4.9	1.8	-	1.0	-	1.9	-	-	-	-	-	-

*Summed features represent groups of two or more components that could not be separated by the MIDI system. Summed feature 2 comprises $C_{12:0}$ aldehyde? and/or unknown 10.928. Summed feature 3 comprises $C_{16:1}$ ω7c/$C_{16:1}$ ω6c and/or $C_{16:1}$ ω6c/$C_{16:1}$ ω7c. Summed feature 5 comprises $C_{18:2}$ ω6,9c anteiso-$C_{18:0}$ and/or $C_{18:0}$ ante/C18:2 ω6,9c. Summed feature 8 comprises $C_{18:1}$ ω7c and/or $C_{18:1}$ ω6c.

Strain1 – data from this study

Strain 2 to 12- data from Tazato et al. [138]

Strain13- data from Ko et al. [146]

Strain 14 to 16- data from Vandamme et al. [147]

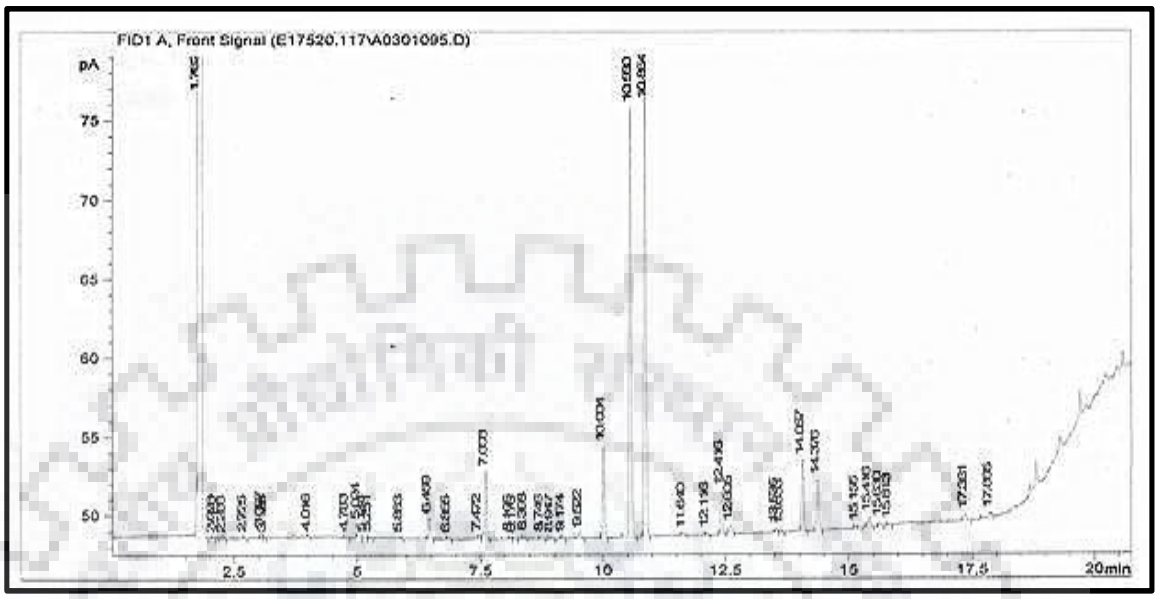

Fig. 5.9 Gas chromatogram of the cellular fatty acids of isolated bacterial strain BTIITR.

E175201.17A [1095] bordetella 1 36hr

Library	Sim Index	Entry Name
	0.444	Grimontia-hollisae (Vibrio)
RTSBA6 6.10	0.669	Kingella-kingae
	0.632	Achromobacter-xylosoxidans-xylosoxidans (Alcaligenes)
	0.573	Achromobacter-xylosoxidans-denitrificans (Alcaligenes)
	0.444	Grimontia-hollisae (Vibrio)
CLIN6 6.10	0.769	Bordetella-bronchiseptica-GC subgroup A
	0.565	Achromobacter-xylosoxidans-denitrificans (Alcaligenes)
	0.513	Proteus-penneri-GC subgroup A
ACTIN1 3.80		(No Match)

Fig. 5.10 Result of the similarity index which were obtained by database of MIDI.

5.1.7. Taxonomic conclusion

All of the characteristics of strain BTIITR were in accordance with those of the members of the genus *Bordetella*, which was placed in family Alcaligenaceae, order Burkholderiales, class Betaproteobacteria, phylum Proteobacteria. Phylogenetic study revealed more than 99 % similarity with the *Bordetella tumbae* and *Bordetella muralis*, which were also isolated from

environmental samples. However, some biochemical characteristics, like assimilation of D-xylose, differentiated it from *B. tumabe*, while assimilation of D-glucose differentiated it from the other members of *Bordetella.* The CFA analysis also confirmed that the isolate belongs to *Bordetlla* genus as library data (CLIN6 6.10) of MIDI showed the maximum similarity index (.769) for *Bordetella bronchiseptica* on the basis of fatty acid composition.

In the above set of experiments, we successfully isolated and identified a bacterium, which was named as *Bordetella* sp. BTIITR. This bacterium was able to grow in the presence of HMF as sole carbon source, which suggested that this bacterium has the advanced metabolic pathways by which it can utilize toxic chemicals, like HMF. This property of *Bordetella* sp. BTIITR was used subsequently to detoxify lignocellulosic hydrolysate liquor.

5.2. Study of the fermentation inhibitor degradation capability of *Bordetella* sp. BTIITR

This Section contains the results for the fermentation inhibitor degradation capability of the isolated microorganism from both simulated and actual hydrolysate liquors. HMF and furfural were used as the model pollutants for the simulated hydrolysate liquor, whereas sugarcane bagasse was used for producing the actual hydrolysate liquor.

5.2.1. Effect of temperature on degradation of *Bordetella* sp. BTIITR

To check the temperature sensitivity of *Bordetella* sp. BTIITR, cell culture was performed in MMH10 medium and the culture was incubated at different temperatures ranging from 25 °C to 40 °C. Then, the optical density was measured at every 4 h time intervals during the incubation, and the results are represented in Fig. 5.11 reveals that *Bordetella* sp. BTIITR can be grown up to 40 °C temperature, however best growth was observed between 30 °C to 35 °C temperature. Below 25 °C and above 35 °C temperature, there was adverse effect of temperature on bacterial growth. Hence, 30 °C temperature was considered to be the optimum temperature for the HMF degradation using *Bordetella* sp. BTIITR strain. Rahman et al. [150] also reported that temperature of 30 °C and pH 7.5 were to be optima for maximum biodegradation of petroleum [151]. Higher temperature increased the rate of hydrocarbon metabolism to a maximum, typically in the range of 30 °C to 40 °C. Above that the membrane toxicity of hydrocarbons was increased.

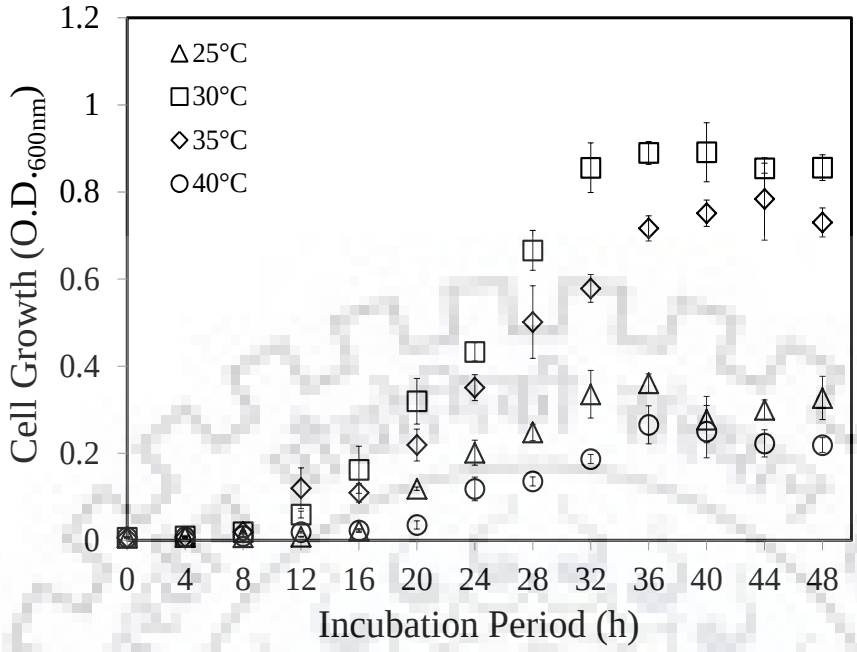

Fig. 5.11 Effect of temperature on the growth of *Bordetella* sp. BTIITR in a medium enriched with 10 mM HMF. The error bar represents the standard deviation, where the number of replicates, n = 3.

5.2.2. Effect of concentration of HMF on degradation of *Bordetella* sp. BTIITR

Typical concentrations of HMF and furfural in dilute acid pretreated lignocellulosic hydrolysate liquor are observed to be around 1-1.5 gL^{-1} (8-12 mM) and 0.5-1 gL^{-1} (5-10 mM), respectively. As a result, overall production of valuable chemicals decreases during the fermentation. Joo et al. [152] reported that on increasing the furfural concentration from 1 gL^{-1} to 3 gL^{-1} the production of 2,3 butanediol using *Enterobacter aerogenes* was decreased from 9.22 gL^{-1} to 3.70 gL^{-1}, when glucose was used as a substrate.Therefore, to determine the inhibitor tolerance of *Bordetella* sp. BTIITR, it was grown in different concentrations of HMF ranging from 3 mM to 24 mM and the results are demonstrated in Fig. 5.12. Lag, exponential and stationary phases can be distinctly observed for 3 mM to 12 mM substrate concentration. However, above 12 mM HMF concentration, the lag phase was extended resulting in less cell growth. For 3 mM and 6 mM substrate concentration, death phase was observed early as compare to the higher substrate concentrations. Maximum and most stable growth was observed at around 10 mM concentration of HMF as demonstrated in Fig. 5.12. The inset plot

of Fig. 5.12 clearly illustrates that the maximum growth of the bacteria was achieved at around 10 mM HMF concentration. On either side of 10 mM HMF concentration, the growth declined. This observation aligns well with an earlier reported study (Wierckx et al.), which mentioned that *Cupriavidus basilensis* HMF14 exhibit no stable growth above 6 mM concentration of furfural and HMF [71]. Since high concentration of HMF (above 10 mM) demonstrated toxic substrate inhibition to the bacterial cells, cells take more time to adapt to the environment. Hence, longer lag phase was observed above 10 mM as mentioned previously. When HMF concentration was less than 10 mM, it was observed that the bacteria attain stationary phase early with slower growth rate than that of 10 mM. From this experiment, it was concluded that the ability of *Bordetella* sp. BTIITR to tolerate HMF remained maximum at around 10 mM (1.26 gL^{-1}) HMF concentration. At HMF concentration greater than 10 mM, the inhibitory effect of HMF on the bacterium is severe, which led to substantially slower rate of detoxification. Mussatto and Roberto [21] reported that a high concentration of furan derivatives (1.5 gL^{-1}) interfered in respiration and growth of the microorganism resulting in reduction of ethanol yield by 90.4%. *Bordetella* sp. BTIITR has the potential to remove the furan derivatives in that concentration range, thereby helping to achieve a higher yield of ethanol.

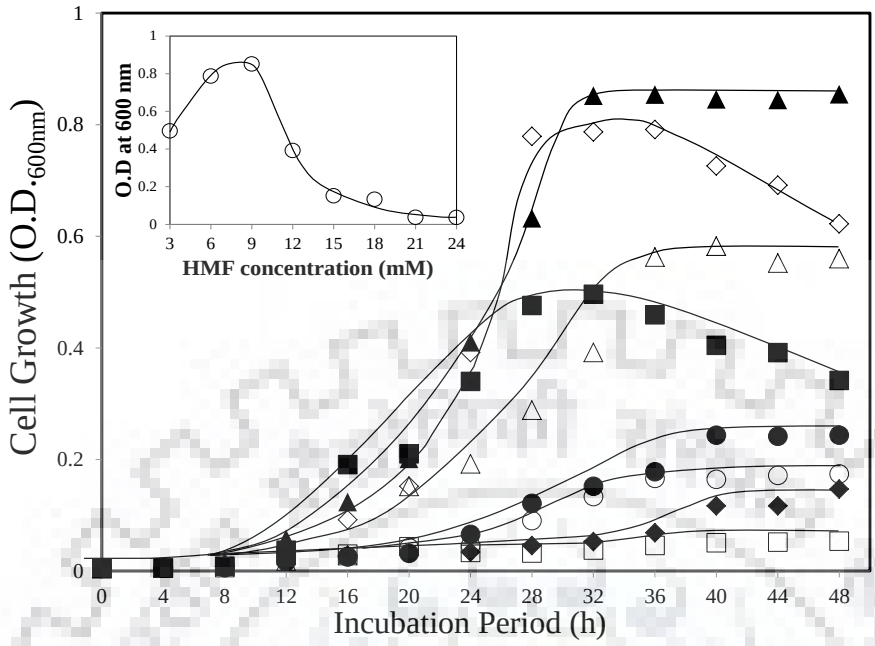

Fig. 5.12 Growth of *Bordetella* sp. BTIITR for different concentrations of HMF. Highest growth was observed at around 10 mM. Inset figure demonstrates the optical density at 32 h of incubation period for different concentrations of HMF. The legends used are as follows: ■ 3 mM; ◇ 6 mM; ▲ 9 mM; △ 12 mM; ●15 mM; ○18 mM; ◆ 21 mM; and □ 24 mM.

5.2.3. Degradation of inhibitory compounds by *Bordetella* sp. BTIITR

5.2.3.1. Degradation of HMF and furfural from MMH10 and MMF10 media

In order to evaluate the degradation performance of *Bordetella* sp. BTIITR, the bacterium was inoculated in a medium having either 10 mM HMF or 10 mM furfural as the sole carbon source (without glucose and xylose supplementation). Broth was analyzed at every 4 h time interval to establish a time course of HMF or furfural degradation. A control medium (without microorganism) was also incubated with culture, where no removal of HMF or furfural was observed. Fig. 5.13(a) and (b) reveal that *Bordetella* sp. BTIITR was able to survive in the presence of fermentation inhibitors and was able to efficiently remove both HMF and furfural. The rate of removal was higher for furfural compare to HMF. As shown in Fig. 5.13(a), HMF concentration was reduced from initial 10 mM to 0.2 mM in 28 h of incubation period, which indicated that when HMF was the only carbon source, *Bordetella* sp. BTIITR was able to degrade 98% of HMF in 28 h. Gradually, with the degradation of HMF, HMF acid was also recorded in minor amount in the broth, however this disappeared soon (Fig. 5.14 a). When

furfural was the only carbon source, furfural was completely disappeared from the culture broth in 24 h of incubation period as shown in Fig. 5.13 (b). Furoic acid and furfural alcohol were observed during the culture of *Bordetella* sp. BTIITR in the MMF10 medium, but they also got consumed with time (Fig. 5.14 b). Approximately, half growth was observed in MMF10 as compared to MMH10 medium. This suggested that furfural is stronger inhibitor as compare to HMF. Hu et al. [153] also reported that furfural and its derivatives furfuryl alcohol and furoic acid inhibited cell growth by 45% at around 1 mM concentration in oleaginous yeast *Rhodosporidium toruloides* Y4. Furfural was identified as the most toxic compound among all the inhibitors synthesized in the hydrolysate for *Cupriavidus necator* [154]. The appearance of HMF acid, furfural alcohol and furoic acid during HMF and furfural degradation conclude that these chemicals are synthesized as intermediate compounds. Similar observations were also reported in earlier studies, where HMF acid, furfural alcohol and furoic acid were formed as intermediate compounds during HMF and furfural degradation pathways in *Cupriavidus basilenisis* HMF14 and *Amorphotheca resinae* ZN1 [71, 155].

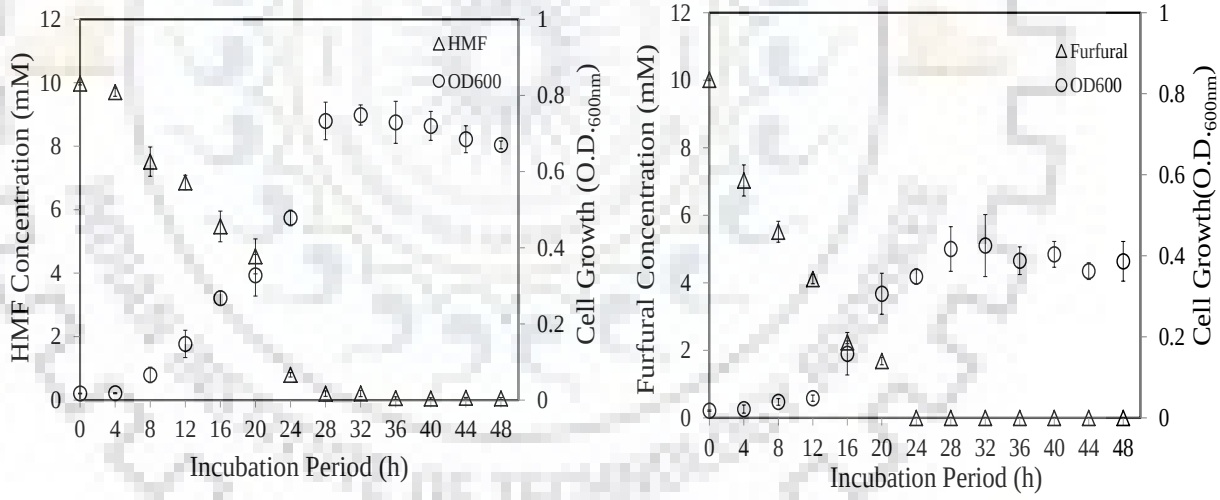

Fig. 5.13 Degradation of (a) HMF and (b) furfural by *Bordetella* sp. BTIITR in MMH10 and MMF10 medium, where either HMF or furfural was used as the sole carbon source. The error bar represents the standard deviation, where n=3.

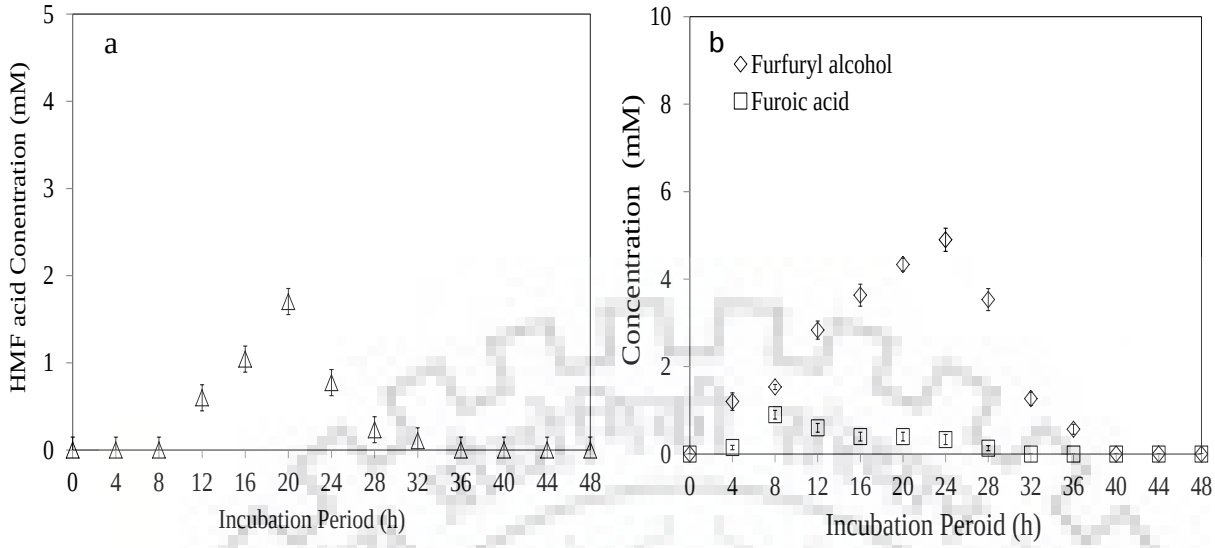

Fig. 5.14 (a) Formation of intermediate HMF acid during degradation of HMF (b) Formation of intermediate furfuryl alcohol and furoic acid during furfural degradation pathway

When *Bordetella sp*. BTIITR was grown in the presence of mixture of 10 mM HMF and 10 mM furfural (MMHF10), it was observed that furfural was consumed at a faster rate than HMF as observed earlier for the individual substrate (Table 5.3). However, an overall slow growth and slow degradation was observed compared to the individual substrate, which could be attributed to the synergistic effect of the inhibitors. Ruan et al. [156] also reported the synergistic effect of these inhibitors reducing 28% of the total fungal growth.

5.2.3.2. Degradation of HMF and furfural from GXH10 and GXF10 simulated hydrolysate

Fig. 5.15 and Fig. 5.16 illustrate the efficiency of the strain BTIITR for detoxification of simulated hydrolysate liquor. When the strain BTIITR was grown in GXH10 media, complete removal of HMF was observed in 24 h of incubation period. The result also revealed that 77 % of HMF was removed in just 8 h of incubation period. It was also very encouraging to observe that the strain utilized insignificant amount of glucose and xylose when the inhibitor was present in the solution (Fig. 5.15 and Fig. 5.16). Once the inhibitor was consumed completely, significant utilization of sugars occurred. During the degradation of HMF, HMF acid was formed in the medium as transient intermediate compounds, which were subsequently consumed. Similarly, as depicted in Fig. 5.16, when the isolated strain was grown in GXF10

media, complete removal of furfural was observed in 20 h of incubation period. Furoic acid and furfuryl alcohol were also observed in medium as transient intermediate compounds. A long lag phase was observed in the GXF10 medium as compared to GXH10 medium, which suggested that furfural was stronger inhibitor as compared to HMF [71]. However, all the phases – lag, log, stationary and declined, were observed for both GXH10 and GXF10 media in 48 h of incubation period. Production of HMF acid, HMF alcohol, furoic acid and furfuryl alcohol during the degradation of HMF and furfural indicated that *Bordetella* was probably following the same degradation pathway as suggested earlier in *Cupriavidus basilenisis* HMF14 and *Amorphotheca resinae* ZN1 [71, 157, 158], where the final product 2-oxoglutaric acid pathway entered into the Kreb's cycle.

Above results clearly establish the potential ability of *Bordetella* sp. BTIITR to efficiently detoxify lignocellulosic biomass hydrolysate liquor. The benefit of detoxification of lignocellulosic biomass hydrolysate liquor on ethanol production was reported earlier. 8.67 gL^{-1} of ethanol was produced when sugarcane bagasse hydrolysate liquor was detoxified with ion exchange method, which was significantly higher than the ethanol produced (3.46 gL^{-1}) without detoxification [85]. The results in Fig. 5.15 and Fig. 5.16 demonstrate that *Bordetella* sp. BTIITR has substrate priority for the furan derivatives over the sugars. Significant utilization of sugars was initiated only when HMF and furfural concentrations reached to a low threshold value. This substrate priority of strain BTIITR makes it a potential candidate for degradation of HMF and furfural from lignocellulosic biomass hydrolysate to improve the ethanol production by fermentation. .

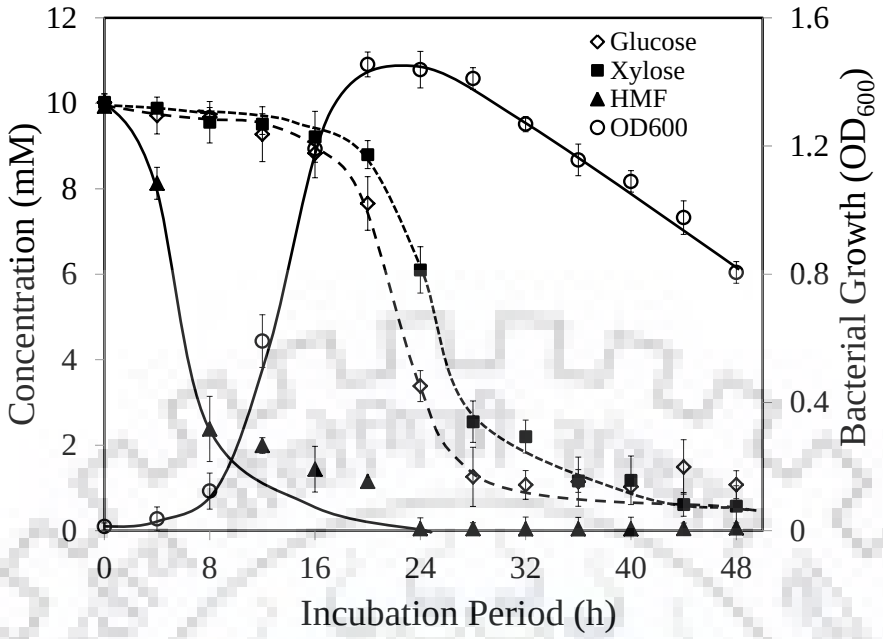

Fig. 5.15 Degradation of HMF from the media containing glucose, xylose and HMF each of 10 mM.

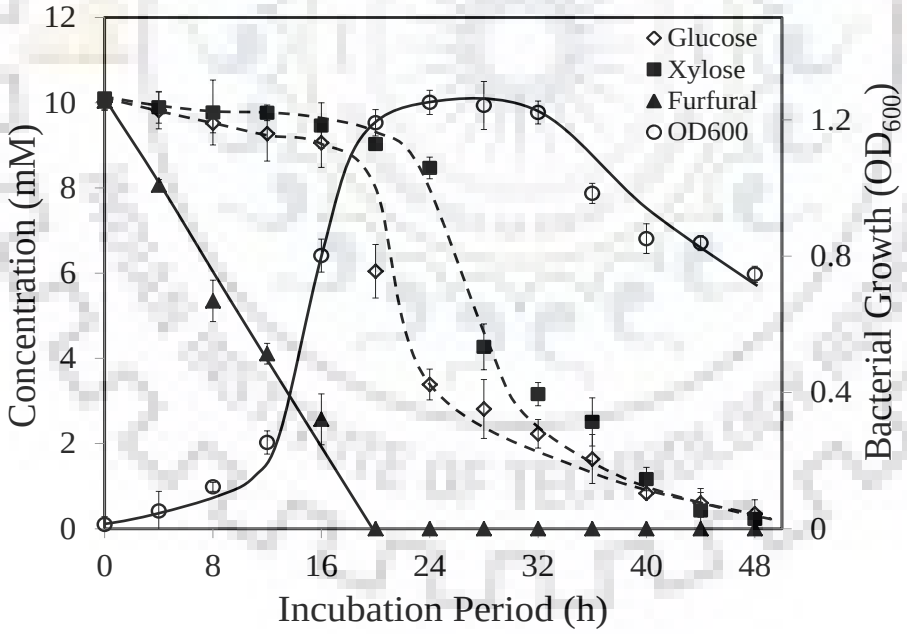

.

Fig. 5.16 Degradation of furfural from the media containing glucose, xylose and furfural each of 10 mM.

5.2.3.3. Degradation of HMF and furfural from simulated hydrolysate liquor (GXHF10)

To check the substrate priority, *Bordetella* sp. BTIITR was grown in a mixture containing 10 mM each of HMF, furfural, glucose and xylose. The main reason to take glucose and xylose as the carbon sources along with HMF and furfural was to simulate the lignocellulosic hydrolysate liquor, where both glucose and xylose constitute more than 90% of total carbohydrate. The result of this experiment was quite interesting as represented in Fig. 5.17. Furfural demonstrated faster rate of removal and was completely disappeared from the culture in 16 h of incubation period. When furfural concentration became negligible at 16 h, sharp degradation of HMF took place to around 1.90 mM. This signifies that *Bordetella* sp. BTIITR was able to remove 100% of furfural and 80% of HMF in just 16 h. Complete removal of HMF (100%) was achieved at 28 h. Compare to MMH10 and MMF10, time reduction in furfural and HMF degradation in GXHF could be due to the presence of glucose and xylose in the medium, which provided favorable environment for bacterial growth compare to only furan derivatives as the sole carbon sources. Point to be noted that during the first 16 h, negligible reduction in sugar concentration took place (at 16 h concentrations of glucose, xylose, HMF and furfural were 8.40 mM, 9.26 mM, 1.90 mM and 0 mM, respectively). After removal of both furfural and HMF from the broth, consumption of glucose and xylose was accelerated. For example, at 28 h, the concentration of glucose, xylose, HMF and furfural were 4.10 mM, 5.0 mM, 0 mM and 0 mM, respectively. These observations indicate that the furan derivatives inhibited the activity of the glycolysis enzymes [16, 17] due to which, initially, glucose and xylose were consumed at a slower rate. Once furfural and HMF were consumed, glucose and xylose were consumed rapidly by the microorganism following the normal glycolysis cycle. From these experimental results, we can speculate that if we incubate the bacterial culture only for 16 h, most of the toxic compounds can be removed from lignocellulosic hydrolysate liquor without sacrificing significant fraction of sugar. This suggests that *Bordetella* sp. BTIITR can be a useful microorganism to detoxify the furan derivatives from the lignocellulosic hydrolysate liquor prior to the downstream fermentation step.

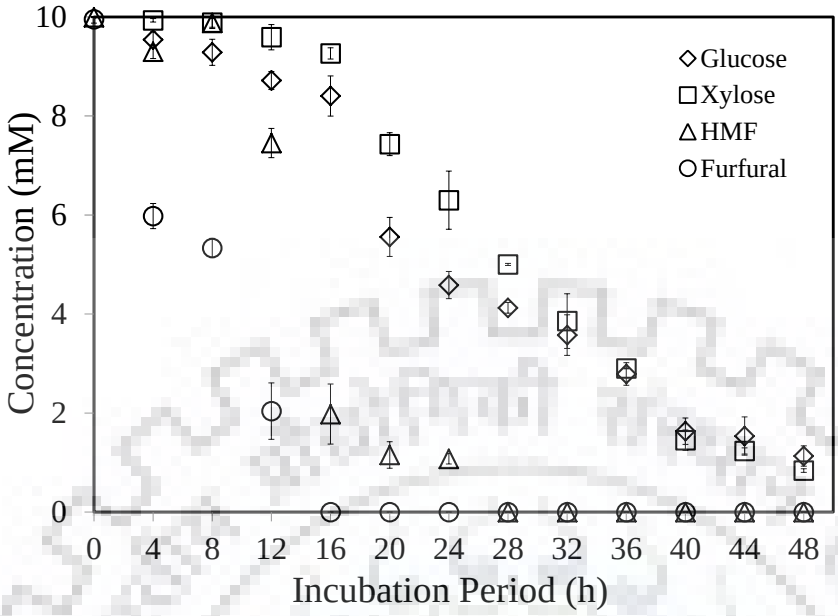

Fig. 5.17 Time course of degradation of fermentation inhibitors present in simulated hydrolysate liquor, where furfural, HMF, glucose and xylose were each taken at 10 mM concentration. The error bar represents the standard deviation, where n=3.

5.2.3.4. Degradation of inhibitory compounds from sugarcane bagasse hydrolysate by *Bordetella* sp. BTIITR

Sugarcane bagasse was vacuum oven dried at 60 °C for overnight and reduced to a particle size range of 5-10 mm. Then, 10 % w/w of sugarcane bagasse was mixed with 1.25 % H_2SO_4 and autoclaved for 2 h at 121 °C and 15 psi pressure for conversion of the complex sugars to the simple sugars. Resulting sugarcane bagasse hydrolysate liquor contained 7.74, 16.5, 3.3, 1.03 and 0.42 gL^{-1} of glucose, xylose, acetic acid, HMF and furfural, respectively. To detoxify the furan derivatives, the hydrolysate liquor (after adjusting the pH to 7.0 using 5 N NaOH) was inoculated with seed culture of *Bordetella* sp. BTIITR and the results are represented in Fig. 5.18. In Fig. 5.18, the concentrations are represented in normalized form by dividing with the initial concentration of the individual components. It was observed that the furan derivatives, HMF and furfural, were almost completely removed (HMF 94% and furfural 100%) from the hydrolysate liquor in 16 h of incubation period in a similar manner as was observed in the previous experiment with simulated hydrolysate liquor. After 16 h of incubation period, sugarcane bagasse hydrolysate liquor contained 6.40, 15.1, 0.6, 0.06 and 0 gL^{-1} of glucose,

xylose, acetic acid, HMF and furfural, respectively. A slow utilization of carbohydrates, compare to the simulated liquor, was observed during the initial 16 h of incubation period, which is even better for the detoxification of furan derivatives from lignocellulosic hydrolysate liquor. In addition, 82% acetic acid was also utilized by the microorganism within 16 h of incubation period. After the utilization of acetic acid, HMF and furfural at around 16 h of incubation period, *Bordetella* started to utilize the carbohydrates with an accelerated rate. Consumption of minor quantity of carbohydrates during the initial 16 h was due to the adverse effect of the furan derivatives on the glycolysis enzymes as explained before. This substrate priority of *Bordetella* sp. BTIITR towards the furfural, HMF and acetic acid makes it a suitable organism for biodetoxification of fermentation inhibitors. The pathways by which these furan derivatives were metabolized are largely unknown, although a degradation route for furfural has been proposed based on enzyme activities [159, 160]. In the proposed pathway, furfural was oxidized to furoic acid, which entered the cellular metabolism as the actual substrate for growth. In the HMF degradation pathway, HMF was first converted into HMF acid, which was then oxidized to 2,5-furan-dicarboxylic acid by aldehyde oxidase or HMF/furfural oxidoreductase enzymes, and finally joined the furfural degradation pathway at furoic acid formation step. Then, furoic acid was converted to 2-oxo-glutaric acid via several intermediate steps, which then joined the tricarboxylic acid or TCA cycle to complete the metabolism [161]. Prior utilization of furfural and HMF as compared to the simple sugars, glucose and xylose, was due to the inhibition effect of furfural and HMF on the central carbon metabolism, which involves the glycolysis. Unless HMF and furfural were reduced to its low threshold concentration, glycolysis or TCA cycle was not initiated for simple sugars utilization. This phenomenon of selective utilization of the fermentation inhibitors over the sugars by *Bordetella* sp. BTIITR can be extremely beneficial for efficient downstream fermentation. The above observations establish *Bordetella* sp. BTIITR as a suitable candidate for detoxification of hydrolysate liquor without significantly affecting the sugar population.

In this study, we examined the ability of *Bordetella* sp. BTIITR for degradation of the inhibitory compounds present in different media and observed that the degradation capability of bacterium depends on the medium composition. For better understanding, the comparative results are summarized in Table 5.3, which highlights the best data point for % degradation and the corresponding degradation time. From the table, it is evident that *Bordetella* sp. BTIITR

performs even better in actual hydrolysate liquor compared to the simulated ones, because of the favorable environment provided by the higher amount of sugars.

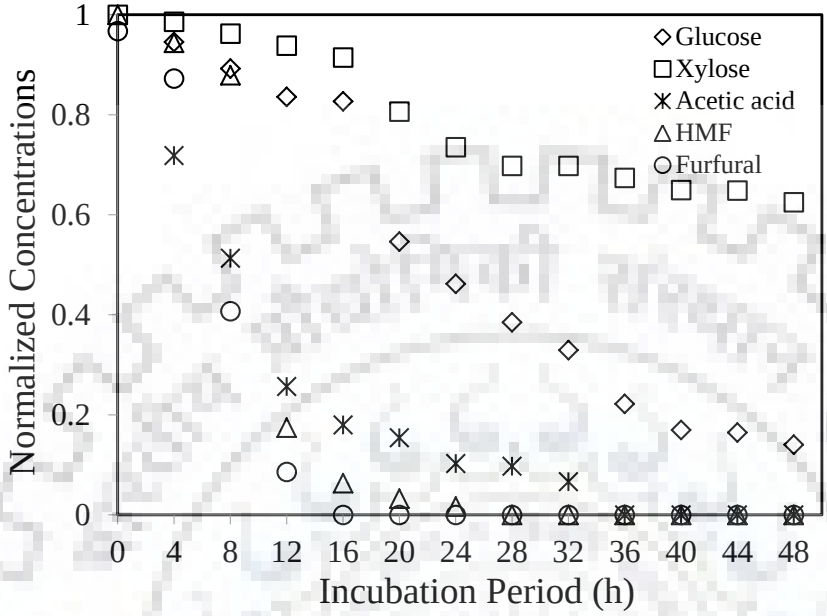

Fig. 5.18 Degradation of inhibitory compounds present in sugarcane bagasse hydrolysate liquor by using *Bordetella* sp. BTIITR. Initial concentrations of glucose, xylose, acetic acid, HMF and furfural in hydrolysate were 7.74, 16.5, 3.3, 1.03 and 0.42 gL^{-1}, respectively. Initial concentrations of different hydrolysate liquor components were used to normalize the concentrations.

Table 5.3 Summary showing the best data point for % degradation of the inhibitors and the corresponding degradation time by the *Bordetella* sp. BTIITR from different types of growth medium. GXH (Glucose, Xylose and HMF each 10 mM), GXHF (Glucose, Xylose, HMF and furfural each 10 mM)

Growth Medium	Inhibitory compounds	Degradation (%)	Degradation time (h)
MMH10	HMF	98	28
MMF10	Furfural	100	24
MMHF10	HMF	38	36
	Furfural	100	36
GXH10	HMF	99.6	24
GXF10	Furfural	100	20
GXHF10	HMF	80	16
	Furfural	100	16
Sugarcane bagasse hydrolysate	HMF	94	16
	Furfural	100	16
	Acetic acid	82	16

5.3. Immobilization of *Bordetella* sp. BTIITR within chitosan beads and study of HMF and furfural degradation from simulated lignocellulosic hydrolysate liquor

In this section, chitosan, cross-linked with sodium tripolyphosphate (TPP) was used to immobilize the cells of the microorganism, *Bordetella* sp. BIITR. The immobilized cells were further used to study the detoxification of the fermentation inhibitors present in lignocellulosic hydrolysate liquor. HMF and furfural degradation efficiency was evaluated at various parameters, such as pH, temperature, biomass loading and inhibitors concentration. In addition, chitosan beads were characterized using various analytical tools.

5.3.1. Characterization of cell-immobilized chitosan beads

5.3.1.1. SEM images of chitosan beads

SEM images of chitosan beads, both immobilized and non-immobilized, were captured to visualize the surface and cross sectional morphology. As shown in Fig. 5.19 (a), the chitosan beads were spherical with diameter of approximately 2 mm. Spherical structure provided maximum surface area per unit volume for diffusional transport of components of the simulated hydrolysate inside the bead. Cross section of bead (Fig. 5.19 b) revealed the presence of small cavities within the internal structure, which probably functioned as reservoirs for hydrolysate liquor. Micro-graph of surface of the chitosan bead illustrated that numerous sub-micron pores were formed due to the cross-linking structure within the chitosan bead (Fig. 5.19 c). These pores helped in efficient mass transfer across the bead area. Smooth, cross-linked fibers were observed in the cross section of non-immobilized bead as demonstrated in Fig. 5.19 (d). These cross-linked fibers became rough after the immobilization of cells inside the bead as shown in Fig. 5.19 (e). The cells were uniformly dispersed in the whole bead, indicating that the bead served as a uniform bio-reactor for the degradation of the target inhibitors. Fig. 5.19 (f) represent the cross sectional image of a bead after 28 h of incubation within the simulated hydrolysate. It can be observed that prolonged incubation resulted into significant growth of the cells, thereby occupying the whole internal surface area of the bead. This indicates that the cells were grown efficiently inside the beads. However, due to the cross-linked stable structure of the beads, it was difficult to measure the actual growth of the cells inside the bead. Since beads possessed hydrogel-like structure, they were always kept in hydrated condition to avoid structural disintegration due to dehydration.

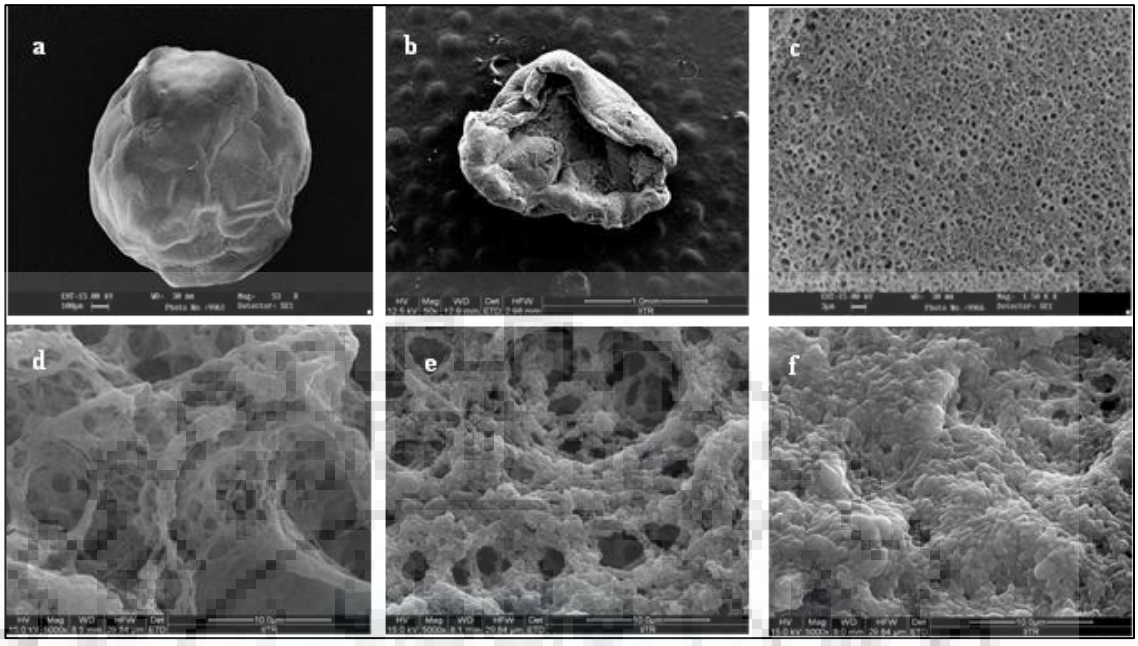

Fig. 5.19 The SEM micrographs of the (a) Whole chitosan bead at 50 X (b) Cross section of chitosan bead at 50 X (c) Surface appearance of chitosan bead at 1500 X (d) Cross section of non-immobilized bead at 5000 X (e) Cross section of *Bordetella* sp. BTIITR immobilized bead indicate bacterial colony at 5000 X (f) Cross section of *Bordetella* sp. BTIITR immobilized bead after detoxification of hydrolysate at 5000 X.

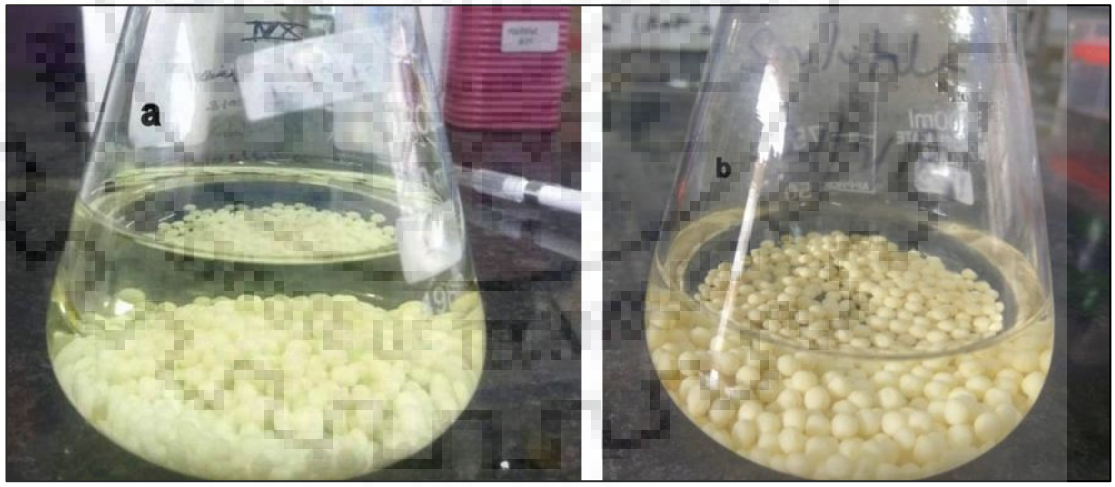

Fig. 5.20 (a) Chitosan immobilized beads before growth in the undetoxified hydrolysate (yellowish in color) (b) chitosan immobilized cells after 20 h of growth in the detoxified hydrolysate (clear solution). Yellowish color of simulated hydrolysate was due presence of HMF and furfural.

Fig. 5.21 Image of single bead at the scale showing the size of bead.

5.3.1.2. Water uptake ratio

Chitosan is a hydrophilic polymer containing number of amine groups, and therefore, functioned as a cationic polymer, whereas, Na-tripolyphosphate (STPP) is an anionic chelating agent. The amine groups of chitosan, in weak acidic condition, remained protonated and interacted with the anionic counter-ions to form a gel-like structure. Then, ionic cross-linking between the gel and STPP led to a solid porous structure of chitosan bead [110]. Chitosan, being a hydrophilic polymer, allowed permeation of water molecules across the porous external barrier and accommodated them in the interstices between the polymer chains. This caused swelling of the chitosan beads.

While ionic cross-linking was necessary for the formation of the beads, it also restricted swelling by providing the necessary rigidity to the beads. With an increase in pH, amine groups of chitosan tend to deprotonate, i.e. the number of cationic groups reduced. This decreased the ionic cross-linking to some extent, promoted stretching of the solid matrix and resulted in higher swelling. Additionally, as amine groups of chitosan deprotonated at higher pH, the tendency of hydrogen bond formation between the nitrogen of amine group and proton of water increased. This enhanced hydrogen bonding was also responsible for the increased swelling at higher pH [162].

Swelling ability of the cell-immobilized chitosan beads, which is expressed here in terms of water uptake ratio, is a major factor to influence the mass transfer across the beads. Typically, the water uptake of polymeric beads is measured with respect to the dry weight of the beads and is represented as swelling ratio. In our case, with encapsulated cells, we hypothesized that rather than using dry beads as the basis, cell-immobilized beads as the basis will be more appropriate representation of the actual scenario. Hence, water uptake experiments

were conducted starting from cell-immobilized beads right after formation. The beads change their ability to adsorb solution, when the environmental pH is altered [163]. Therefore, to test the dynamic swelling properties of the prepared chitosan beads, they were suspended in phosphate buffer of pH 6, 7, 8, and 9, and the results are shown in Fig. 5.22. Fig. 5.22 reveals that maximum water uptake ratio was obtained at pH 8, which was recorded as 3.7 and 3.8 at 16 and 24 h, respectively. Water uptake ratio increased with increase in pH from 6 to 8 due to the reasons explained in previous paragraph. Wang et al. [162] observed that hydrogel beads composed of chitosan-g-poly (acrylic acid)/vermiculite and sodium alginate showed a pH sensitive swelling, where swelling ratio increased to 44.6 with increase in pH from 2 to 7, and then, decreased sharply to 2.8 with further increase in pH to 12. These observations also support the results obtained in section 3.3, where pH 8 was found to be the most suitable to degrade HMF and furfural from the simulated hydrolysate. pH 9 also provided similar water uptake as pH 8, although there was large difference between the degradation efficiency at pH 8 and 9. The lower degradation efficacy at pH 9 was probably due to the harsh effect of higher pH on the immobilized microbial cells.

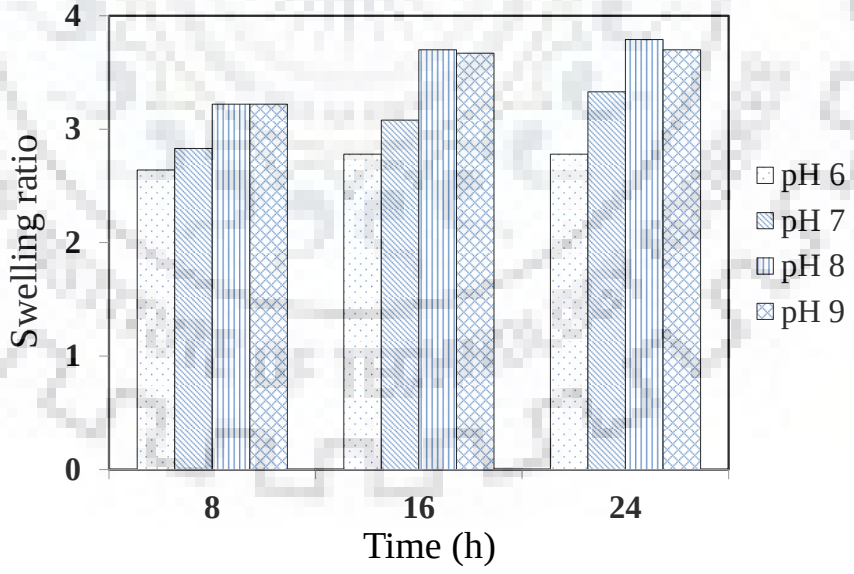

Fig. 5.22 Variation of water uptake for chitosan beads in solutions of different pH at different time periods. Water uptake was defined as the ratio of the weight of adsorbed water to the

weight of the cell-immobilized beads right after as the ratio of the weight of adsorbed water to the weight of the cell-immobilized beads right after formation.

5.3.1.3. FTIR spectroscopy of cell-immobilized chitosan beads

To get information about the chemical structure of the chitosan beads and to differentiate between the empty beads and the cell-immobilized beads, FTIR spectra of the chitosan beads were obtained. Three samples of beads were prepared – empty bead, cell-immobilized bead and immobilized bead after treating the simulated hydrolysate. The spectra for the three cases are demonstrated in Fig. 5.23. Some of the peaks for empty, cell-immobilized and used cell-immobilized beads in Fig. 5.23 are as follows – the peaks at 3311, 3370 and 3304 are assigned to -OH stretching [164], peaks at 1100, 1123 and 1108 are assigned to -C-O-C- bridge stretching [165], peaks at 1636, 1639 and 1637 are assigned to -NH bend stretching [165], peaks at 897, 898 and 897 are due to the –CH deformation of β-glycosidic bond, and peak at 1400 is assigned to $-CH_2$ stretching [166]. Although, peaks are observed at the same locations for all three cases, there are variations in the % transmittance values for the peaks due to changes in the number of entrapped cells. The additional peaks at 604, 603 and 617 are corresponding to asymmetric bending in $-PO_4$ [167], which was probably due to washing of chitosan beads in potassium phosphate solution. This shows that there was some electrostatic interaction between the amino groups of chitosan and the phosphate groups of buffer. In addition, it can be observed that % transmittance has varied considerably in all three spectra. % transmittance represents the absorption of light by the material. Maximum % transmittance (least absorption) was observed for the empty beads, which was decreased substantially in the cell-immobilized beads and in the used cell-immobilized beads. Increase of the absorption of light suggested that the numbers of bacterial cells had increased after culturing the immobilized cells in the simulated hydrolysate.

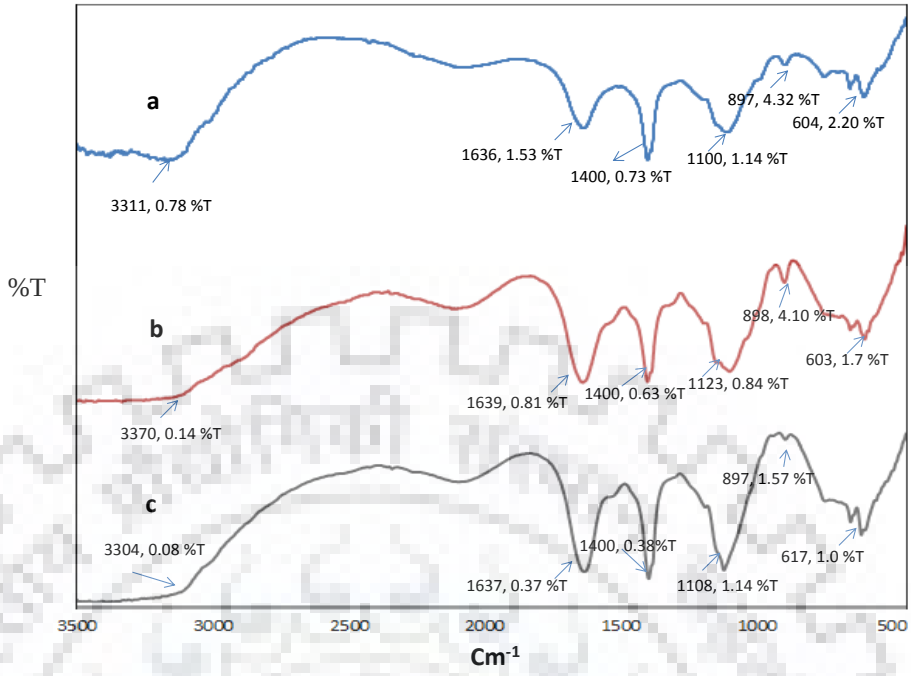

Fig. 5.23 FTIR spectra of (a) Empty chitosan bead (b) Fresh microbial cells immobilized chitosan bead (c) Microbial cells immobilized chitosan bead after culturing in hydrolysate for time period 28 h.

5.3.2. Effect of initial biomass loading on HMF and furfural degradation

The effect of initial biomass loading within the chitosan beads on HMF and furfural degradation is elucidated in Fig. 5.24. For furfural, almost complete removal was achieved within 24-28 h of incubation time using 5 mg, 10 mg and 20 mg of initial biomass loading in 50 ml of 2 wt% chitosan solutions. For HMF, degradation was lower compare to furfural in most of the cases and almost complete removal was achieved after 28 h of incubation time using 10 mg and 15 mg of initial biomass loading in 50 ml of 2 wt% chitosan solutions. It is also evident from Fig. 5.24 that degradation of the inhibitors was significantly affected by the initial biomass loading. The HMF and furfural degradation rates were increased with increase of biomass loading till 10 mg of initial biomass loading / 50 ml of 2 wt% chitosan, but gradually leveled off on further increasing the biomass loading. In fact, when the biomass loading was 20 mg, the removal % was lower than the 10 and 15 mg biomass loadings. Therefore, 10 mg of initial biomass loading / 50 ml of 2 wt% chitosan was found most suitable to degrade the inhibitors from simulated lignocellulosic hydrolysate. The ‘‘leveling-off’’ trend can be

attributed to the lower availability of free space for cell growth with increase in initial biomass loading beyond 10 mg within the beads. The higher initial cell loading led to saturation within the beads, thereby resulting in the decreases of mass transfer efficiency within the beads [168, 169]. Oxygen diffusion limitation inside the beads may be another factor for this "leveling-off" trend. With increasing biomass loading in the beads, the rate of oxygen consumption became greater than the rate of oxygen transport by diffusion within the beads, and the whole degradation efficiency was reduced [170]. Hence 10 mg of initial biomass loading per 50 ml of 2 wt% chitosan was considered to be the optimum biomass loading and further experiments were conducted with this initial biomass loading.

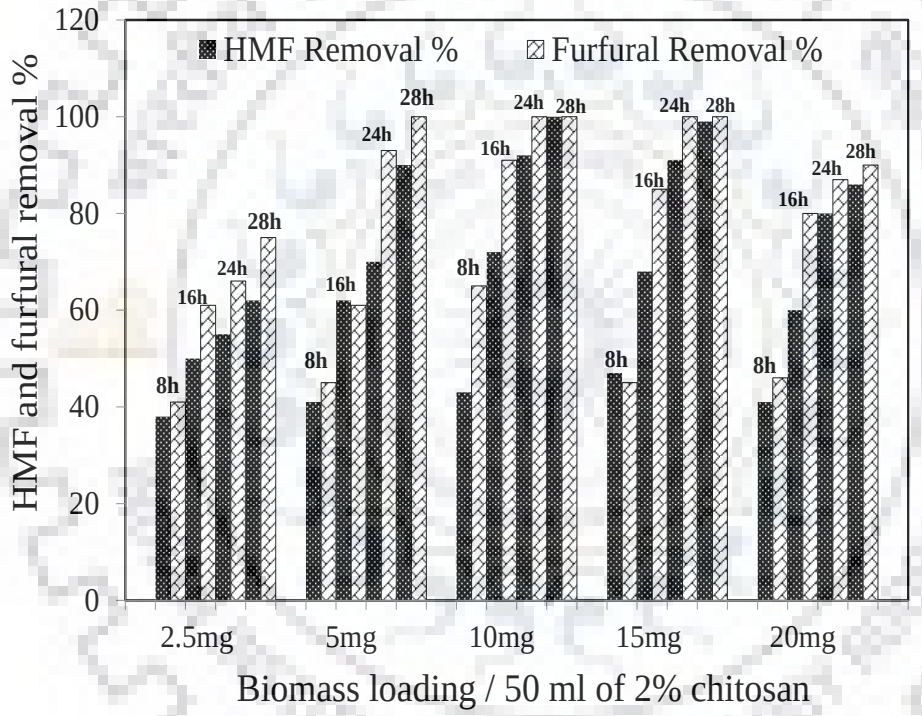

Fig. 5.24 The effect of initial biomass loading within the beads on the degradation of HMF and furfural from the simulated hydrolysate. Inhibitors removal % were analyzed at 8 h, 16 h, 24 h and 28 h for each biomass loading.

5.3.3. Effect of pH on HMF and furfural degradation

pH is a major factor that affects the growth of microorganisms. The effect of initial pH on degradation by both suspended and immobilized *Bordetella* sp. BTIITR is illustrated in Fig. 5.25 (a) and (b), respectively. For the suspended cells, pH 7 was observed to be the most

suitable for degradation, whereas degradation rate was significantly deceased at pH 8 and 9 due to the slower growth of the microorganism (Fig. 5.25). This can be attributed to the higher stress on the organism's metabolic abilities at higher pH [171]. In contrary, the plots in Fig. 5.26 reveal that the inhibitors were degraded satisfactorily both at pH 7 and 8, with pH 8 being marginally better than 7. This can be attributed to the higher swelling of the chitosan beads at higher pH, leading to higher uptake of the inhibitors, which eventually resulted in satisfactory degradation of the inhibitors in spite of the metabolic stress. Even at pH 9, satisfactory degradation was observed for the immobilized cells. At an initial pH of 6, chitosan beads got dissolved in the medium after 16 h of incubation period. Degradation reaction led to the formation of acidic intermediates, such as HMF acid and furoic acid [157], which decreased the pH of the medium to 5.3, and chitosan dissolves below a pH of 5.5. It has also been suggested that with higher positive charges on chitosan, the positively charged surface of chitosan interacts with the negatively charged microbial cell membranes, leading to the leakage of intercellular constituents [172]. Chen et al. [107] reported that pHzpc (point of zero charge) of chitosan beads is around 7.0 to 7.5. Therefore, pH below 7.5 may cause the surface of chitosan to be positively charged, and hence, suppression of the activity of the microorganism.

Comparison of the degradation data between the suspended and the immobilized cells from Fig. 5.25 and Fig. 5.26 reveal some interesting facts. Suspended cells were easily accessible by the inhibitors due to the absence of any significant external mass transfer resistance. In contrary, the inhibitors were subjected to an external mass transfer resistance in presence of the immobilized (encapsulated) cells. This caused delayed response for the immobilized cells in comparison to the suspended cells. The data at pH 7 correspond to this explanation with complete furfural and HMF removal time of 16 and 24 h, respectively for the suspended cells, while 20 and 28 h, respectively for the immobilized cells. However, the data at pH 8 exhibit opposite trend. For the suspended cells, complete furfural and HMF removal time were around 28 and 32 h, respectively, while that for the immobilized cells were 20 and 24 h, respectively. Better degradation with the immobilized cells compare to the suspended cells at pH 8 can be attributed to the protective ambience provided by the chitosan beads. Higher pH of 8 was associated with slower growth of microorganisms due to higher stress on the organisms' metabolic abilities. However, due to the protective barrier of the chitosan beads, the stress experienced by the immobilized cells was lower than the suspended cells.

So, metabolic stress and swelling counteracted each other, and the dominated one dictated the final result. Overall, a pH of 8 was observed to be the most suitable one for the immobilized cells, and therefore, all the experiments with chitosan beads were conducted at pH 8. Similar finding was reported by Nguyen et al. [109], where an optimum pH of 8.7 was observed for absorption of the dye, sulfur blue (SB15), using chitosan beads. Chitosan immobilized cells showed better tolerance for pH as compare to the suspended cells. At higher pH condition, the amine groups present in chitosan became less protonated, resulting in less ionic cross-linking, which led to more permeable surface barrier of chitosan [110].

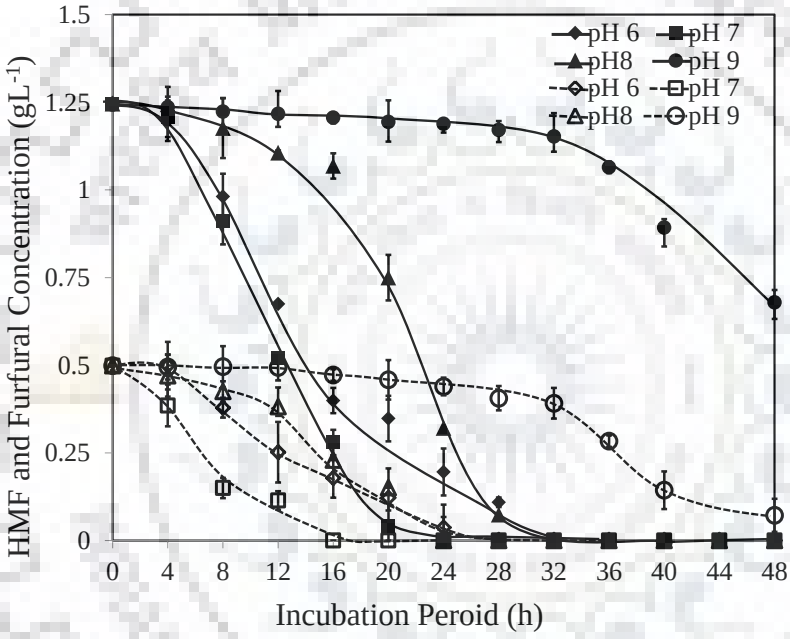

Fig. 5.25 Effect of initial pH on degradation of HMF and furfural from the simulated hydrolysate in free cell culture of *Bordetella* sp. BTIITR. Continuous lines represent HMF and discontinuous lines represent furfural.

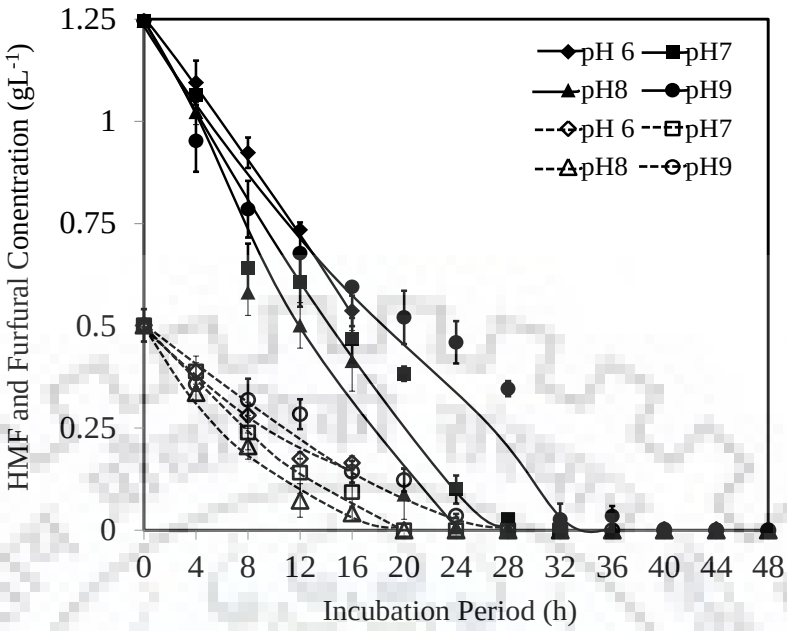

Fig. 5.26 Effect of initial pH on degradation of HMF and furfural from the simulated hydrolysate using immobilized cells of *Bordetella* sp. BTIITR within chitosan beads. Initial biomass loading was 10 mg / 50 ml of 2 wt% chitosan. Continuous lines represent HMF and discontinuous lines represent furfural.

5.3.4. Effect of temperature on HMF and furfural degradation

Most of the microbial species have a specific range of temperature in which they can grow, but they show maximum growth at a particular temperature within that range [173]. Microbial growth is controlled by the rate of chemical reaction catalyzed by enzymes within the cell [173]. Hence, like pH, temperature is also expected to have significant impact on the degradation of the fermentation inhibitors by the microbes. The influence of temperature on the degradation of HMF and furfural from the simulated hydrolysate using the immobilized cells was observed between the temperature range of 25 to 45 °C and the results are represented in Fig. 5.27. The results reveal that the degradation did not vary significantly with temperature up to a shorter incubation period of 8 h. After that the effect of temperature was prominent. 35 to 40 °C was found to be the most suitable range for the HMF and furfural degradation. 96 % HMF and complete furfural removal was observed at 40 °C temperature by immobilized cells in 20 h of incubation period. Earlier, we have reported that the non-immobilized *Bordetella* sp. BTIITR cells were able to degrade 94 % HMF and 100 % furfural at 30 °C from the sugarcane

bagasse hydrolysate. It was also observed that the free cells were more sensitive to the temperature as they showed very little growth below 30 °C and above 35 °C [174] . In contrary, the immobilized cells could degrade the inhibitors at a wider range of temperature. Entrapment of microbial cells inside the chitosan beads played an important role in keeping the cells active at wider range of temperature. Dilute acid pretreatment of lignocellulosic biomass is typically conducted at 120 °C. With immobilized cells, the temperature needs to be brought down to 40 °C, whereas for free cells, temperature needs to be decreased to 30 °C. This indicates a possibility of significant energy savings.

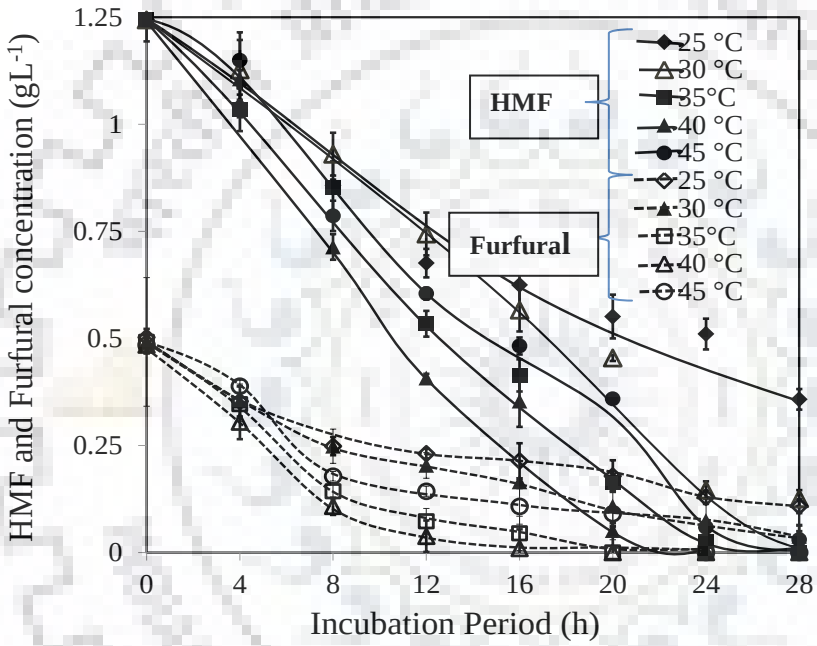

Fig. 5.27 Effect of temperature on the degradation of HMF and furfural from the simulated hydrolysate using chitosan immobilized cells of *Bordetella* sp. BTIITR. Initial biomass loading was taken 10 mg / 50 ml of 2 wt% chitosan at pH 8. Continuous lines represent HMF and discontinuous lines represent furfural.

5.3.5. Effect of HMF concentration on immobilized biomass

Typical concentrations of HMF and furfural in dilute acid pretreated lignocellulosic hydrolysate liquor are found to be around 1-1.5 gL^{-1} (8-12 mM) and 0.5-1 gL^{-1} (5-10 mM), respectively. Degradation of furan compounds by microbial cells has generally been known to be inhibited by the higher concentration of furan itself, leading to extended lag time for degradation [71, 174]. HMF and furfural are the major inhibitors for the growth of microorganisms. As a result, overall production of chemicals decreases during fermentation. Joo et al. [152] reported that on increasing the furfural concentration from 1 gL^{-1} to 3 gL^{-1}, the production of 2,3 butanediol was decreased from 9.22 gL^{-1} to 3.70 gL^{-1}, when glucose was used as a substrate. *Bordetella* sp. BTIITR, in suspension cell culture, showed a tolerance limit of 10 mM HMF concentration [174]. Therefore, to determine the inhibitor tolerance of immobilized *Bordetella* sp. BTIITR, it was grown in different concentrations of HMF ranging from 5 mM to 25 mM, and the results are demonstrated in Fig. 5.28. Chitosan immobilized cells were able to completely degrade 10 mM (1.26 gL^{-1}) HMF in 20 h of incubation period. As expected, with increase in HMF concentration, degradation time increased. 90 % of 25 mM HMF was degraded in 28 h of incubation period. This indicates that the immobilized cells in chitosan beads can tolerate higher inhibitor concentrations compare to the free cells. This observation aligns well with an earlier reported study, which mentioned that chitosan entrapped *Pseudomonas putida* degraded up to 1500 mgL^{-1} (~15mM) phenol compare to that of 1000 mgL^{-1} (~10 mM) for suspension culture [110]. Chitosan beads formed a cross-networking structure, which functioned as protective barrier against the toxicity of the inhibitors. In addition, the active metabolites produced by the entrapped cells, were retained within the beads for longer time and provided a better environment for inhibitor degradation within the beads [175]. The cumulative effect of these factors reduced the substrate inhibition by fermentation inhibitors while using the immobilized microbes.

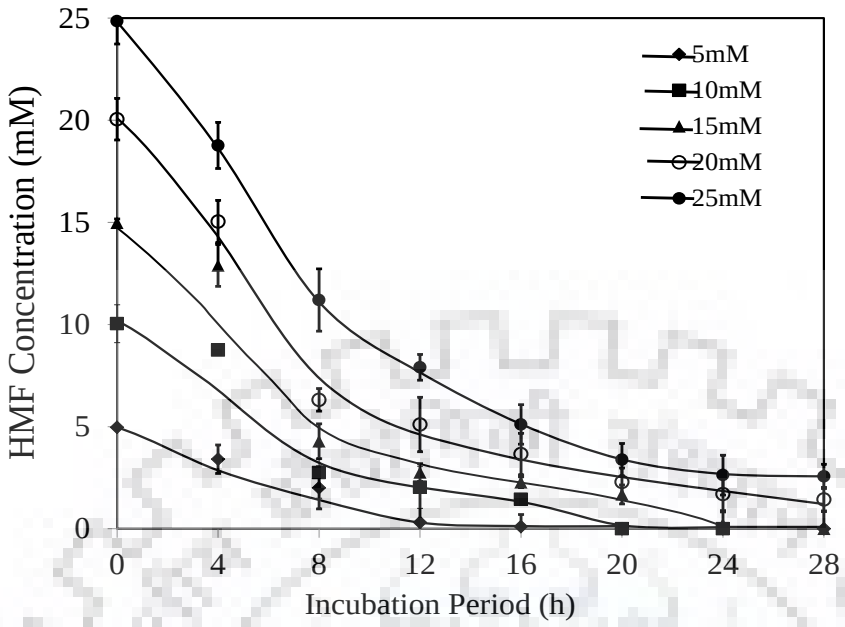

Fig. 5.28 Effect of initial HMF concentration on the degradation of HMF from the simulated hydrolysate using chitosan bead immobilized cells of *Bordetella* sp. BTIITR. In this experiment initial biomass loading 10 mg / 50 ml of 2 wt% chitosan, was used and prepared beads were inoculated in the hydrolysate liquor having pH 8 and incubated at temperature of 40 °C for 48 h.

5.3.6. Biodetoxification of sugarcane bagasse hydrolysate liquor using immobilized cells

The detoxification ability of the immobilized cells was investigated using acid-treated sugarcane bagasse hydrolysate liquor. After acid treatment, HMF and furfural were quantified as 1.30 g/L and 0.6 g/L, respectively in the bagasse hydrolysate liquor. After pH neutralization, 100 mL of bagasse hydrolysate liquor was inoculated with the immobilized cells at pH 8 and 40 °C temperature, and the results are represented in Fig. 5.29. The figure reveals degradation of 86 % of HMF and 100 % of furfural in 20 h of incubation period by the immobilized cells. Hence, the immobilized cells were able to satisfactorily degrade both HMF and furfural, and the degradation pattern was similar as observed earlier for the simulated hydrolysate liquor. This established the efficacy of the immobilized cells in degrading the fermentation inhibitors from actual hydrolysate liquor. Point to note that earlier we have reported degradation of 94 % of HMF and 100 % of furfural in 16 h of incubation period from acid-treated sugarcane bagasse hydrolysate liquor using the free cells of *Bordetella* sp. BTIITR [174]. It was also important to observe that only 10 % of total sugar was consumed in 20 h of detoxification with the

immobilized cells (glucose + xylose concentration reduced from 25 g/L to 22.5 g/L). Significant sugar consumption took place only after HMF and furfural reduced to a lower level. Therefore, the immobilized cells also demonstrated the substrate priority towards the inhibitors over the sugars as observed for the free cells in our previous study [20]. Although the degradation was somewhat slower for the immobilized cells than the free cells, presumably due to the diffusional resistance, other process benefits, such as easier downstream processing and reusability, render the former a preferred choice over the later.

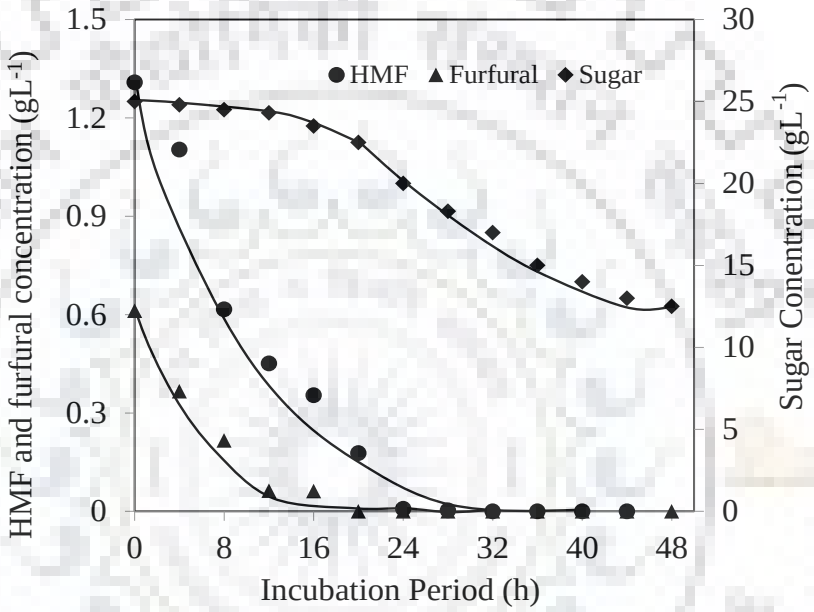

Fig. 5.29 Biodetoxification of sugarcane bagasse hydrolysate liquor containing 1.30 g/L HMF and 0.6 g/L furfural by immobilized cells at pH 8 and 40 °C temperature. Immobilization of cells was conducted using 10 mg biomass/50 mL of 2 wt% chitosan.

5.3.7. Reusability of the immobilized cells

Reuse of immobilized cells is beneficial, because it reduces wastage of cells and significantly improves the time and cost of cultivation. Further, the reusability of the immobilized cells can be utilized to develop a long term continuous bioprocess for degradation of the inhibitors. Therefore, we performed multiple successive HMF and furfural degradation cycles with the simulated hydrolysate liquor by reusing the immobilized cells. Immobilized cells were filtered, washed and transferred after each cycle of 20 h to fresh hydrolysate liquor. This was repeated for 7 consecutive cycles and it was observed that the immobilized cells efficiently degraded

HMF and furfural from the simulated hydrolysate liquor with almost constant degradation efficiency in each of the cycles (Fig. 5.30). Even after 7 cycles, no apparent change in the physical appearance of the bead structure was observed. The constant degradation efficiency and physical appearance indicated no adverse effect on the structural integrity of the immobilized cells. Hence, it can be hypothesized that the immobilized cells can possibly be reused for even more cycles or can be used to develop a continuous bioreactor for longer period of operation. Of course after certain point of time, the degradation capability of the cells will be exhausted. But, for the existing conditions, the immobilized cells are capable of providing steady performance at least up to 7 consecutive cycles. These results align well with the previously reported results, where immobilized cells in chitosan beads were used continuously for 3 month to degrade 100 mg/L of phenol from waste water. During this period, degradation ability of immobilized cells were unaffected [110]. Apart from this, the long term storage stability of the immobilized cells was examined by storing the immobilized cells for 15 days at 4 °C. After 15 days of storage, when immobilized cells of *Bordetella* sp. BTIITR were inoculated in the simulated hydrolysate, 88 % of HMF and 100 % of furfural were degraded in 20 h of incubation period at 40 °C and pH 8. Therefore, storage of chitosan beads at 4 °C neither led to the inactivation of the inhibitor-degrading capability of the entrapped cells nor decreased the mass transfer efficiency of the chitosan beads. Moreover, no breakage or leakage or morphological changes in the structure of the beads was observed after the long-term storage. This observation indicated that *Bordetella* sp. BTIITR-immobilized chitosan beads can easily be stored and reused for an extended period of operation.

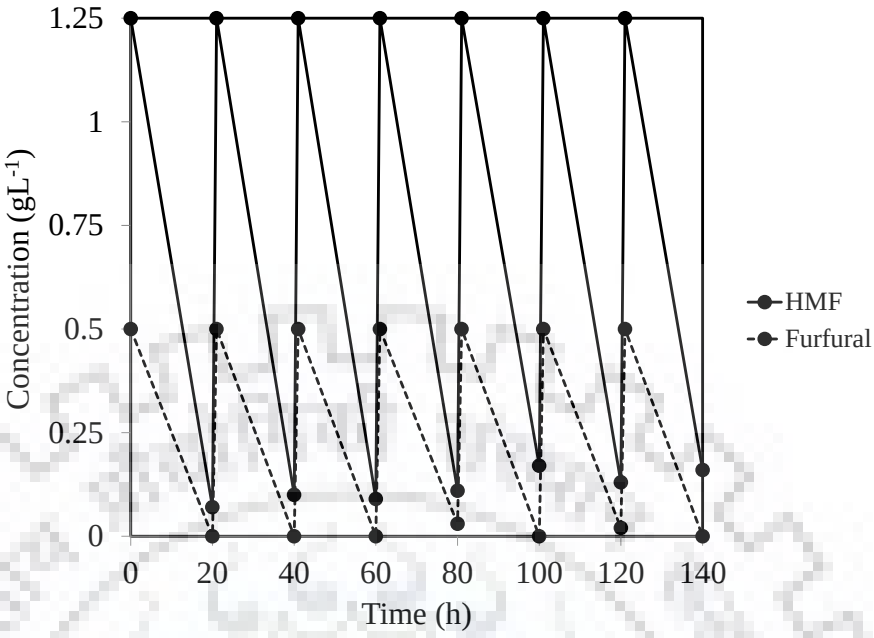

Fig. 5.30 Degradation of HMF and furfural by chitosan-immobilized cells for 7 successive cycles. For every cycle previously used beads were filtered, recovered and reused to detoxify fresh simulated hydrolysate.

5.4. Development and application of a packed bed reactor (PBR) using immobilized cells for detoxification of lignocellulosic hydrolysate liquor

To deliver a translational technology using the immobilized cells of *Bordetella* sp. BTIITR, demonstration of long term biodetoxification within a continuous reactor is essential. Towards that goal, a packed bed reactor (PBR) was developed and implemented for degradation of HMF and furfural from both simulated and actual hydrolysate liquors. This section contains the results of the biodetoxification experiments conducted within the PBR by varying the bed height and flow rate. Analysis of kinetic parameters is also presented in this section.

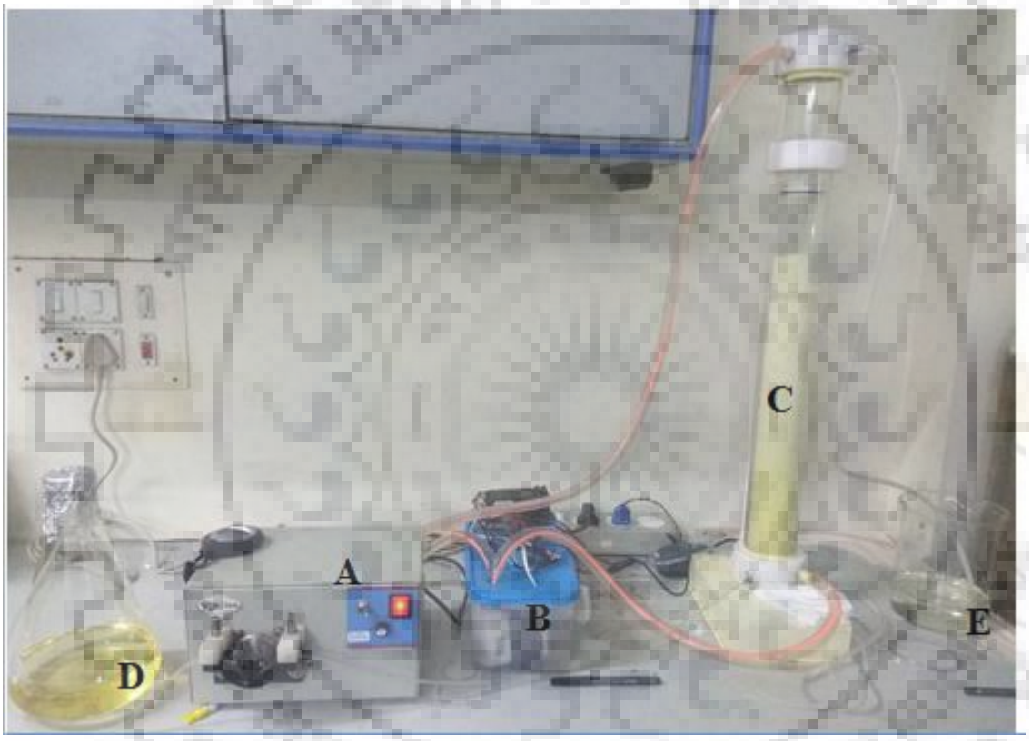

Fig. 5.31 Experimental set-up of the packed bed reactor (PBR) A- Peristaltic pump, B- Temperature controller, C- Packed bed reactor, D- Feed, E- Biodetoxified hydrolysate.

An acrylamide column with inside diameter of 4.4 cm was packed with cell-immobilized beads to form the PBR. To study the effect of bed height on degradation, bed height was varied between 25 cm, 37.5 cm and 50 cm, while keeping the flow rate constant at 4 ml/min using a peristaltic pump. To study the effect of flow rate (residence time) on degradation, a constant bed height of 37.5cm was used, while the flow rate was varied between 2 -5 ml/min. In all the

experiments, temperature of 37 °C was maintained by continuous flow of water through a jacket surrounding the reactor and connected to a heater.

List of symbols

CH_{in} - HMF concentration in the feed (gL^{-1})

CH_{out} - HMF concentration in the effluent from the PBR (gL^{-1})

CF_{in} - Furfural concentration in the feed (gL^{-1})

CF_{out} - Furfural concentration in the effluent from the PBR (gL^{-1})

C_{in} - Total furan concentration in the feed (gL^{-1})

C_{out} Total furan concentration in the effluent (gL^{-1})

k_H - Apparent rate constant (min^{-1}) for HMF degradation

k_F - Apparent rate constant (min^{-1}) for furfural degradation

τ - Residence time or space time of the liquid within the PBR (min)

Q - Flow rate of the feed (ml/min)

V_{PBR} - Total volume of the PBR (ml)

ε - Voidage

εV_{PBR} - Void volume of the PBR

5.4.1. Determination of the kinetic parameters of the degradation reaction

The PBR was assumed to be a continuous, steady state reactor; similar to a plug flow reactor (PFR), i.e. no mixing condition in the direction of flow was assumed to prevail. Therefore, the reactant concentration within the PBR decreased gradually along the length of the reactor from the entrance to the exit. Hence, it is imperative to say that the design equation of a PBR would be a differential equation obtained from reactant mass balance within a differential element. Overall, concentration within the PBR was a function of location, but independent of time; similar to that observed in a PFR. Space time (τ) of a PFR is defined as the time needed to treat unit volume of feed under specified operating conditions [176].

$$\tau = \frac{\varepsilon V_{PBR}}{Q} \quad (7)$$

For bed height of 25 cm, $\tau = \frac{0.29*\pi*2.2^2*25}{4} = \frac{0.29*380}{4} = 27.5\ min$

Similarly, for bed height of 37.5 cm, $\tau = \frac{0.29*\pi*2.2^2*37.5}{4} = \frac{0.29*570}{4} = 41.3\ min$

And, for bed height of 50 cm, $\tau = \frac{0.29*\pi*2.2^2*50}{4} = \frac{0.29*760}{4} = 55\ min$

Where, voidage of PBR, ε, is determined by W/W_h as explained in the Chapter 4. 100 ml cylinder was used to calculate the ε.

$$\varepsilon = \frac{W}{W_h} = \frac{29}{100} = 0.29$$

Integral method of analysis of experimental data was adopted to estimate the kinetic parameters, such as the apparent order of the degradation reaction (n) and the apparent rate constant (k). In this method, a particular form of rate equation is first assumed, and then, after integration with proper limits and mathematical rearrangement, an expression of concentration is obtained that is linearly dependent on τ [176]. This is known as performance equation of the reactor. Then, that particular expression of concentration is plotted as a function of τ to check whether a straight line is obtained, thereby verifying the rate equation. For an irreversible, first order, constant volume reaction in a PBR, the performance equation is as given below.

$$\tau = \frac{\varepsilon V_{PFR}}{Q} = \frac{1}{k}[-\ln(1-X)] = \frac{1}{k}\left[-\ln\frac{C_{out}}{C_{in}}\right] \quad (8)$$

$$\left[-\ln\frac{C_{out}}{C_{in}}\right] = k\tau \quad (9)$$

$$or, C_{out} = C_{in}e^{-k\tau} \quad (10)$$

According to equation (9), if a plot of $-\ln(C_{out}/C_{in})$ vs. τ results in a straight line, then it can be inferred that the reaction follows first order kinetics. Besides, the apparent rate constant can also be determined from the slope of the straight line.

Kinetic experiments were conducted for HMF and furfural degradation using 2 L of simulated hydrolysate liquor. HMF and furfural concentration as a function of time was analyzed to determine the individual kinetic parameters of HMF and furfural degradation. Space time, τ, of

the PBR was varied by changing the bed height to 25 cm, 37.5 cm and 50 cm with same volumetric flow rate of 4 ml/min. These resulted into three different values of τ of 27.5, 41.3 and 55 min, respectively. Then, $-\ln(C_{out}/C_{in})$ vs. τ was plotted as demonstrated in Fig. 5.32 and Fig. 5.33 for HMF and furfural degradation, respectively. The figures reveal linear dependency of the concentration expression on τ with regression coefficient close to unity. This indicates that the degradation reaction of both HMF and furfural by the immobilized bacterium followed pseudo first order kinetics. Although, both the biomass and the inhibitors participated in a complex degradation reaction, we speculate that due to the presence of the excess biomass in our experiments, it behaved as a pseudo first order reaction, i.e. independent of the biomass concentration.

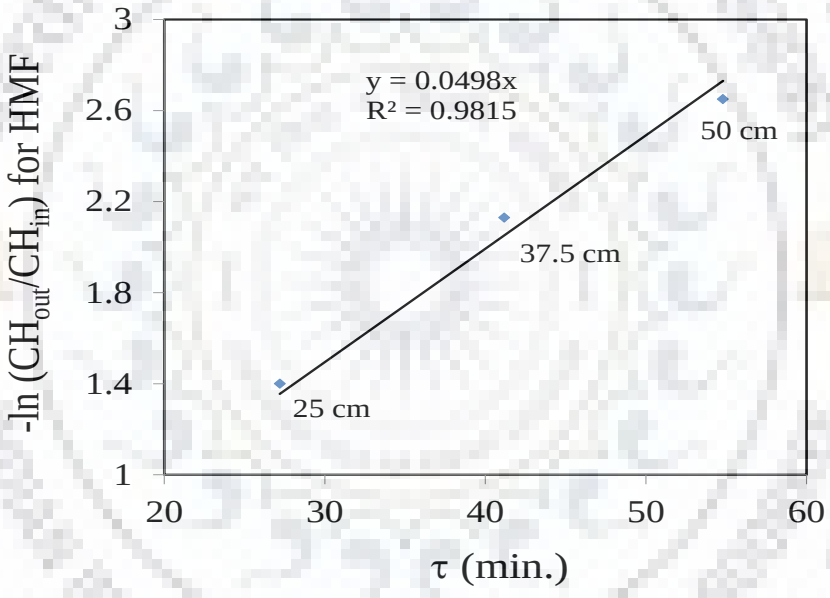

Fig. 5.32 Plot of $-\ln(CH_{out}/CH_{in})$ vs. τ for HMF degradation in the packed bed reactor with flow rate of 4 ml/min and varying bed height of 50 cm, 37.5 cm and 25 cm

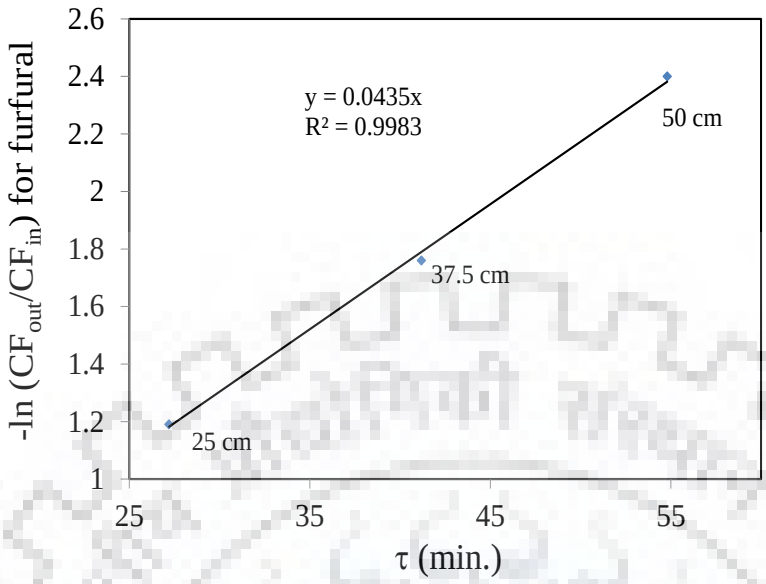

Fig. 5.33 Plot of $-\ln(CF_{out}/CF_{in})$ vs. τ for furfural degradation in the packed bed reactor with flow rate of 4 ml/min and varying bed height of 50 cm, 37.5 cm and 25 cm.

Hence, pseudo first-order kinetics offers a good approximation for the rate of reaction between the inhibitors (both HMF and furfural) and the immobilized cells in a PBR. Accordingly, the rate of degradation of the inhibitors can be written as follows.

$$(-r_H) = k_H C_H \quad (11)$$

$$(-r_F) = k_F C_F \quad (12)$$

Where, the apparent rate constants for HMF and furfural degradation reactions can be calculated from the slopes of Fig. 5.32and Fig. 5.33, respectively as per equation (9).

$$k_H = slope\ of\ Fig.5.4.1 = 0.0498\ min^{-1}$$

$$k_F = slope\ of\ Fig.5.4.2 = 0.0435\ min^{-1}$$

Point to note that this kinetic analysis appears to neglect the effect of mass transfer resistance, although in reality, diffusional transport of the reactants and the products has profound influence on the degradation. In the kinetic analysis, we have taken a simplified approach and

assumed that the effects of mass transfer were clubbed within the apparent rate constant (k). Hence, separate analysis of mass transfer was not conducted in this simplified model.

5.4.2. Effect of column bed height on degradation

Bed height of the PBR (h) was varied from 25 to 50 cm at a flow rate of 4 ml/min and temperature was maintained at 37 ^{o} C. Variation in the bed height caused variation in space time (equal to residence time for constant volume reaction). Fig. 5.34 and Fig. 5.35 represent removal of HMF and furfural per unit volume (CH_{in}-CH_{out}), respectively for different bed height as a function of clock time. It can be observed from the figures that HMF and furfural removal increased with increase in bed height for a fixed flow rate due to increase in τ. Fig. 5.36 represents removal of total furans (HMF+furfural) per unit volume (C_{in}-C_{out}) for different bed height as a function of clock time. Maximum removal of 90.2 % was achieved with 50 cm bed height, whereas 86.3 % and 73.8 % removals were observed for 37.5 cm and 25 cm bed heights, respectively. Residual sugar (leftover sugar after 8 h of operation) was 16.4 gL^{-1}, 21.5 gL^{-1} and 22.5 gL^{-1} for the 50, 37.5 and 25 cm bed height, respectively (

Table 5.4). Comparison of both % degradation and residual sugars for the three bed heights reveal that 37.5 cm is the most suitable bed height to treat the hydrolysate as it maintained a proper balance between the degradation and residual sugar, i.e. it enabled higher degradation with an affordable loss of sugars. Fig. 5.36 shows the breakthrough curve as a function of clock time for different bed heights. It can be observed that the breakthrough time increases with increasing bed height at a fixed flow rate. As the bed height increases, the amount of biomass increases and consequently the total number of binding sites also increases, thereby offering a delayed breakthrough time [136, 177].

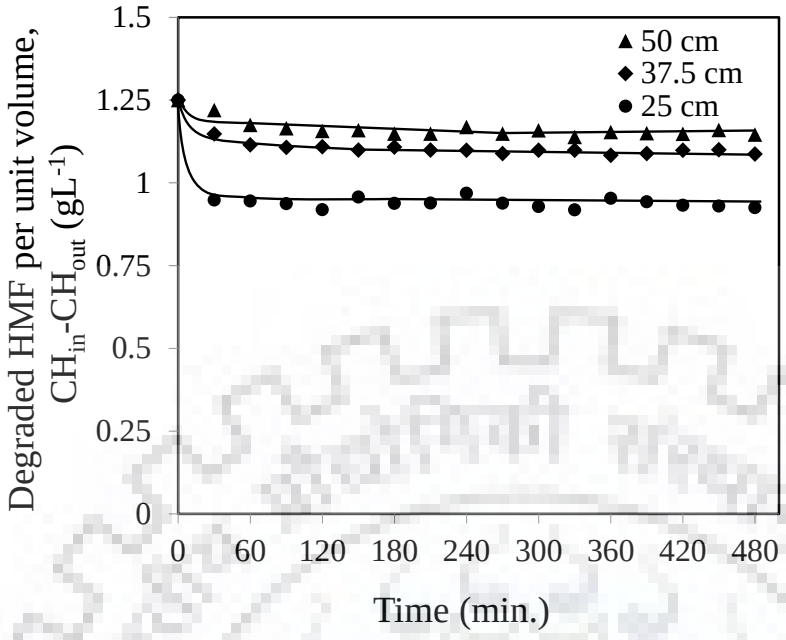

Fig. 5.34 Effect of bed height on degradation of HMF (CH_{in}-CH_{out})in packed bed column (Flow rate: 4 ml/min, Initial HMF concentration: 1.25 gL^{-1}, pH: 8.

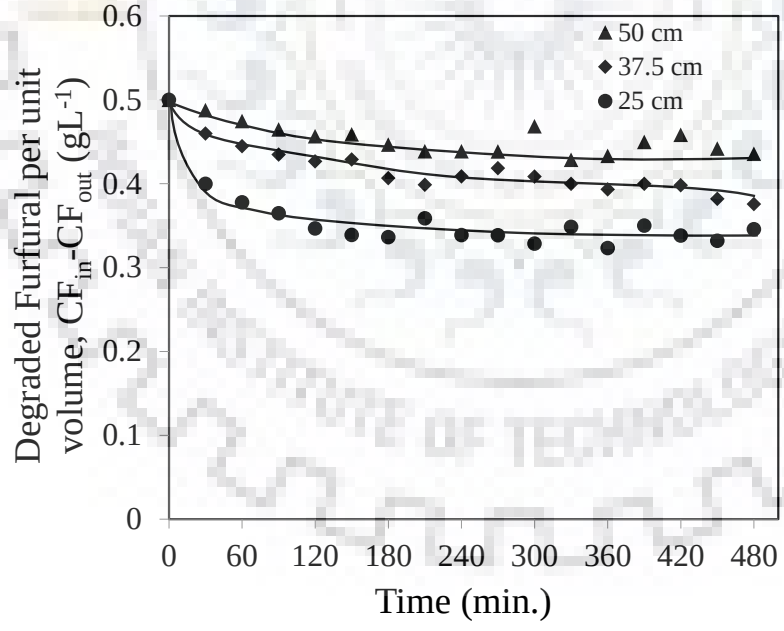

Fig. 5.35 Effect of bed height on degradation of Furfural in packed bed column (Flow rate: 4 ml/min, Initial Furfural concentration: 0.5 gL^{-1}, pH: 8.

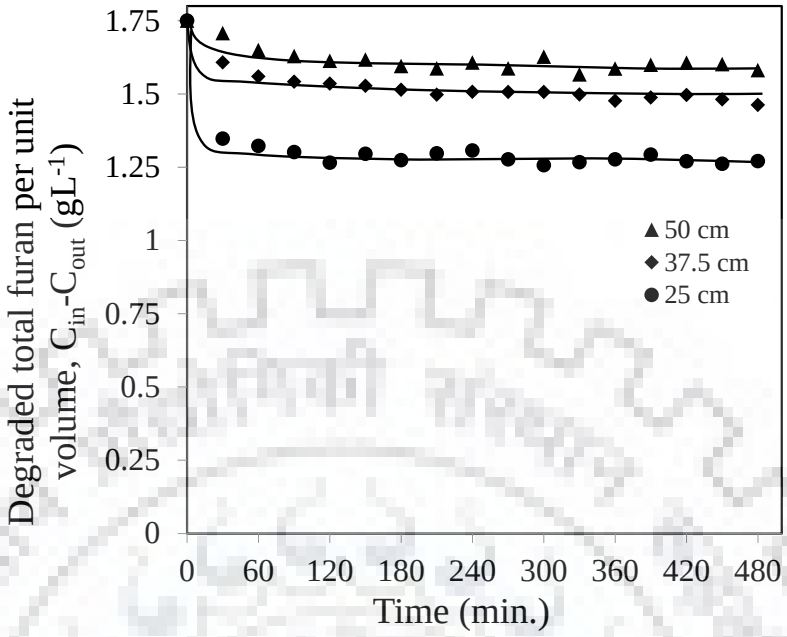

Fig. 5.36 Effect of bed height on degradation of total furan in packed bed column (Flow rate: 4 ml/min, Initial total furan (HMF+Furfural) concentration: 1.75 gL^{-1}, pH: 8.

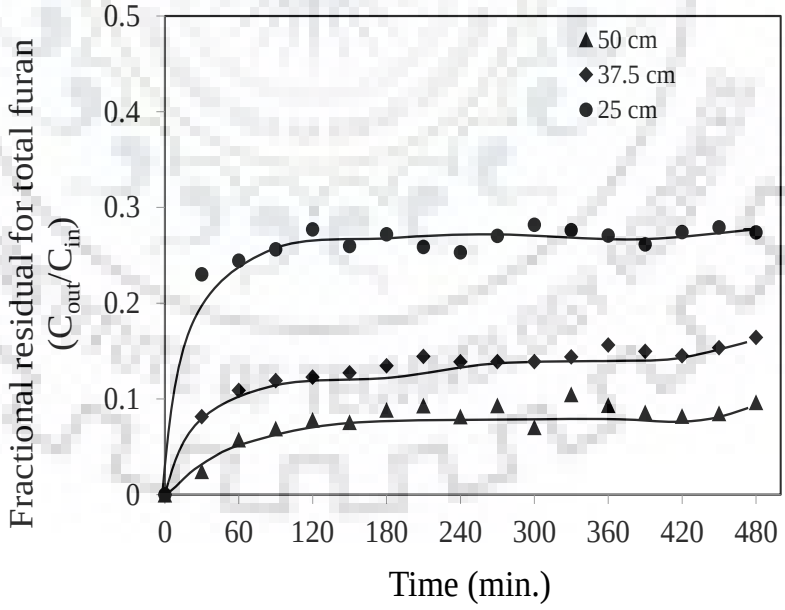

Fig. 5.37 Breakthrough curve obtained at different bed height for total furan degradation (flow rate was fixed at 4 ml/min., initial furan concentration: 1.75 gL^{-1}, pH: 8.

Table 5.4 Removal % of total inhibitors and residual sugars at different bed height and flow rate

Bed height, h (cm)	Flowrate, Q (ml/min.)	Total furan conc. C_{in} (gL^{-1})	Area under the curve,A ($g.minL^{-1}$)	q_{total} (g)	m_{total} (g)	Removal %	Residual total sugar (gL^{-1})
25	4	1.75	620.7	2.8	3.36	73.8	22.5
37.5	4	1.75	730.5	2.90	3.36	86.3	21.5
50	4	1.75	775.4	3.1	3.36	92.2	16.4
37.5	2	1.75	765.2	1.53	1.68	91	17.2
37.5	5	1.75	648.2	3.24	4.2	77.1	22

*Area under the curve was calculated with help of Excel

5.4.3. Effect of flow rate

After bed height optimization, flow rate was also optimized for efficient degradation of the inhibitors from the lignocellulosic hydrolysate at a fixed bed height of 37.5 cm. Flow rate of feed was varied from 2 to 5 ml/min using a peristaltic pump. Total inhibitors concentration (HMF and furfural) was 1.75 gL^{-1} in the simulated hydrolysate. The degradation of inhibitors was found to decrease with increasing flow rate as shown in Fig. 5.38. It was due to the reduction in the residence time with increase in flow rate. Fig. 5.39 represents the breakthrough curve in terms of the total furans ($C_{in} = CH_{in} + CF_{in}$ and $C_{out} = CH_{out} + CF_{out}$) at different flow rates. Maximum removal of inhibitors (91%) was obtained at feed flow rate of 2 ml/min, however it was associated with substantial loss of sugars as shown in the
Table 5.4. In comparison, when 5 ml/min of flow rate was used, 77 % degradation of the inhibitors was observed along with reduction of total sugars from 24 gL^{-1} to 22 gL^{-1}. The best results were obtained for the flow rate of 4 ml/min, where nearly 86% of inhibitors were degraded with affordable loss of sugars (24 gL^{-1} to 21.5 gL^{-1}) as demonstrated in
Table 5.4. Hence, in our case, 37.5 cm bed height and 4 ml/min feed flow rate were found to be the most suitable parameters to detoxify hydrolysate using a cell-immobilized packed bed reactor.

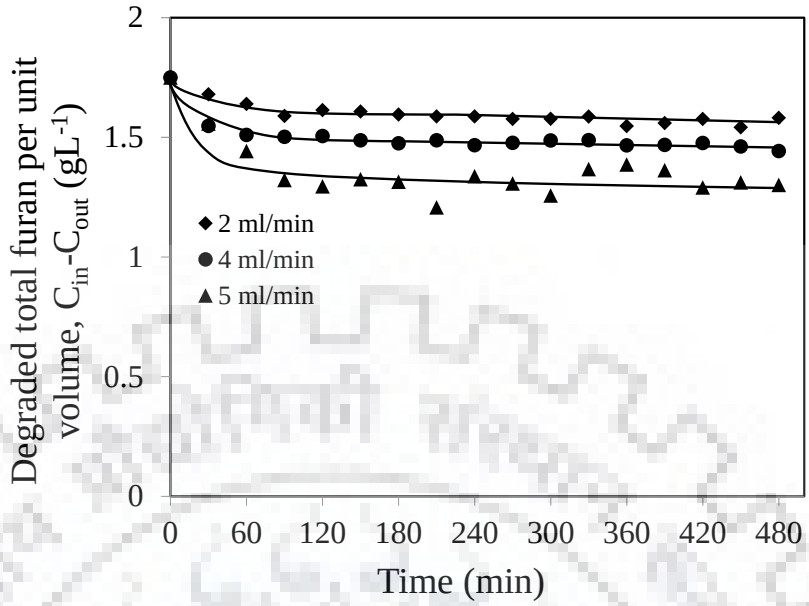

Fig. 5.38 Effect of feed flow rate on degradation of total furan in packed bed column (bed height was 37.5 cm, Initial furan concentration: 1.75 gL^{-1}, pH: 8.

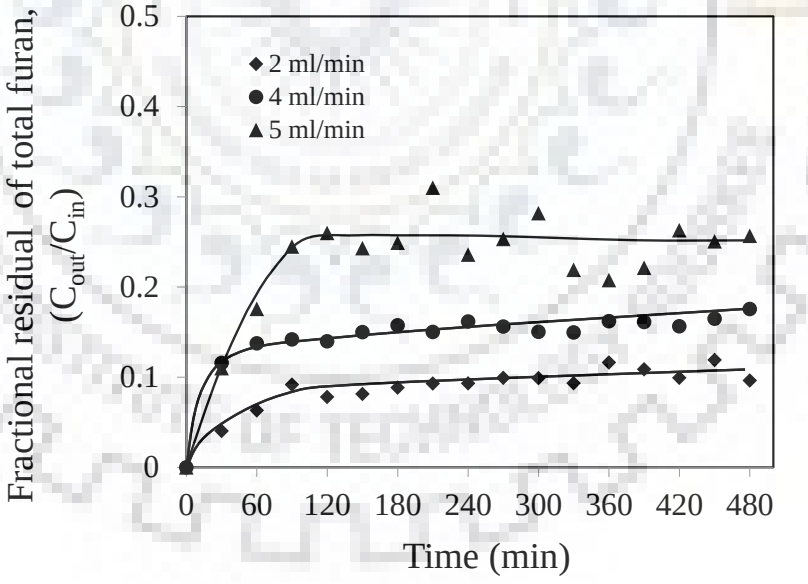

Fig. 5.39 Breakthrough curve obtained at different flow rate of feed for total furan degradation (bed height was fixed at 37.5 cm, initial furan concentration: 1.75 gL^{-1}, pH: 8.

5.4.4. Biodetoxification of sugarcane bagasse hydrolysate liquor using PBR

Detoxification of sugarcane bagasse hydrolysate liquor was conducted in a PBR of 37.5 cm bed height filled with cell-immobilized chitosan beads and operated at 4 ml/min flow rate. 4 L of sugarcane bagasse hydrolysate liquor containing 1.35 gL^{-1} of HMF, 0.55 gL^{-1} of furfural, 8.4 gL^{-1} of glucose and 17.3 gL^{-1} of xylose was obtained from dilute acid pretreatment of sugar cane bagasse as discussed earlier. This hydrolysate liquor was passed through the PBR for 900 min and samples were collected at every 60 min for analysis using HPLC. The results obtained during the experiment are shown in Fig. 5.40. The figure demonstrates that the PBR was able to efficiently degrade the inhibitors as observed earlier for the simulated hydrolysate. The observed conversion was 86 % at 540 min and then the conversion decreased to 74 % at 900 min. The breakthrough curve, represented in Fig. 5.41, depicts that the PBR was able to maintain around 10-12 % of the inlet concentration in the exit till 9 h of operation. Then, the exit concentration increased rapidly and reached to 26 % of the inlet concentration after 15 h of operation. Both of the figures clearly illustrate the capability of the PBR to detoxify sugar cane bagasse hydrolysate liquor for longer period of operation in a continuous mode of feed flow. Point to note that due to inadequate quantity of hydrolysate liquor, complete saturation of the bed is not achieved. However, it is evident that with longer period of operation with higher volume of solution, eventually, the bed (biomass) will lose its degradation capability.

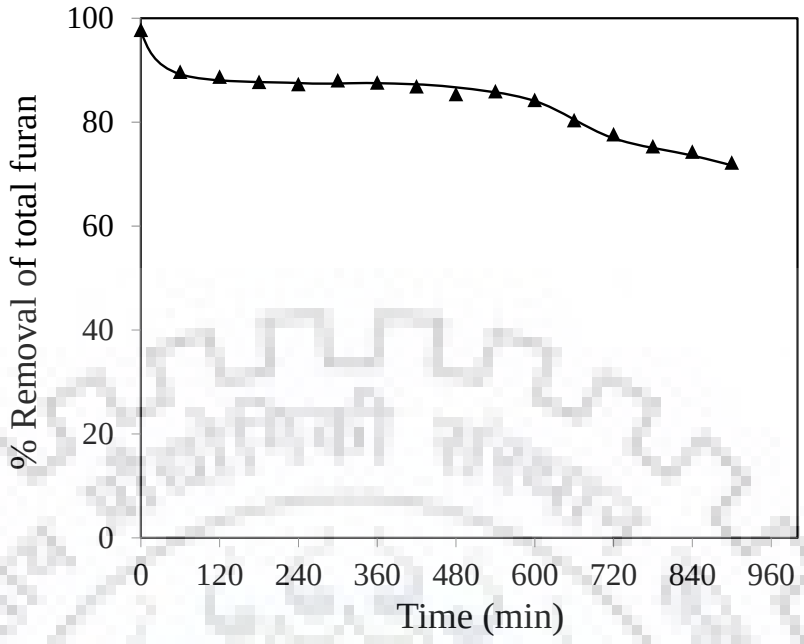

Fig. 5.40 Time course of the % degradation of total furan from the actual sugarcane bagasse hydrolysate in the packed bed reactor (Initial concentration of Total furan (HMF + furfural) was 1.85gL^{-1} respectively).

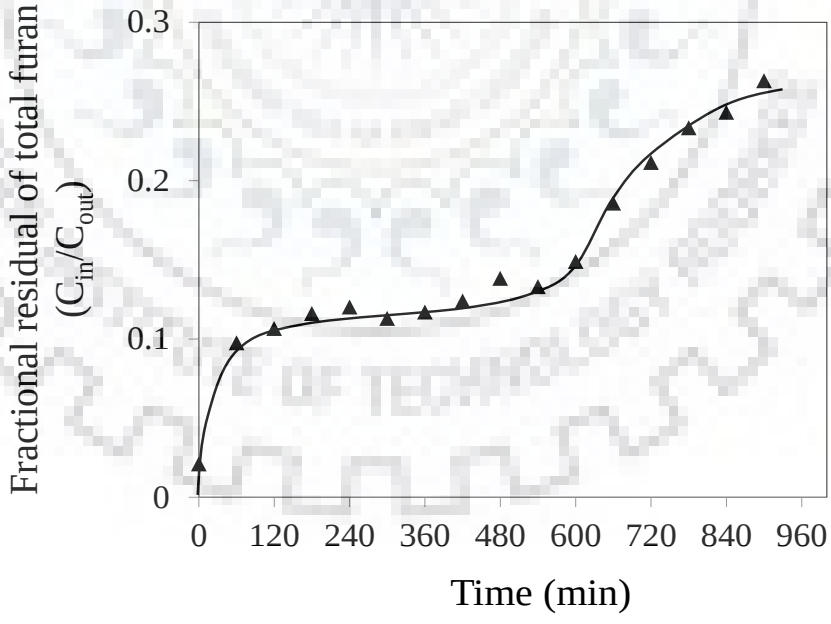

Fig. 5.41 Breakthrough curve for the degradation of furan derivatives from the sugarcane bagasse hydrolysate.

5.5. Study of the effect of biodetoxification on bioethanol production

5.5.1. Ethanol production from simulated hydrolysate liquor detoxified with free cells of *Bordetella* sp. BTIITR

A simulated medium containing 8 gL^{-1} glucose, 8 gL^{-1} xylose, 1.25 gL^{-1} HMF and 0.5 gL^{-1} furfural (total sugar 16 gL^{-1} and total furan 1.75 gL^{-1}) was inoculated with *Bordetella* sp. BTIITR for detoxification. After incubation for 16 h, it was observed that 81 % HMF and 100 % furfural were removed from the simulated hydrolysate. Total sugar was marginally reduced to 14.2 gL^{-1} from the initial sugar concentration of 16 gL^{-1} after the detoxification (Results discussed in Section 5.2). Then, *Pichia stipitis* NCIM 3498 was inoculated in the detoxified and undetoxified hydrolysate liquors and allowed to ferment.

Fig. 5.42 demonstrates that *Pichia stipitis* exhibited a faster growth in the detoxified hydrolysate as compare to the undetoxified hydrolysate. In the undetoxified hydrolysate, HMF and furfural inhibited the growth of *P. stipitis* and a prolonged lag phase was observed. Similar findings were reported by Yee et al. [178] where 27 % less biomass was obtained in furfural-containing media as compare to the control and 58 % less biomass was obtained in HMF-containing media as compare to the control. Fig. 5.43 demonstrates the results for ethanol production and sugar consumption from the undetoxified (control) and the detoxified hydrolysate liquors. In the undetoxified hydrolysate, maximum ethanol concentration of 3.0 gL^{-1} was observed after 48 h of fermentation with ethanol volumetric productivity (Q_p) of 0.062 $gL^{-1}h^{-1}$. Whereas, in the detoxified hydrolyste, maximum ethanol concentration of 4.6 gL^{-1} ethanol was observed in 32 h of incubation period, which corresponds to an ethanol volumetric productivity (Q_p) of 0.14 $gL^{-1}h^{-1}$. Therefore, 1.53 times higher ethanol yield and 2.3 times

higher Q_p were achieved from the detoxified hydrolysate as compare to the undetoxified hydrolysate. Similar findings were reported by Fonseca et al. [179] where they observed 1.96 times higher ethanol concentration in detoxified rice straw hydrolysate as compare to the undetoxified rice straw hydrolysate. Zhu et al. [115] reported 21.8 gL^{-1} of ethanol from detoxified corn stover hydrolysate against 3.79 gL^{-1} from undetoxified corn stover hydrolysate. The fate of total sugar, starting from an initial concentration of 14.2 gL^{-1} and 16 gL^{-1} in detoxified hydrolysate and undetoxified hydrolyate , respectively, is also depicted in Fig. 5.43. 96 % of total sugar was consumed in 48 h from the detoxified hydrolysate, while only 62.5 % of total sugar was consumed in 48 h from the undetoxified hydrolysate.

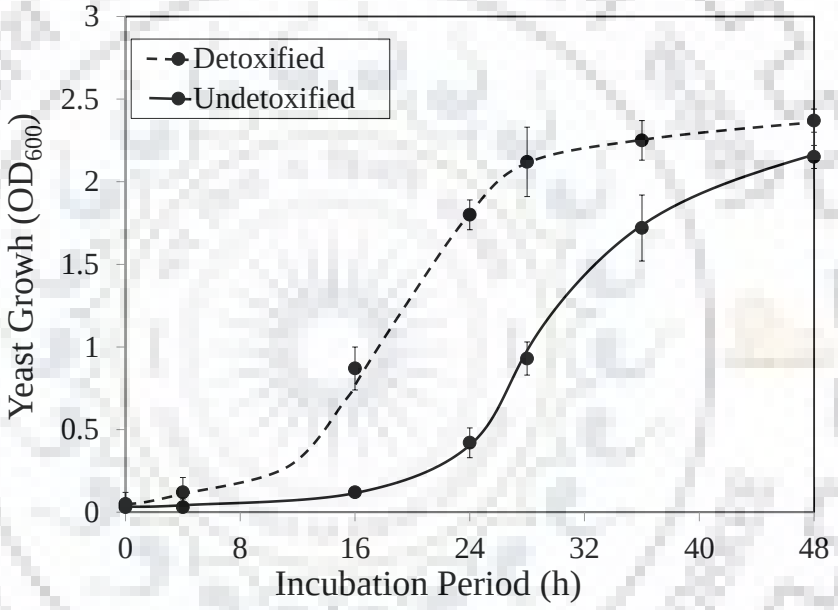

Fig. 5.42 Growth of *Pichia stipitis* in the detoxified and undetoxified simulated hydrolysate liquors.

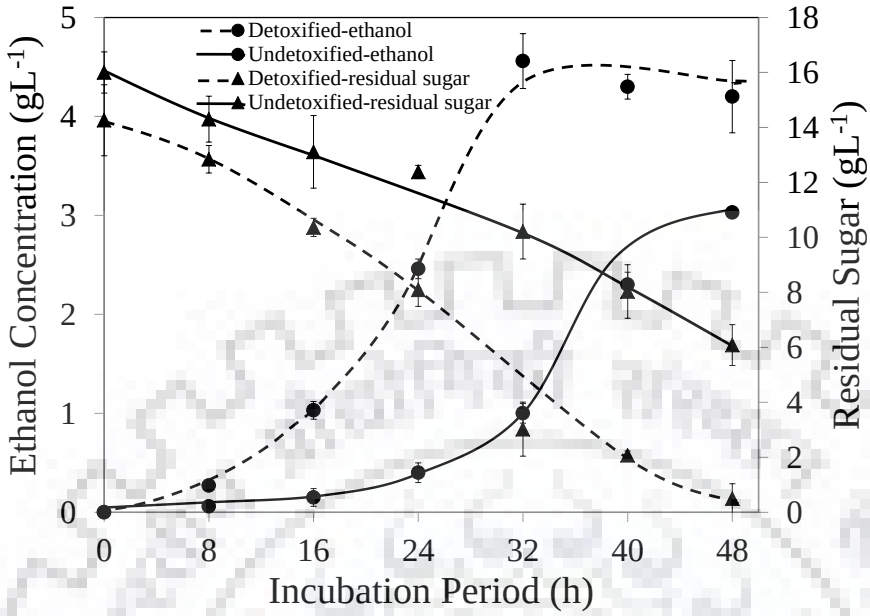

Fig. 5.43 Ethanol production and sugar consumption during the fermentation of the detoxified and the undetoxified simulated hydrolysate liquors using *Pichia stipitis* as fermenting microorganism.

5.5.2. Ethanol production from sugarcane bagasse hydrolysate liquor detoxified with free cells of *Bordetella* sp. BTIITR

To investigate the effect of detoxification on ethanol production in the real system, sugarcane bagasse hydrolysate liquor was used. This hydrolysate was containing 27.3 gL^{-1} of sugars (glucose + xylose) and 1.85 gL^{-1} of furan derivatives (HMF + furfural). The actual lignocellulosic hydrolysate liquor was detoxified by inoculating *Bordetella* sp. BTIITR cells for 16 h. It was observed that most of the HMF and furfural were disappeared from the broth. Total sugar left in sugarcane bagasse hydrolysate after detoxification was 24.5 gL^{-1}. Detoxified and undetoxified (control) hydrolysate liquors were fermented using *Pichia stipitis* for 48 h. Fig. 5.44 demonstrates the ethanol production from the undetoxified (control) and detoxified hydrolysate liquors. In the undetoxified hydrolysate, maximum ethanol concentration of 5.2 gL^{-1} was observed after 48 h of fermentation with volumetric productivity (Q_p) of 0.11 $gL^{-1}h^{-1}$. While in the detoxified hydrolysate, maximum ethanol concentration of 8.4 gL^{-1} was observed in 32 h of incubation period, which corresponds to an ethanol volumetric productivity (Q_p) of

0.26 $gL^{-1}h^{-1}$. Therefore, 1.61 times higher ethanol yield and 2.6 times higher Q_p were achieved from the detoxified bagasse hydrolysate as compare to the undetoxified bagasse hydrolysate. Fig. 5.44 also demonstrates the fate of sugars for the detoxified and the undetoxified bagasse liquors during fermentation. 64.7 % of sugar was consumed for the undetoxified liquor, whereas 93 % of sugar was consumed for the detoxified liquor. Therefore, the benefit of biological detoxification using the free cells of *Bordetella* sp. BTIITR on ethanol formation was evident from the above study using sugar cane bagasse hydrolysate liquor.

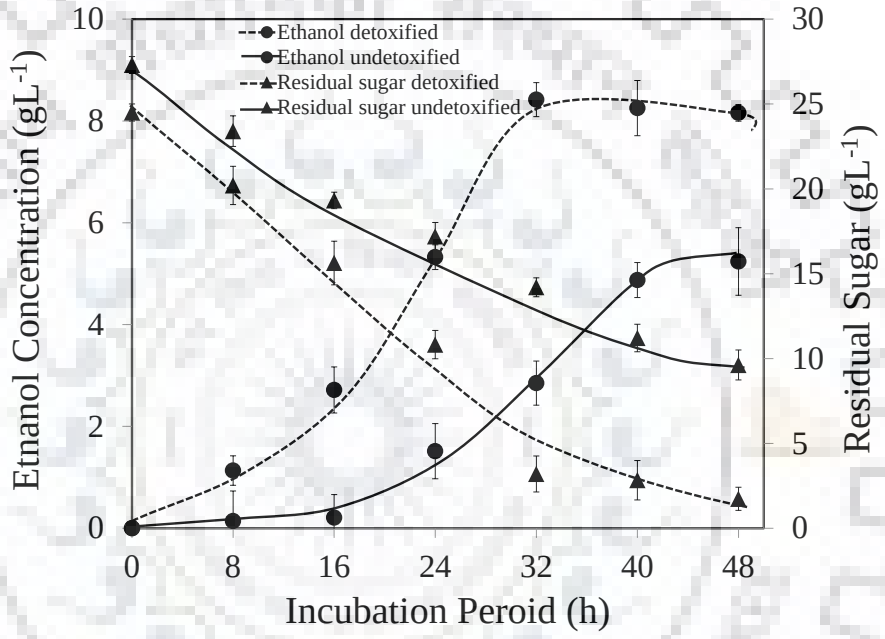

Fig. 5.44 Ethanol production and sugar consumption during the fermentation of the detoxified and undetoxified sugarcane bagasse hydrolysate liquors using *Pichia stipitis* as fermenting microorganism (hydrolysate before detoxification contained 27.3 gL^{-1} of total sugar and 1.85 gL^{-1} of total furans).

5.5.3. Ethanol production from simulated hydrolysate liquor detoxified using packed bed reactor (PBR) containing immobilized cells.

The simulated hydrolysate, containing 16 gL^{-1} xylose, 8 gL^{-1} glucose 1.25 gL^{-1} HMF and 0.5 gL^{-1} furfural, (total 24 gL^{-1} sugars and 1.75 of furan derivatives), was detoxified using the PBR of different bed heights. Detoxified hydrolysates were containing 16.4 gL^{-1}, 21.5 gL^{-1} and 22.5 gL^{-1} sugars from 50 cm, 37.5 cm and 25 cm bed height, respectively as discussed earlier in

Section 5.4. All three detoxified hydrolysate liquors and an undetoxified liquor were fermented using *Pichia stipitis* as demonstrated in Fig. 5.46. Maximum ethanol concentration of 7.24 gL^{-1} was obtained from the detoxified hydrolysate treated with PBR of bed height 37.5 cm after 32 h of incubation period. Then, 7.0 gL^{-1} of ethanol was produced from the hydrolysate detoxified with 25 cm bed height in 40 h. The ethanol produced from the detoxified hydrolysate from 50 cm bed was lower than the 37.5 and 25 cm bed heights due to low remaining concentration of sugars. Maximum ethanol was obtained from the hydrolysate detoxified with the 37.5 bed height. However maximum inhibitors removal was obtained in the 50 cm bed height
Table 5.4). From the undetoxified simulated hydrolysate, only 4.7 gL^{-1} ethanol was produced, which shows that furan inhibitors, like HMF and furfural, decrease the efficiency of fermenting microorganism *Pichia stipitis*. Corresponding residual sugar curves also demonstrate better utilization of sugars for the detoxified hydrolyte liquors in 48 h of incubation period compare to the undetoxified one. Overall, detoxified simulated hydrolysate liquors led to a significantly improved ethanol production pathway as evident from up to 54 % [i.e. (7.24-4.7)/4.7] higher production of ethanol compare to the undetoxified one.

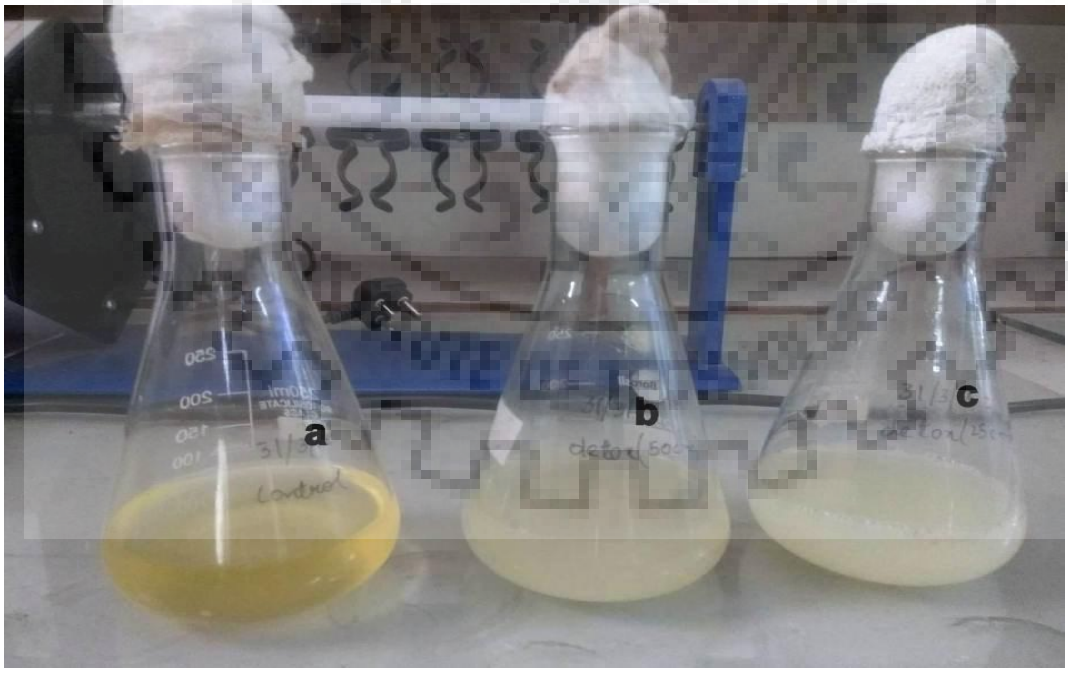

Fig. 5.45 (a) growth of *Pichia stipitis* in undetoxified hydrolysate liquor at 32 h; (b) and (c) growth of *Pichia stipitis* in detoxified hydrolyate liquor at 32 h.

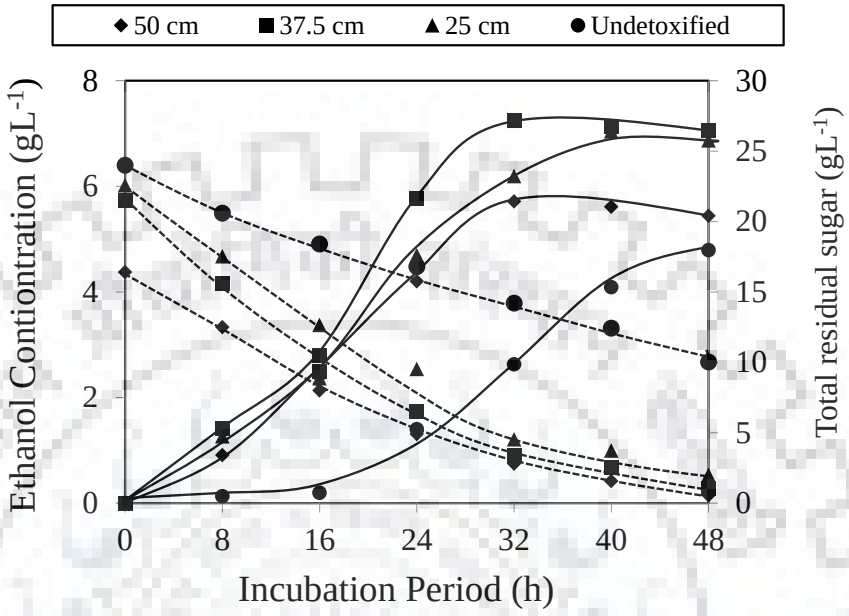

Fig. 5.46 Ethanol production from detoxified hydrolysate obtained from different bed heights of packed bed reactor containing the immobilized cells of *Bordetella* sp BTIITR. Continuous lines represent ethanol production and discontinuous lines denote the residual sugars.

5.5.4. Ethanol production from sugarcane bagasse hydrolysate liquor detoxified using packed bed reactor (PBR) containing immobilized cells

Sugarcane bagasse hydrolysate liquor containing 24.7 gL^{-1} sugars and 1.8 gL^{-1} of furan derivatives was detoxified using the PBR as discussed in Section 5.4. After detoxification, the sugar (glucose and xylose) concentration of the detoxified hydrolysate liquor was measured as 22.7 gL^{-1}. This detoxified hydrolysate was filter-sterilized and inoculated with fermenting microorganism, *Pichia stipitis*, and allowed to ferment for 48 h. Undetoxified (control) sugarcane bagasse hydrolysate was also incubated for fermentation.

Fig. 5.47 and Fig. 5.48 illustrate the fermentation time course of sugar consumption, ethanol production, sugar utilization ratio, and ethanol yield (in terms of % of theoretical yield). Sugar utilization ratio is the ratio of consumed sugar to total sugar in %. Theoretical yield of ethanol is known to be 0.51. As shown in Fig. 5.48, for the fermentation of undetoxified hydrolysate,

4.8 gL^{-1} of ethanol was produced in 48 h. The sugar utilization ratio was 61 % in 48 h. Maximum % of theoretical ethanol yield was 62% in the undetoxified hydrolysate fermentation. The fermentation of the detoxified sugarcane bagasse hydrolysate was easier than that of undetoxified hydrolysate, as illustrated in Fig. 5.47. The initial sugar concentration was 22.7 gL^{-1} in the detoxified hydrolysate. 83 % of sugar utilization was observed in 32 h and 95 % was observed in 48 h of fermentation. Ethanol reached its highest concentration of 7.7 gL^{-1} at 32 h, with a sugar utilization ratio of 83% and an ethanol yield of 80 % of theoretical yield. After 48 h of incubation period, around 95 % sugar was consumed in detoxified hydrolysate against only 61% in the undetoxified hudrolysate. In summary, it can be concluded that the PBR containing the immobilized cells was an efficient tool to detoxify sugarcane bagasse hydrolysate liquor. After detoxification, significantly improved fermentation of sugarcane bagasse hydrolysate was achieved in comparison to the undetoxified hydrolysate by the yeast, *Pichia stipits*.

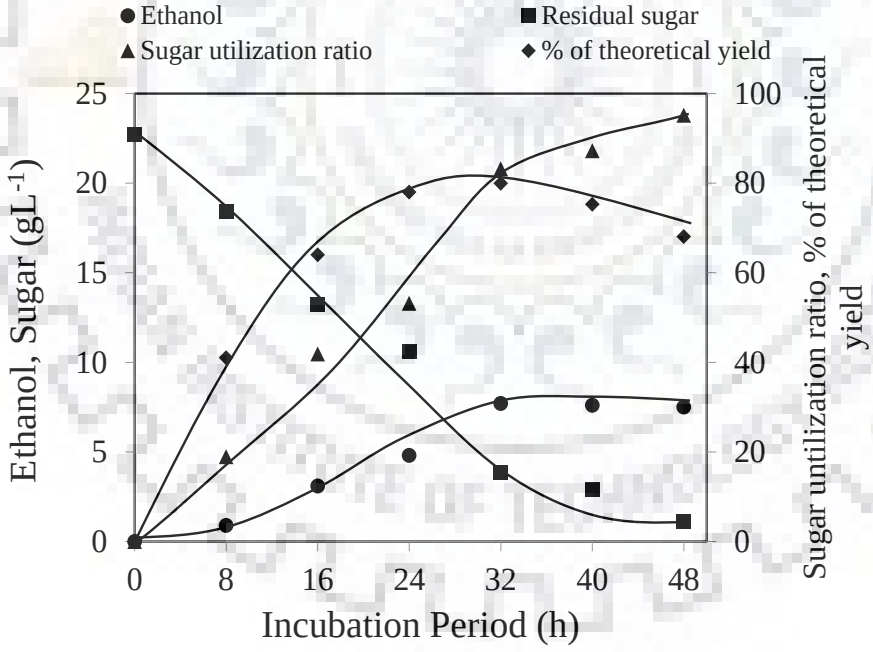

Fig. 5.47 Time course of the fermentation of the detoxified bagasse hydrolysate liquor showing ethanol production, sugar consumption, sugar utilization ratio and % of theoretical yields.

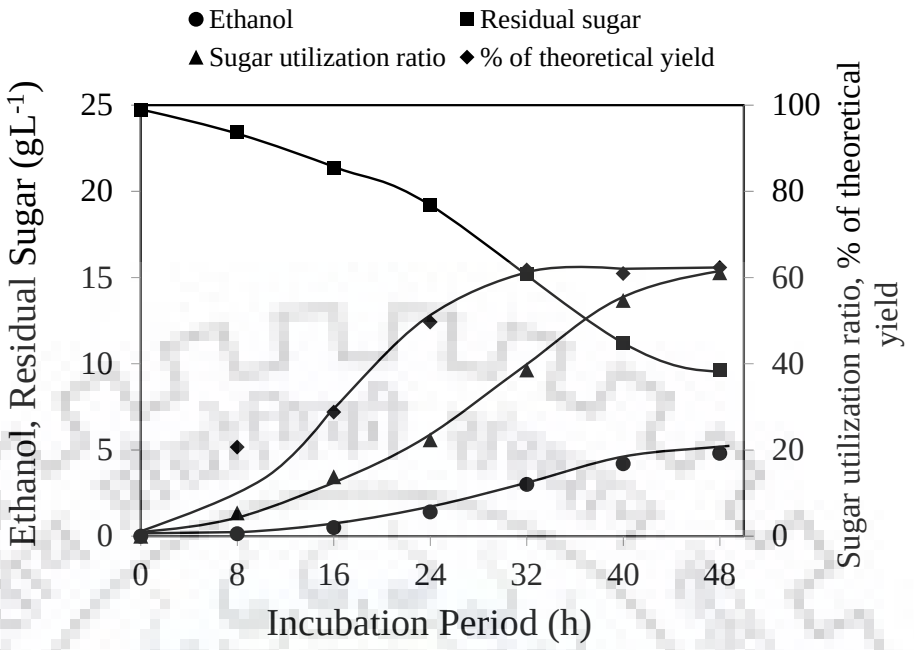

Fig. 5.48 Time course of the fermentation of the undetoxified bagasse hydrolysate liquor showing ethanol production, sugar consumption, sugar utilization ratio and % of theoretical yields.

CHAPTER 6: CONCLUSIONS

We report isolation of a bacterium from soil that utilized HMF as the sole carbon source. The bacterium was characterized and identified as a new strain of *Bordetella* sp. and was designated as *Bordetella* sp BTIITR. All of the characteristics of strain BTIITR were in accordance with those of the members of the genus *Bordetella*, which was placed in family Alcaligenaceae, order Burkholderiales, class Betaproteobacteria, phylum Proteobacteria. Phylogenetic study revealed more than 99 % similarity with the *Bordetella tumbae* and *Bordetella muralis*, which were also isolated from environmental samples. However, some biochemical characteristics, like assimilation of D-xylose, differentiated it from *B. tumabe*, while assimilation of D-glucose differentiated it from the other members of *Bordetella*. This bacterium demonstrated satisfactory degradation of the fermentation inhibitors, HMF and furfural, from lignocellulosic biomass hydrolysate liquor. Cells of the strain BTIITR were observed to be Gram stain-negative, coccobacillus and non-motile. The optimum temperature and pH for growth of bacterium were found to be 30-35 °C and 6-7, respectively. G+C content of the isolated strain was recorded 59.6 to 60 %.

Maximum and most stable growth of the bacterium was observed at around 10 mM concentration of HMF. High concentration of furan derivatives retarded the growth of organism. Since high concentration of HMF (above 10 mM) demonstrated toxic substrate inhibition to the bacterial cells, they took more time to adapt to the environment, resulting into longer lag phase above 10 mM HMF concentration. 30 °C temperature was observed to be the optimum temperature for the HMF degradation using the free cells of *Bordetella* sp. BTIITR strain.

In order to evaluate the degradation performance of *Bordetella* sp. BTIITR, the bacterium was inoculated in a medium having either 10 mM HMF or 10 mM furfural as the sole carbon source. When HMF was the only carbon source in MMH10 medium, *Bordetella* sp. BTIITR was able to degrade 98 % of HMF in 28 h. When furfural was the only carbon source in MMF10 medium, furfural was completely disappeared from the culture broth in 24 h of incubation period. HMF acid, Furoic acid and furfural alcohol were observed as intermediate substance during the degradation of HMF and furfural.

To check the substrate priority, *Bordetella* sp. BTIITR was grown in a mixture containing 10 mM each of HMF, furfural, glucose and xylose in different combinations. When the strain BTIITR was grown in GXH10 media, complete removal of HMF was observed in 24 h of incubation period. When the isolated strain was grown in GXF10 media, complete removal of furfural was observed in 20 h of incubation period. When the strain was grown in GXHF10 medium furfural demonstrated faster rate of removal and was completely disappeared from the culture in 16 h of incubation period. *Bordetella* sp. BTIITR was able to remove 100 % of furfural and 80 % of HMF in just 16 h from the GXHF10 medium. It was also observed that the furan derivatives, HMF and furfural, were almost completely removed (HMF 94 % and furfural 100 %) from the sugarcane bagasse hydrolysate liquor in 16 h of incubation period. The furan derivatives inhibited the activity of the glycolysis enzymes, due to which, initially, glucose and xylose were consumed at a slower rate. Once furfural and HMF were consumed, glucose and xylose were consumed rapidly by the microorganism following the normal glycolysis cycle. From these experimental results, we can speculate that, if we incubate the bacterial culture only for 16 h, most of the toxic compounds can be removed from lignocellulosic hydrolysate liquor without sacrificing significant fraction of sugars. Due to the substrate priority of *Bordetella* sp. BTIITR towards HMF and furfural, fermentable sugars were not consumed significantly before the furfural and HMF reached to lower threshold levels. This suggested that *Bordetella* sp. BTIITR can be a useful microorganism to detoxify the furan derivatives from lignocellulosic hydrolysate liquor prior to the downstream fermentation step.

Bacterial cells were successfully immobilized within the chitosan beads, which were able to maintain the mechanical and chemical integrity during the course of detoxification. Characterization of cell-immobilized beads was done by FESEM, FTIR and swelling ratio. 10 mg of initial biomass loading / 50 ml of 2 wt % chitosan was found most suitable to degrade the inhibitors from simulated lignocellulosic hydrolysate. Detoxification results suggested that the immobilized *Bordetella* sp. BTIITR cells have several advantages over the free cells. Immobilized cells were able to detoxify lignocellulosic hydrolysate liquor at broader range of operating pH, temperature and inhibitor concentration as compare to the free cells. 96 % HMF and 100 % furfural removal was observed at 40 °C temperature by immobilized cells in 20 h of incubation period. 90 % of 25 mM HMF was degraded in 28 h of incubation period, which indicated that the immobilized cells in chitosan beads can tolerate higher inhibitor

concentrations compare to the free cells. A major highlight of immobilized cell study was the reusability of the immobilized cells for seven consecutive cycles without significant loss of the degradation efficiency. After 15 days of storage at 4 °C, when immobilized cells of *Bordetella* sp. BTIITR were inoculated in the simulated hydrolysate, immobilized cells degraded 88 % HMF and 100 % furfural in 20 h of incubation period at 40 °C, thereby manifesting the storage stability of the immobilized cells.

A packed bed reactor (PBR) was designed and developed with the cell-immobilized chitosan beads. The PBR was assumed to be a continuous, steady state reactor; similar to a plug flow reactor (PFR), i.e. no mixing condition in the direction of flow was assumed to prevail. The space time (τ) was varied by varying the bed height. τ was calculated as 21.5, 41.3 and 55 min for 25, 37.5 and 50 cm bed height, respectively. Simplified kinetic studies revealed that the degradation reaction of HMF and furfural followed first order kinetics. Apparent rate constants, k_H and , were measured as 0.049 min^{-1} and 0.043 min^{-1} for HMF and furfural degradation from simulated hydrolysate. Maximum removal of 92.2 % was achieved with 50 cm bed height, whereas 86.3 % and 73.8 % removals were observed for 37.5 cm and 25 cm bed heights, respectively. Residual sugar (leftover sugar after 8 h of operation) was 16.4 gL^{-1}, 21.5 gL^{-1} and 22.5 gL^{-1} for the 50, 37.5 and 25 cm bed height, respectively. Comparison of both % degradation and residual sugars for the three bed heights reveal that 37.5 cm is the most suitable bed height to treat the hydrolysate as it maintained a proper balance between the degradation and residual sugar, i.e. it enabled higher degradation without significant loss of sugars.

To explore the optimum flow rate for inhibitors degradation, feed flow rate was maintained at 2, 4 and 5 ml/min for a fixed bed height 37.5 cm. Maximum removal of inhibitors (91%) was obtained at feed flow rate of 2 ml/min and a bed height of 37.5 cm. However, in comparison, when 5 ml/min of flow rate was used, 77 % degradation of the inhibitors was observed along with reduction of total sugars from 24 gL^{-1} to 22 gL^{-1}. The best results were obtained for the flow rate of 4 ml/min, where nearly 86 % of inhibitors were degraded with a marginal loss of sugars from 24 gL^{-1} to 21.5 gL^{-1}. For the sugarcane bagasse hydrolysate liquor, the observed inhibitors degradation was 86 % at 540 min and then the conversion decreased to 74 % at 900 min.

This study showed that detoxified hydrolysate provided better environment to the fermenting microorganism as compare to the undetoxified hydrolysate. *Pichia stipitis* exhibited a faster growth in the detoxified hydrolysate as compare to the undetoxified hydrolysate. After detoxification with free cells of *Bordetella* sp. BTIITR, fermentation results revealed 1.53 times higher ethanol yield and 2.3 times higher volumetric productivity from the detoxified simulated hydrolysate liquor as compare to the undetoxified simulated hydrolysate liquor. Similarly, 1.61 times higher ethanol yield and 2.6 times higher volumetric productivity was obtained from the detoxified sugarcane bagasse hydrolysate liquor in comparison to the undetoxified sugarcane bagasse hydrolysate liquor. Concentration of ethanol was 8.4 gL^{-1} and 5.2 gL^{-1} for detoxified bagasse and undetoxified bagasse hydrolysate liquors, respectively.

Fermentation of detoxified simulated hydrolysate liquors from different bed heights of PBR showed that maximum ethanol concentration of 7.24 gL^{-1} was associated with the bed height of 37.5 cm in 32 h of incubation period. Then, 7.0 gL^{-1} ethanol was produced from the hydrolysate detoxified with 25 cm bed height in 40 h. The ethanol produced from the detoxified hydrolysate from 50 cm bed was lower than the 37.5 and 25 cm bed height due to low residual sugar concentration. This study suggested that 37.5 cm bed height of PBR is optimum to detoxify the hydrolysate.

The fermentation study of sugarcane bagasse detoxified with the PBR using 37.5 cm bed height and 4 ml/min flow rate shows that fermentation of the detoxified sugarcane bagasse hydrolysate was easier than that of undetoxified hydrolysate. From the undetoxified hydrolysate, 4.8 gL^{-1} of ethanol was produced in 48 h. Also, the sugar utilization ratio was 61 % in 48 h and the maximum % of theoretical ethanol yield was 62% during fermentation. While in detoxified sugarcane bagasse, maximum ethanol concentration of 7.7 gL^{-1} was achieved in 32 h with a sugar utilization ratio of 83 % and an ethanol yield of 80 % (% of theoretical yield). In 48 h of incubation period, around 95 % sugars were consumed in detoxified hydrolysate against only 61 % for the undetoxified hydrolysate.

In summary, this study promises to deliver a translational technology for biological detoxification of lignocellulosic biomass hydrolysate liquor, which subsequently leads to significant improvement in the overall economics of bioethanol production.

CHAPTER 7: MAJOR SCIENTIFIC ACCOMPLISHMENTS

- A bacterium, *Bordetella* sp. BTIITR, capable of degrading the fermentation inhibitors, furfural and HMF, was isolated from soil, identified and characterized.
- *Bordetella* sp. BTIITR demonstrated the ability to selectively consume furfural and HMF from lignocellulosic hydrolysate liquor without significantly affecting the sugars.
- The immobilized cells of *Bordetella sp.* BTIITR enabled further process improvements in terms of tolerance for wider range of operating parameters, reusability for subsequent cycles and easier downstream processing.
- A packed bed reactor was developed using the immobilized cells and was successfully employed for continuous detoxification of lignocellulosic hydrolysate liquor.
- The detoxified hydrolysate liquor led to improved ethanol production as compare to the undetoxified hydrolysate liquor.

CHAPTER 8: REFERENCES

[1] Althuri A, Chintagunta AD, Sherpa KC, Banerjee R. Simultaneous Saccharification and Fermentation of Lignocellulosic Biomass. Biorefining of Biomass to Biofuels: Springer; 2018. p. 265-85.

[2] Althuri A, Banerjee R. Separate and simultaneous saccharification and fermentation of a pretreated mixture of lignocellulosic biomass for ethanol production. Biofuels. 2017:1-12.

[3] Sivakumar G, Vail DR, Xu J, Burner DM, Lay JO, Ge X, et al. Bioethanol and biodiesel: Alternative liquid fuels for future generations. Engineering in Life Sciences. 2010;10:8-18.

[4] Ho S-H, Huang S-W, Chen C-Y, Hasunuma T, Kondo A, Chang J-S. Bioethanol production using carbohydrate-rich microalgae biomass as feedstock. Bioresource technology. 2013;135:191-8.

[5] Nigam PS, Singh A. Production of liquid biofuels from renewable resources. Progress in energy and combustion science. 2011;37:52-68.

[6] Taherzadeh M, Gustafsson L, Niklasson C, Lidén G. Physiological effects of 5-hydroxymethylfurfural on Saccharomyces cerevisiae. Applied microbiology and biotechnology. 2000;53:701-8.

[7] Datta S, Lin YJ, Schell DJ, Millard C, Ahmad SF, Henry MP, et al. Removal of acidic impurities from corn stover hydrolysate liquor by resin wafer based electrodeionization. Industrial & Engineering Chemistry Research. 2013;52:13777-84.

[8] Mosier N, Wyman C, Dale B, Elander R, Lee Y, Holtzapple M, et al. Features of promising technologies for pretreatment of lignocellulosic biomass. Bioresource technology. 2005;96:673-86.

[9] Parawira W, Tekere M. Biotechnological strategies to overcome inhibitors in lignocellulose hydrolysates for ethanol production: review. Critical reviews in biotechnology. 2011;31:20-31.

[10] Liu Z, Slininger P, Dien B, Berhow M, Kurtzman C, Gorsich S. Adaptive response of yeasts to furfural and 5-hydroxymethylfurfural and new chemical evidence for HMF conversion to 2, 5-bis-hydroxymethylfuran. Journal of Industrial Microbiology and Biotechnology. 2004;31:345-52.

[11] Palmqvist E, Hahn-Hägerdal B. Fermentation of lignocellulosic hydrolysates. I: inhibition and detoxification. Bioresource technology. 2000;74:17-24.

[12] Malav MK, Prasad S, Kharia SK, Kumar S, Sheetal K, Kannojiya S. Furfural and 5-HMF: Potent fermentation inhibitors and their removal techniques. Int J Curr Microbiol App Sci. 2017;6:2060-6.

[13] Gorsich S, Dien B, Nichols N, Slininger P, Liu Z, Skory C. Tolerance to furfural-induced stress is associated with pentose phosphate pathway genes ZWF1, GND1, RPE1, and TKL1 in Saccharomyces cerevisiae. Applied microbiology and biotechnology. 2006;71:339-49.

[14] Phitsuwan P, Sakka K, Ratanakhanokchai K. Improvement of lignocellulosic biomass in planta: a review of feedstocks, biomass recalcitrance, and strategic manipulation of ideal plants designed for ethanol production and processability. Biomass and bioenergy. 2013;58:390-405.

[15] Taherzadeh MJ, Karimi K. Pretreatment of lignocellulosic wastes to improve ethanol and biogas production: a review. International journal of molecular sciences. 2008;9:1621-51.

[16] Horváth IS, Franzén CJ, Taherzadeh MJ, Niklasson C, Lidén G. Effects of furfural on the respiratory metabolism of Saccharomyces cerevisiae in glucose-limited chemostats. Applied and environmental microbiology. 2003;69:4076-86.

[17] Modig T, Liden G, Taherzadeh MJ. Inhibition effects of furfural on alcohol dehydrogenase, aldehyde dehydrogenase and pyruvate dehydrogenase. Biochemical Journal. 2002;363:769-76.

[18] Sanchez B, Bautista J. Effects of furfural and 5-hydroxymethylfurfural on the fermentation of Saccharomyces cerevisiae and biomass production from Candida guilliermondii. Enzyme and Microbial Technology. 1988;10:315-8.

[19] Allen SA, Clark W, McCaffery JM, Cai Z, Lanctot A, Slininger PJ, et al. Furfural induces reactive oxygen species accumulation and cellular damage in Saccharomyces cerevisiae. Biotechnology for Biofuels. 2010;3:1.

[20] Palmqvist E, Hahn-Hägerdal B. Fermentation of lignocellulosic hydrolysates. II: inhibitors and mechanisms of inhibition. Bioresource technology. 2000;74:25-33.

[21] Mussatto SI, Roberto IC. Alternatives for detoxification of diluted-acid lignocellulosic hydrolyzates for use in fermentative processes: a review. Bioresource technology. 2004;93:1-10.

[22] Qi B, Luo J, Chen X, Hang X, Wan Y. Separation of furfural from monosaccharides by nanofiltration. Bioresource technology. 2011;102:7111-8.

[23] Cantarella M, Cantarella L, Gallifuoco A, Spera A, Alfani F. Comparison of different detoxification methods for steam-exploded poplar wood as a substrate for the bioproduction of ethanol in SHF and SSF. Process Biochemistry. 2004;39:1533-42.

[24] Nilvebrant N-O, Reimann A, Larsson S, Jönsson LJ. Detoxification of lignocellulose hydrolysates with ion-exchange resins. Applied biochemistry and biotechnology. 2001;91:35-49.

[25] Dong H, Bao J. Metabolism: biofuel via biodetoxification. Nature chemical biology. 2010;6:316-8.

[26] Koopman F, Wierckx N, de Winde JH, Ruijssenaars HJ. Efficient whole-cell biotransformation of 5-(hydroxymethyl) furfural into FDCA, 2, 5-furandicarboxylic acid. Bioresource technology. 2010;101:6291-6.

[27] Kourkoutas Y, Bekatorou A, Banat IM, Marchant R, Koutinas A. Immobilization technologies and support materials suitable in alcohol beverages production: a review. Food Microbiology. 2004;21:377-97.

[28] Aksu Z, Bülbül G. Determination of the effective diffusion coefficient of phenol in Ca-alginate-immobilized P. putida beads. Enzyme and microbial technology. 1999;25:344-8.

[29] Haq F, Ali H, Shuaib M, Badshah M, Hassan SW, Munis MFH, et al. Recent progress in bioethanol production from lignocellulosic materials: A review. International Journal of Green Energy. 2016;13:1413-41.

[30] Slininger PJ, Shea-Andersh MA, Thompson SR, Dien BS, Kurtzman CP, Sousa LD, et al. Techniques for the Evolution of Robust Pentose-fermenting Yeast for Bioconversion of Lignocellulose to Ethanol. J Vis Exp. 2016:15.

[31] Van Maris AJ, Abbott DA, Bellissimi E, van den Brink J, Kuyper M, Luttik MA, et al. Alcoholic fermentation of carbon sources in biomass hydrolysates by Saccharomyces cerevisiae: current status. Antonie Van Leeuwenhoek. 2006;90:391-418.

[32] De Bhowmick G, Sarmah AK, Sen R. Lignocellulosic biorefinery as a model for sustainable development of biofuels and value added products. Bioresource technology. 2017.

[33] Vohra M, Manwar J, Manmode R, Padgilwar S, Patil S. Bioethanol production: feedstock and current technologies. Journal of Environmental Chemical Engineering. 2014;2:573-84.

[34] Prasad S. Ethanol production from stalk juice of selected sorghum cultivars using efficient Saccharomyces cerevisiae strains: Indian Agricultural Research Institute; New Delhi; 2005.

[35] Banerjee S, Mudliar S, Sen R, Giri B, Satpute D, Chakrabarti T, et al. Commercializing lignocellulosic bioethanol: technology bottlenecks and possible remedies. Biofuels, Bioproducts and Biorefining: Innovation for a sustainable economy. 2010;4:77-93.

[36] Pan S-Y, Lin YJ, Snyder SW, Ma H-W, Chiang P-C. Development of low-carbon-driven bio-product technology using lignocellulosic substrates from agriculture: Challenges and perspectives. Current Sustainable/Renewable Energy Reports. 2015;2:145-54.

[37] Schenk PM, Thomas-Hall SR, Stephens E, Marx UC, Mussgnug JH, Posten C, et al. Second generation biofuels: high-efficiency microalgae for biodiesel production. Bioenergy research. 2008;1:20-43.

[38] Karemore A, Sen R. Downstream processing of microalgal feedstock for lipid and carbohydrate in a biorefinery concept: a holistic approach for biofuel applications. RSC Advances. 2016;6:29486-96.

[39] Scott SA, Davey MP, Dennis JS, Horst I, Howe CJ, Lea-Smith DJ, et al. Biodiesel from algae: challenges and prospects. Current opinion in biotechnology. 2010;21:277-86.

[40] Banerjee S, Mudliar S, Sen R, Giri B, Satpute D, Chakrabarti T, et al. Commercializing lignocellulosic bioethanol: technology bottlenecks and possible remedies. Biofuels, Bioproducts and Biorefining. 2010;4:77-93.

[41] Timung R, Mohan M, Chilukoti B, Sasmal S, Banerjee T, Goud VV. Optimization of dilute acid and hot water pretreatment of different lignocellulosic biomass: a comparative study. biomass and bioenergy. 2015;81:9-18.

[42] Rajak RC, Banerjee R. An eco-friendly process integration for second generation bioethanol production from laccase delignified Kans grass. Energy Conversion and Management. 2018;157:364-71.

[43] Rajak RC, Banerjee R. Enzyme mediated biomass pretreatment and hydrolysis: a biotechnological venture towards bioethanol production. RSC Advances. 2016;6:61301-11.

[44] Banerjee S, Sen R, Morone A, Chakrabarti T, Pandey R, Mudliar S. Improved wet air oxidation pretreatment for enhanced enzymatic hydrolysis of rice husk for bioethanol production. Dyn Biochem Process Biotechnol Mol Biol. 2012;6:43-5.

[45] Sims RE, Mabee W, Saddler JN, Taylor M. An overview of second generation biofuel technologies. Bioresource technology. 2010;101:1570-80.

[46] Das SP, Ravindran R, Deka D, Jawed M, Das D, Goyal A. Bioethanol production from leafy biomass of mango (Mangifera indica) involving naturally isolated and recombinant enzymes. Preparative Biochemistry and Biotechnology. 2013;43:717-34.

[47] Deshavath NN, Mohan M, Veeranki VD, Goud VV, Pinnamaneni SR, Benarjee T. Dilute acid pretreatment of sorghum biomass to maximize the hemicellulose hydrolysis with minimized levels of fermentative inhibitors for bioethanol production. 3 Biotech. 2017;7:12.

[48] Ruane J, Sonnino A, Agostini A. Bioenergy and the potential contribution of agricultural biotechnologies in developing countries. Biomass and bioenergy. 2010;34:1427-39.

[49] Das SP, Deka D, Ghosh A, Das D, Jawed M, Goyal A. Scale up and efficient bioethanol production involving recombinant cellulase (Glycoside hydrolase family 5) from Clostridium thermocellum. Sustainable Chemical Processes. 2013;1:19.

[50] Datta S, Bals B, Lin YJ, Negri M, Datta R, Pasieta L, et al. An attempt towards simultaneous biobased solvent based extraction of proteins and enzymatic saccharification of cellulosic materials from distiller's grains and solubles. Bioresource technology. 2010;101:5444-8.

[51] Kumar AK, Sharma S. Recent updates on different methods of pretreatment of lignocellulosic feedstocks: a review. Bioresources and bioprocessing. 2017;4:7.

[52] Aditiya H, Mahlia T, Chong W, Nur H, Sebayang A. Second generation bioethanol production: A critical review. Renewable and sustainable energy reviews. 2016;66:631-53.

[53] Lai CH, Li X, Zhu JJ, Yu SY, Yong Q. Detoxification of Steam-Exploded Corn Stover Prehydrolyzate with Organobentonite Enhances Ethanol Fermentation by Pichia stipitis. Bioresources. 2016;11:1905-18.

[54] Iwaki A, Kawai T, Yamamoto Y, Izawa S. Biomass conversion inhibitors furfural and 5-hydroxymethylfurfural induce formation of messenger RNP granules and attenuate translation activity in Saccharomyces cerevisiae. Applied and environmental microbiology. 2013;79:1661-7.

[55] de Oliveira RA, Rossell CEV, Venus J, Rabelo SC, Maciel Filho R. Detoxification of sugarcane-derived hemicellulosic hydrolysate using a lactic acid producing strain. J Biotechnol. 2018;278:56-63.

[56] Galbe M, Zacchi G. Pretreatment of lignocellulosic materials for efficient bioethanol production. Biofuels: Springer; 2007. p. 41-65.

[57] Olofsson K, Bertilsson M, Lidén G. A short review on SSF–an interesting process option for ethanol production from lignocellulosic feedstocks. Biotechnology for biofuels. 2008;1:7.
[58] Mutreja R, Das D, Goyal D, Goyal A. Bioconversion of agricultural waste to ethanol by SSF using recombinant cellulase from Clostridium thermocellum. Enzyme research. 2011;2011.
[59] Wang J, Gao Q, Zhang H, Bao J. Inhibitor degradation and lipid accumulation potentials of oleaginous yeast Trichosporon cutaneum using lignocellulose feedstock. Bioresource technology. 2016;218:892-901.
[60] Huang C-F, Lin T-H, Guo G-L, Hwang W-S. Enhanced ethanol production by fermentation of rice straw hydrolysate without detoxification using a newly adapted strain of Pichia stipitis. Bioresource Technology. 2009;100:3914-20.
[61] Landaeta R, Aroca G, Acevedo F, Teixeira JA, Mussatto SI. Adaptation of a flocculent Saccharomyces cerevisiae strain to lignocellulosic inhibitors by cell recycle batch fermentation. Appl Energy. 2013;102:124-30.
[62] Larsson S, Cassland P, Jönsson LJ. Development of a Saccharomyces cerevisiae strain with enhanced resistance to phenolic fermentation inhibitors in lignocellulose hydrolysates by heterologous expression of laccase. Applied and environmental microbiology. 2001;67:1163-70.
[63] Larsson S, Nilvebrant N-O, Jönsson L. Effect of overexpression of Saccharomyces cerevisiae Pad1p on the resistance to phenylacrylic acids and lignocellulose hydrolysates under aerobic and oxygen-limited conditions. Applied microbiology and biotechnology. 2001;57:167-74.
[64] Petersson A, Almeida JR, Modig T, Karhumaa K, Hahn-Hägerdal B, Gorwa-Grauslund MF, et al. A 5-hydroxymethyl furfural reducing enzyme encoded by the Saccharomyces cerevisiae ADH6 gene conveys HMF tolerance. Yeast. 2006;23:455-64.
[65] Hasunuma T, Sung K-m, Sanda T, Yoshimura K, Matsuda F, Kondo A. Efficient fermentation of xylose to ethanol at high formic acid concentrations by metabolically engineered Saccharomyces cerevisiae. Applied microbiology and biotechnology. 2011;90:997-1004.

[66] Parawira W, Tekere M. Biotechnological strategies to overcome inhibitors in lignocellulose hydrolysates for ethanol production. Critical reviews in biotechnology. 2011;31:20-31.

[67] Chandel AK, Singh OV, Rao LV, Chandrasekhar G, Narasu ML. Bioconversion of novel substrate Saccharum spontaneum, a weedy material, into ethanol by Pichia stipitis NCIM3498. Bioresource technology. 2011;102:1709-14.

[68] Zhuang J, Liu Y, Wu Z, Sun Y, Lin L. Hydrolysis of wheat straw hemicellulose and detoxification of the hydrolysate for xylitol production. BioResources. 2009;4:674-86.

[69] Pan S-Y, Lin YJ, Snyder SW, Ma H-W, Chiang P-C. Assessing the environmental impacts and water consumption of pretreatment and conditioning processes of corn stover hydrolysate liquor in biorefineries. Energy. 2016;116:436-44.

[70] Jönsson LJ, Alriksson B, Nilvebrant N-O. Bioconversion of lignocellulose: inhibitors and detoxification. Biotechnology for Biofuels. 2013;6:16.

[71] Wierckx N, Koopman F, Bandounas L, De Winde JH, Ruijssenaars HJ. Isolation and characterization of Cupriavidus basilensis HMF14 for biological removal of inhibitors from lignocellulosic hydrolysate. Microbial biotechnology. 2010;3:336-43.

[72] Ran H, Zhang J, Gao Q, Lin Z, Bao J. Analysis of biodegradation performance of furfural and 5-hydroxymethylfurfural by Amorphotheca resinae ZN1. Biotechnology for biofuels. 2014;7:51.

[73] Okuda N, Soneura M, Ninomiya K, Katakura Y, Shioya S. Biological detoxification of waste house wood hydrolysate using Ureibacillus thermosphaericus for bioethanol production. Journal of bioscience and bioengineering. 2008;106:128-33.

[74] Alriksson B, Sjöde A, Nilvebrant N-O, Jönsson LJ. Optimal conditions for alkaline detoxification of dilute-acid lignocellulose hydrolysates. Applied Biochemistry and Biotechnology. 2006;130:599-611.

[75] Alriksson B, Cavka A, Jönsson LJ. Improving the fermentability of enzymatic hydrolysates of lignocellulose through chemical in-situ detoxification with reducing agents. Bioresource technology. 2011;102:1254-63.

[76] Cavka A, Jönsson LJ. Detoxification of lignocellulosic hydrolysates using sodium borohydride. Bioresource technology. 2013;136:368-76.

[77] Soudham VP, Brandberg T, Mikkola J-P, Larsson C. Detoxification of acid pretreated spruce hydrolysates with ferrous sulfate and hydrogen peroxide improves enzymatic hydrolysis and fermentation. Bioresource technology. 2014;166:559-65.

[78] Deng F, Aita GM. Detoxification of dilute ammonia pretreated energy cane bagasse enzymatic hydrolysate by soluble polyelectrolyte flocculants. Ind Crop Prod. 2018;112:681-90.

[79] Jönsson L, Palmqvist E, Nilvebrant N-O, Hahn-Hägerdal B. Detoxification of wood hydrolysates with laccase and peroxidase from the white-rot fungus Trametes versicolor. Applied microbiology and biotechnology. 1998;49:691-7.

[80] Gurram RN, Datta S, Lin YJ, Snyder SW, Menkhaus TJ. Removal of enzymatic and fermentation inhibitory compounds from biomass slurries for enhanced biorefinery process efficiencies. Bioresource technology. 2011;102:7850-9.

[81] Mussatto SI, Santos JC, Roberto IeC. Effect of pH and activated charcoal adsorption on hemicellulosic hydrolysate detoxification for xylitol production. Journal of Chemical Technology & Biotechnology: International Research in Process, Environmental & Clean Technology. 2004;79:590-6.

[82] Horváth IS, Sjöde A, Nilvebrant N-O, Zagorodni A, Jönsson LJ. Selection of anion exchangers for detoxification of dilute-acid hydrolysates from spruce. Proceedings of the Twenty-Fifth Symposium on Biotechnology for Fuels and Chemicals Held May 4–7, 2003, in Breckenridge, CO: Springer; 2004. p. 525-38.

[83] Lopez MJ, del Carmen Vargas-García M, Suárez-Estrella F, Nichols NN, Dien BS, Moreno J. Lignocellulose-degrading enzymes produced by the ascomycete Coniochaeta ligniaria and related species: application for a lignocellulosic substrate treatment. Enzyme and Microbial Technology. 2007;40:794-800.

[84] Larsson S, Reimann A, Nilvebrant N-O, Jönsson LJ. Comparison of different methods for the detoxification of lignocellulose hydrolyzates of spruce. Applied biochemistry and biotechnology. 1999;77:91-103.

[85] Chandel AK, Kapoor RK, Singh A, Kuhad RC. Detoxification of sugarcane bagasse hydrolysate improves ethanol production by Candida shehatae NCIM 3501. Bioresource Technology. 2007;98:1947-50.

[86] Chandel AK, da Silva SS, Singh OV. Detoxification of lignocellulosic hydrolysates for improved bioethanol production. Biofuel production-Recent developments and prospects: InTech; 2011.

[87] Converti A, Perego P, Domínguez JM. Xylitol production from hardwood hemicellulose hydrolysates by Pachysolen tannophilus, Debaryomyces hansenii, and Candida guilliermondii. Applied biochemistry and biotechnology. 1999;82:141-51.

[88] Wilson JJ, Deschatelets L, Nishikawa NK. Comparative fermentability of enzymatic and acid hydrolysates of steam-pretreated aspenwood hemicellulose by Pichia stipitis CBS 5776. Applied microbiology and biotechnology. 1989;31:592-6.

[89] Grzenia DL, Schell DJ, Wickramasinghe SR. Membrane extraction for removal of acetic acid from biomass hydrolysates. Journal of Membrane Science. 2008;322:189-95.

[90] Fonseca BG, de Oliveira Moutta R, de Oliveira Ferraz F, Vieira ER, Nogueira AS, Baratella BF, et al. Biological detoxification of different hemicellulosic hydrolysates using Issatchenkia occidentalis CCTCC M 206097 yeast. Journal of industrial microbiology & biotechnology. 2011;38:199-207.

[91] Zhang Y-Q, Tao M-L, Shen W-D, Zhou Y-Z, Ding Y, Ma Y, et al. Immobilization of L-asparaginase on the microparticles of the natural silk sericin protein and its characters. Biomaterials. 2004;25:3751-9.

[92] Rahman RNZA, Ghazali FM, Salleh AB, Basri M. Biodegradation of hydrocarbon contamination by immobilized bacterial cells. The Journal of Microbiology. 2006;44:354-9.

[93] Jack T, Zajic J. The immobilization of whole cells. Advances in Biochemical Engineering, Volume 5: Springer; 1977. p. 125-45.

[94] Leon R, Fernandes P, Pinheiro H, Cabral J. Whole-cell biocatalysis in organic media. Enzyme and Microbial Technology. 1998;23:483-500.

[95] Groboillot A, Boadi D, Poncelet D, Neufeld R. Immobilization of cells for application in the food industry. Critical Reviews in Biotechnology. 1994;14:75-107.

[96] Trelles JA, Rivero CW. Whole cell entrapment techniques. Immobilization of Enzymes and Cells: Springer; 2013. p. 365-74.

[97] López A, Lázaro N, Marqués AM. The interphase technique: a simple method of cell immobilization in gel-beads. Journal of microbiological methods. 1997;30:231-4.

[98] Bickerstaff GF. Immobilization of enzymes and cells. Immobilization of enzymes and cells: Springer; 1997. p. 1-11.

[99] Bayat Z, Hassanshahian M, Cappello S. Immobilization of microbes for bioremediation of crude oil polluted environments: a mini review. The open microbiology journal. 2015;9:48.

[100] Dursun AY, Tepe O. Internal mass transfer effect on biodegradation of phenol by Ca-alginate immobilized Ralstonia eutropha. Journal of hazardous materials. 2005;126:105-11.

[101] Sarin C, Sarin S. Removal of cadmium and zinc from soil using immobilized cell of biosurfactant producing bacteria. Environment Asia. 2010;3:49-53.

[102] Overmeyer C, Rehm H-J. Biodegradation of 2-chloroethanol by freely suspended and adsorbed immobilized Pseudomonas putida US2 in soil. Applied microbiology and biotechnology. 1995;43:143-9.

[103] Wang Y, Tian Y, Han B, Zhao H-b, Bi J-n, Cai B. Biodegradation of phenol by free and immobilized Acinetobacter sp. strain PD12. Journal of Environmental Sciences(China). 2007;19:222-5.

[104] Dwyer DF, Krumme ML, Boyd SA, Tiedje JM. Kinetics of phenol biodegradation by an immobilized methanogenic consortium. Applied and Environmental Microbiology. 1986;52:345-51.

[105] Wu L, Ge G, Wan J. Biodegradation of oil wastewater by free and immobilized Yarrowia lipolytica W 29. Journal of Environmental Sciences(China). 2009;21:237-42.

[106] Tope A, Jamil K, Baggi T. Transformation of 2, 4, 6-trinitrotoluene (TNT) by immobilized and resting cells of Arthrobacter sp. Journal of Hazardous Substance Research. 1999;2:3.

[107] Chen Y-M, Lin T-F, Huang C, Lin J-C, Hsieh F-M. Degradation of phenol and TCE using suspended and chitosan-bead immobilized Pseudomonas putida. Journal of hazardous materials. 2007;148:660-70.

[108] Barreto R, Hissa D, Paes F, Grangeiro T, Nascimento R, Rebelo L, et al. New approach for petroleum hydrocarbon degradation using bacterial spores entrapped in chitosan beads. Bioresource technology. 2010;101:2121-5.

[109] Nguyen TA, Fu C-C, Juang R-S. Effective removal of sulfur dyes from water by biosorption and subsequent immobilized laccase degradation on crosslinked chitosan beads. Chemical Engineering Journal. 2016;304:313-24.

[110] Hsieh F-M, Huang C, Lin T-F, Chen Y-M, Lin J-C. Study of sodium tripolyphosphate-crosslinked chitosan beads entrapped with Pseudomonas putida for phenol degradation. Process Biochemistry. 2008;43:83-92.

[111] Nawaz MS, Franklin W, Cerniglia CE. Degradation of acrylamide by immobilized cells of a Pseudomonas sp. and Xanthomonas maltophilia. Canadian journal of microbiology. 1993;39:207-12.

[112] Vorlop K, Klein J. [22] Entrapment of microbial cells in chitosan. Methods in enzymology: Elsevier; 1987. p. 259-68.

[113] Berger J, Reist M, Mayer JM, Felt O, Peppas N, Gurny R. Structure and interactions in covalently and ionically crosslinked chitosan hydrogels for biomedical applications. European Journal of Pharmaceutics and Biopharmaceutics. 2004;57:19-34.

[114] Nichols NN, Sharma LN, Mowery RA, Chambliss CK, Van Walsum GP, Dien BS, et al. Fungal metabolism of fermentation inhibitors present in corn stover dilute acid hydrolysate. Enzyme and microbial technology. 2008;42:624-30.

[115] Zhu J, Yong Q, Xu Y, Yu S. Detoxification of corn stover prehydrolyzate by trialkylamine extraction to improve the ethanol production with Pichia stipitis CBS 5776. Bioresource technology. 2011;102:1663-8.

[116] Yu Y, Feng Y, Xu C, Liu J, Li D. Onsite bio-detoxification of steam-exploded corn stover for cellulosic ethanol production. Bioresource technology. 2011;102:5123-8.

[117] Banerjee A, Ghoshal AK. Biodegradation of phenol by calcium-alginate immobilized@@ Bacillus cereus in a packed bed reactor and determination of the mass transfer correlation. Journal of Environmental Chemical Engineering. 2016;4:1523-9.

[118] Pazarlioğlu NK, Telefoncu A. Biodegradation of phenol by Pseudomonas putida immobilized on activated pumice particles. Process Biochemistry. 2005;40:1807-14.

[119] Banerjee A, Ghoshal AK. Biodegradation of an actual petroleum wastewater in a packed bed reactor by an immobilized biomass of Bacillus cereus. Journal of environmental chemical engineering. 2017;5:1696-702.

[120] Kumar SS, Kumar MS, Siddavattam D, Karegoudar T. Generation of continuous packed bed reactor with PVA–alginate blend immobilized Ochrobactrum sp. DGVK1 cells for effective removal of N, N-dimethylformamide from industrial effluents. Journal of hazardous materials. 2012;199:58-63.

[121] Kathiravan MN, Rani RK, Karthick R, Muthukumar K. Mass transfer studies on the reduction of Cr (VI) using calcium alginate immobilized Bacillus sp. in packed bed reactor. Bioresource technology. 2010;101:853-8.

[122] Yadav M, Srivastva N, Singh RS, Upadhyay SN, Dubey SK. Biodegradation of chlorpyrifos by Pseudomonas sp. in a continuous packed bed bioreactor. Bioresource technology. 2014;165:265-9.

[123] Deka D, Das SP, Sahoo N, Das D, Jawed M, Goyal D, et al. Enhanced cellulase production from Bacillus subtilis by optimizing physical parameters for bioethanol production. ISRN biotechnology. 2013;2013.

[124] Hartmans S, Smits J, Van der Werf M, Volkering F, De Bont J. Metabolism of styrene oxide and 2-phenylethanol in the styrene-degrading Xanthobacter strain 124X. Applied and Environmental Microbiology. 1989;55:2850-5.

[125] Kim O-S, Cho Y-J, Lee K, Yoon S-H, Kim M, Na H, et al. Introducing EzTaxon-e: a prokaryotic 16S rRNA gene sequence database with phylotypes that represent uncultured species. International journal of systematic and evolutionary microbiology. 2012;62:716-21.

[126] Altschul SF, Gish W, Miller W, Myers EW, Lipman DJ. Basic local alignment search tool. Journal of molecular biology. 1990;215:403-10.

[127] Kumar S, Stecher G, Tamura K. MEGA7: Molecular Evolutionary Genetics Analysis version 7.0 for bigger datasets. Molecular biology and evolution. 2016;33:1870-4.

[128] Tajima F, Nei M. Estimation of evolutionary distance between nucleotide sequences. Molecular biology and evolution. 1984;1:269-85.

[129] Felsenstein J. Confidence limits on phylogenies: an approach using the bootstrap. Evolution. 1985;39:783-91.

[130] Sasser M. Identification of bacteria by gas chromatography of cellular fatty acids. 1990.

[131] Goodfellow M, Minnikin DE, bacteriology Sfa. Chemical methods in bacterial systematics: Academic Press London; 1985.

[132] Woo PC, Tam DM, Leung K-W, Lau SK, Teng JL, Wong MK, et al. Streptococcus sinensis sp. nov., a novel species isolated from a patient with infective endocarditis. Journal of clinical microbiology. 2002;40:805-10.

[133] Cheng K-K, Cai B-Y, Zhang J-A, Ling H-Z, Zhou Y-J, Ge J-P, et al. Sugarcane bagasse hemicellulose hydrolysate for ethanol production by acid recovery process. Biochemical Engineering Journal. 2008;38:105-9.

[134] Cheng Y, Lin H, Chen Z, Megharaj M, Naidu R. Biodegradation of crystal violet using Burkholderia vietnamiensis C09V immobilized on PVA–sodium alginate–kaolin gel beads. Ecotoxicology and environmental safety. 2012;83:108-14.

[135] Rai L, Mallick N, Singh J, Kumar H. Physiological and biochemical characteristics of a copper tolerant and a wild type strain of Anabaena doliolum under copper stress. Journal of plant physiology. 1991;138:68-74.

[136] Adhikari S, Chattopadhyay P, Ray L. Continuous removal of malathion by immobilised biomass of Bacillus species S14 using a packed bed column reactor. Chemical Speciation & Bioavailability. 2012;24:167-75.

[137] Aksu Z, Gönen F. Biosorption of phenol by immobilized activated sludge in a continuous packed bed: prediction of breakthrough curves. Process biochemistry. 2004;39:599-613.

[138] Tazato N, Handa Y, Nishijima M, Kigawa R, Sano C, Sugiyama J. Novel environmental species isolated from the plaster wall surface of mural paintings in the Takamatsuzuka tumulus: Bordetella muralis sp. nov., Bordetella tumulicola sp. nov. and Bordetella tumbae sp. nov. International journal of systematic and evolutionary microbiology. 2015;65:4830-8.

[139] von Wintzingerode F, Schattke A, Siddiqui RA, Rösick U, Göbel UB, Gross R. Bordetella petrii sp. nov., isolated from an anaerobic bioreactor, and emended description of the genus Bordetella. International journal of systematic and evolutionary microbiology. 2001;51:1257-65.

[140] Vandamme P, Hommez J, Vancanneyt M, Monsieurs M, Hoste B, Cookson B, et al. Bordetella hinzii sp. nov., isolated from poultry and humans. International Journal of Systematic and Evolutionary Microbiology. 1995;45:37-45.

[141] Kersters K, Hinz K-H, Hertle A, Segers P, Lievens A, Siegmann O, et al. Bordetella avium sp. nov., isolated from the respiratory tracts of turkeys and other birds. International Journal of Systematic and Evolutionary Microbiology. 1984;34:56-70.

[142] Vandamme P, Heyndrickx M, Vancanneyt M, Hoste B, De Vos P, Falsen E, et al. Bordetella trematum sp. nov., isolated from wounds and ear infections in humans, and

reassessment of Alcaligenes denitrificans Rüger and Tan 1983. International Journal of Systematic and Evolutionary Microbiology. 1996;46:849-58.

[143] Weyant RS. Identification of unusual pathogenic gram-negative aerobic and facultatively anaerobic bacteria: Williams & Wilkins; 1996.

[144] Weyant RS, Hollis DG, Weaver RE, Amin M, Steigerwalt AG, O'Connor SP, et al. Bordetella holmesii sp. nov., a new gram-negative species associated with septicemia. Journal of clinical microbiology. 1995;33:1-7.

[145] Goodnow RA. Biology of Bordetella bronchiseptica. Microbiological reviews. 1980;44:722.

[146] Ko KS, Peck KR, Oh WS, Lee NY, Lee JH, Song J-H. New species of Bordetella, Bordetella ansorpii sp. nov., isolated from the purulent exudate of an epidermal cyst. Journal of clinical microbiology. 2005;43:2516-9.

[147] Vandamme PA, Peeters C, Cnockaert M, Inganäs E, Falsen E, Moore ER, et al. Bordetella bronchialis sp. nov., Bordetella flabilis sp. nov. and Bordetella sputigena sp. nov., isolated from human respiratory specimens, and reclassification of Achromobacter sediminum Zhang et al. 2014 as Verticia sediminum gen. nov., comb. nov. International journal of systematic and evolutionary microbiology. 2015;65:3674-82.

[148] Busse H, Auling G. Family Alcaligenaceae De Ley, Segers, Kersters, Mannheim and Lievens 1986, 412VP. Bergey's Manual of Systematic Bacteriology. 2005;2:647-53.

[149] Austin B. The family Alcaligenaceae. The Prokaryotes: Springer; 2014. p. 729-57.

[150] Bossert I, Bartha R. The fate of petroleum in soil ecosystems. 1984.

[151] Rahman K, Thahira-Rahman J, Lakshmanaperumalsamy P, Banat I. Towards efficient crude oil degradation by a mixed bacterial consortium. Bioresource technology. 2002;85:257-61.

[152] Joo J, Lee SJ, Yoo HY, Kim Y, Jang M, Lee J, et al. Improved fermentation of lignocellulosic hydrolysates to 2, 3-butanediol through investigation of effects of inhibitory compounds by Enterobacter aerogenes. Chemical Engineering Journal. 2016;306:916-24.

[153] Hu C, Zhao X, Zhao J, Wu S, Zhao ZK. Effects of biomass hydrolysis by-products on oleaginous yeast Rhodosporidium toruloides. Bioresource Technology. 2009;100:4843-7.

[154] Wang W, Yang S, Hunsinger GB, Pienkos PT, Johnson DK. Connecting lignin-degradation pathway with pre-treatment inhibitor sensitivity of Cupriavidus necator. Frontiers in microbiology. 2014;5:247.

[155] Ran H, Zhang J, Gao Q, Lin Z, Bao J. Analysis of biodegradation performance of furfural and 5-hydroxymethylfurfural by Amorphotheca resinae ZN1. Biotechnology for biofuels. 2014;7:1.

[156] Ruan Z, Hollinshead W, Isaguirre C, Tang YJ, Liao W, Liu Y. Effects of inhibitory compounds in lignocellulosic hydrolysates on Mortierella isabellina growth and carbon utilization. Bioresource technology. 2015;183:18-24.

[157] Koopman F, Wierckx N, de Winde JH, Ruijssenaars HJ. Identification and characterization of the furfural and 5-(hydroxymethyl) furfural degradation pathways of Cupriavidus basilensis HMF14. Proceedings of the National Academy of Sciences. 2010;107:4919-24.

[158] Wang X, Gao Q, Bao J. Transcriptional analysis of Amorphotheca resinae ZN1 on biological degradation of furfural and 5-hydroxymethylfurfural derived from lignocellulose pretreatment. Biotechnology for biofuels. 2015;8:136.

[159] Trudgill PW. The metabolism of 2-furoic acid by Pseudomanas F2. Biochem J. 1969;113:577-87.

[160] Nichols NN, Mertens JA. Identification and transcriptional profiling of Pseudomonas putida genes involved in furoic acid metabolism. FEMS Microbiol Lett. 2008;284:52-7.

[161] Koopman F, Wierckx N, de Winde JH, Ruijssenaars HJ. Identification and characterization of the furfural and 5-(hydroxymethyl)furfural degradation pathways of Cupriavidus basilensis HMF14. Proc Natl Acad Sci U S A. 2010;107:4919-24.

[162] Wang Q, Xie X, Zhang X, Zhang J, Wang A. Preparation and swelling properties of pH-sensitive composite hydrogel beads based on chitosan-g-poly (acrylic acid)/vermiculite and sodium alginate for diclofenac controlled release. International Journal of Biological Macromolecules. 2010;46:356-62.

[163] Mi F-L, Sung H-W, Shyu S-S, Su C-C, Peng C-K. Synthesis and characterization of biodegradable TPP/genipin co-crosslinked chitosan gel beads. Polymer. 2003;44:6521-30.

[164] Yasmeen S, Kabiraz MK, Saha B, Qadir M, Gafur MA, Masum SM. Chromium (VI) ions removal from tannery effluent using chitosan-microcrystalline cellulose composite as adsorbent. Int Res J Pure Appl Chem. 2016;10:1-14.

[165] Saber-Samandari S, Yekta H, Saber-Samandari S. Effect of Iron Substitution in Hydroxyapatite Matrix on Swelling Properties of Composite Bead. Journal of Mineral, Metal and Material Engineering. 2015;1:19-25.

[166] Kumirska J, Czerwicka M, Kaczyński Z, Bychowska A, Brzozowski K, Thöming J, et al. Application of spectroscopic methods for structural analysis of chitin and chitosan. Marine drugs. 2010;8:1567-636.

[167] Pasparakis G, Bouropoulos N. Swelling studies and in vitro release of verapamil from calcium alginate and calcium alginate–chitosan beads. International journal of pharmaceutics. 2006;323:34-42.

[168] Banerjee I, Modak JM, Bandopadhyay K, Das D, Maiti B. Mathematical model for evaluation of mass transfer limitations in phenol biodegradation by immobilized Pseudomonas putida. J Biotechnol. 2001;87:211-23.

[169] Jia X, Wen J, Jiang Y, Bai J, Cheng X, Zheng Y. Modeling for batch phenol biodegradation with immobilized Alcaligenes faecalis. AIChE journal. 2006;52:1294-303.

[170] Jianlong W, Liping H, Hanchang S, Yi Q. Biodegradation of quinoline by gel immobilized Burkholderia sp. Chemosphere. 2001;44:1041-6.

[171] Göksungur Y, Güvenç U. Batch and continuous production of lactic acid from beet molasses by Lactobacillus delbrueckii IFO 3202. Journal of chemical technology and biotechnology. 1997;69:399-404.

[172] Liu H, Du Y, Wang X, Sun L. Chitosan kills bacteria through cell membrane damage. International journal of food microbiology. 2004;95:147-55.

[173] Idris A, Suzana W. Effect of sodium alginate concentration, bead diameter, initial pH and temperature on lactic acid production from pineapple waste using immobilized Lactobacillus delbrueckii. Process Biochemistry. 2006;41:1117-23.

[174] Singh B, Verma A, Pooja, Mandal PK, Datta S. A biotechnological approach for degradation of inhibitory compounds present in lignocellulosic biomass hydrolysate liquor using Bordetella sp BTIITR. Chemical Engineering Journal. 2017;328:519-26.

[175] Chen K-C, Lin Y-H, Chen W-H, Liu Y-C. Degradation of phenol by PAA-immobilized Candida tropicalis. Enzyme and Microbial technology. 2002;31:490-7.

[176] Levenspiel O. Chemical reaction engineering. Industrial & engineering chemistry research. 1999;38:4140-3.

[177] Maiti SK, Bera D, Chattopadhyay P, Ray L. Determination of Kinetic Parameters in the Biosorption of Cr (VI) on Immobilized Bacillus cereus M1 16 in a Continuous Packed Bed Column Reactor. Applied Biochemistry and Biotechnology. 2009;159:488-504.

[178] Yee KL, Jansen LE, Lajoie CA, Penner MH, Morse L, Kelly CJ. Furfural and 5-hydroxymethyl-furfural degradation using recombinant manganese peroxidase. Enzyme and microbial technology. 2018;108:59-65.

[179] Fonseca BG, Mateo S, Moya AJ, Roberto IC. Biotreatment optimization of rice straw hydrolyzates for ethanolic fermentation with Scheffersomyces stipitis. Biomass and Bioenergy. 2018;112:19-28.